

**Hydraulic properties of Amazonian trees:
spatial variation and consequences for
vulnerability to drought**

Julia Valentim Tavares

Submitted in accordance with the requirements for the degree of
Doctor of Philosophy

The University of Leeds
School of Geography

September 2019

The candidate confirms that the work submitted is her own, except where work which has formed part of jointly-authored publications has been included. The contribution of the candidate and the other authors to this work has been explicitly indicated below. The candidate confirms that appropriate credit has been given within the thesis where reference has been made to the work of others.

Chapter 2

In preparation to be submitted to *Nature*. Authors design the study; all authors contributed to data collection and/or data management; Author analysed the data and wrote the paper. RAINFOR network provided forest inventory data;

Chapter 3

In preparation to be submitted to *Nature Ecology and Evolution*. Authors design the study; all authors contributed to data collection and/or data management; Author analysed the data and wrote the paper. RAINFOR network provided forest inventory data;

Chapter 4

In preparation to be submitted to *Ecology letters*. Authors design the study; all authors contributed to data collection and/or data management; Author analysed the data and wrote the paper.

This copy has been supplied on the understanding that it is copyright material and that no quotation from the thesis may be published without proper acknowledgement.

Assertion of moral rights:

The right of Julia Valentim Tavares to be identified as Author of this work has been asserted by her in accordance with the Copyright, Designs and Patents Act 1988.

© 2019 The University of Leeds and Julia Valentim Tavares

Acknowledgements

I apologise in advance because it is not possible to be concise in this part of my thesis. The work presented below has been constructed, piece by piece, by several wonderful people. I would not be able to do all of this without you. It is time to say out loud: Thank you very much!

I would like to thank CAPES foundation, Ministry of Education of Brazil (DPE-1293/2015-00) for funding my PhD and this research. Additionally, I would like to thank NERC (NE/N004655/1) and Climate Research Bursary Fund for field work support.

I could not possibly be better supervised than I have been. What I team I have by my side, teaching, challenging and, most importantly, encouraging me in every single step I have walked in this journey. A thousand thanks would not be enough to say to David Galbraith, Emmanuel Gloor and Oliver Phillips. I would like to specially thank David firstly for answering so kindly that poorly written email I sent to him back in 2014, on which I presented myself and asked if he would be interested in supervising me. Secondly, thank you very much, David, for offering me the opportunity to be part of the TREMOR project and for trusting me to immerse in Amazon and lead all its campaigns. Special thanks also to Emmanuel for trust and for giving me opportunity to share what I have been learning in the Ecophysiology workshop in India and also to help the Ron's campaign.

My absolutely fantastic supervision team has not been fully acknowledged yet. Maurizio Mencuccini and Rafael Oliveira, you both have been also fundamental to my work and development as a researcher. Thank you for opening the doors of your labs and showing me this completely new hydraulic world. Thank you for the meetings, the teaching, the revisions, discussions and for joining David and I in our pilot campaign. Thank you for training me. Your support and incentive have been crucial for me.

I would like to say thanks to Roel Brienen, Tim Baker and Jordi Martínez-Vilalta for accepting to be part of my viva panel and for dedicating their time to read my work.

Representativeness is important to me. Looking ahead and seeing women as researchers helps me to carry on my goal of following an academic career. I would like to thank all women in science. Thank all of you that have walked this path before me. Special thanks to Lucy Rowland, Beatriz Marimon, Flavia Costa, Michelle Johnson,

Erika Berenguer, Indu Murthy, Sara Batterman, Thaise Emilio, Rita Mesquita, Lisa Bentley, Euridice Honorio, Imma Oliveiras, Sophie Fauset, Adriane Esquivel Muelbert, Halina Jancoski, Marta Giannichi, Fernanda Coelho, Mariana Lima, Carolina Freitas, Carolina Allage, Thais Pontes, Juliana Bonanomi, Isabela Aleixo and Juliana Schietti. Your pathway inspires me.

I could not be luckier, during my four years journey, I had by my side long distance friends. Thanks to Karina and Bruno Ladvocat, with whom I shared a flowery walk since university, passing through master's degree in Manaus and then reaching Leeds. Thank you, my friends, for always being the home feeling and safe harbour. I thank Fernanda Coelho, with whom I also shared my journey before. Thanks Fe, for your incentive and support since the very beginning when this PhD was still a distant plan (almost impossible) plan until now in the very last week of it.

Ecology Global Change research cluster became a family to me, not only because we basically spend 90% of our life in the department, but also because it is the starting point for colleagues to become true friends. Thank you to Adriane Esquivel, meu encontro de almas, for all your help with my work since the very beginning until nowadays, but thank you specially for the emotional support, for guide me in this marathon, for all the love and for introducing me Clinton, our musical therapist! Thank you to Marta Giannichi and Alfredão Santos Filho, amigos para a vida inteira que eu precisei vir para Leeds para conhecer, for inspiring me calm, for teaching how to be #serene, for all the love and support. By your side I always felt that everything was absolutely ok. I could not be more grateful for also having by my side: Yunxia Wang (my PhD twin), Amy Bennett (my ukulady), Mathew Richardson (the best hug in the UK), Arthur Coimbra, Gabriel Hidalgo (mi compañero de oficina y lema: "no termina ni se queda corto"), Ana Pacheco, Emma Dochert, Ricardo Dal'Agnol, Paloma, Camila Farrapo, Luciene Gomes, Jessica and Jimmy Baker, Nadir Pallqui, Bart Crezee, Nikee Groot, Antonio Maffei, Suzanne Stas, Will Barker and specially Alex Chambers-Ostler, Rakesh Tiwari and Ron Sunny for literally seating next to me in the final writing moments, sharing weekends and nights in Geography with me and giving me strength for the final push. Thank you, my friends, for the wonderful moments and all the support.

Apart from EGC family, life in Leeds was more colourful due to very special people. I thank Erica, Lucas and Lara Galbraith, Luciana and Ana Sophia Gloor, and

Tiago for recharging my batteries every time we were together. Also, thanks to my Ashtanga yoga teacher Alex Hardern, who inspires me calm and balance. Each short centring mediation was a restart in my mind.

More than thanks have to be said to Fernanda Barros, Caroline Signori, Paulo Bitterncourt, Luciano Pereira and Mauro Brum for giving me your time, for training me in the methodologies, for all on-going help and support. Thanks also to Teresa Rosas for being the first one to introduce me to the hydraulic world. My thanks also to Erika Berenguer and Lisa Bentley for sharing their experiences with long field campaigns and how to lead big field teams. You helped me to prepare myself for this great adventure.

Each PhD is a particular world, with different challenges, learnings and limits. During my PhD experience I spent almost one year in the field immersed in our beloved Amazonia, collecting an enormous amount of data, knowing lovely people and seeing beautiful landscapes. What a beautiful opportunity, which will be eternally grateful for. I am definitely especially lucky to have worked with the most wonderful teams in the world! Thank you Kallpa Team, ustedes son el mas puro exito! Obrigada equipe só otoridade, aqui não tem tempo ruim!

An entire paragraph and more special thanks have to be dedicated to my fixed partners of Amazonian journey: Martin Gilpin, Carolina Signori and Francisco Diniz. Together, we build and rebuild “portable” labs across many sites, we shocked all the passengers in all airports by carrying our 16 massive bags of equipment, plus telescopic scissors. Together we faced impressive storms, we measured traits for more than 12 hours a day, we got very exhausted and stressed. Also, together we sang, we danced and we accomplished a beautiful piece of work. I could not be more grateful to have you in my life!

For the success of the campaigns, there were more than 100 people involved: researcher that received us in each site, people helping locally with logistics, climbers, field assistants, cooks, people from the accommodations and others. People that gave their best for this work and to whom I am infinitely grateful for. I would like to thank specially the TREMOR core team: Manuel Marca, Carlos Salas, Flor Maria Mullisaca and Martin Acosta. Thank you to Don Pedro and Dora from Bolivia. Special thanks to Alejandro Murakami-Araujo, always prompt to help with all information needed: ¡ Muchas gracias, Alejandro! I would like also to thank AIDER for your support in Puerto Maldonado and

specially thanks to Vanessa Hilaes. Vane, yo no tengo palabras para agradecerle todo su apoyo y compromiso sin restricciones para con nosotros. Su apoyo fue esencial para el éxito en cada campaña. ¡Muchas gracias infinitas!

Thank you very much for all the collaborators that shared their hydraulic data with me and to all RAINFOR and ForestPlots collaborators. Thank you all for making this work possible. Special thanks to Aurora Levesley, Karina Ladvocat and Georgia Pickavance.

Thanks to all my friend in Brazil that, in one way or another, made themselves very close to me, transpassing the little Atlantic sea barrier. Special thanks to Carolina Allage, Mariana Lima, Maira Rizzi and Juliana Bonanomi, we have been always so connected that I cannot tell we have not been in the same place. Thanks to Ignez (Diva Magnânima) Leo, Letícia, Pedro, Elisa, Deco, Janaína, Bento e Benjamim for all love and support.

Words are not enough to thank who taught me that there is no reason to be afraid, that we are always learning in life and that learning is such a beautiful process. Thank you very much to my father, mother and sister: Helio Tavares, Maria Eni Valentim and Camila Valentim Tavares for all your trust, infinite support, for holding my hand and showing that yes, we can learn this. Special thanks to our beloved Cristal and Rubisco.

Last, but not least, I would like to thank my husband Francisco Carvalho Diniz for have joined me in every single little track of this marathon: from moving abroad, passing through long field work adventures, measuring plant hydraulics together and finally submitting this piece of work by my side. You make my life bright, light and colourful. To you and our yet to arrive little ones, Teresa and Violeta, I dedicate this thesis.

Abstract

The Amazon rainforest is the largest and most diverse tropical forest on the planet and it plays a fundamental role in global biogeochemical cycles and carbon sequestration from atmosphere. Changes on temperature and precipitation regime due climate change are likely to cause permanent disturbance in Amazon rainforest, a biome highly dependent of water availability. Studies carried in Amazonia have documented increased rates of tree mortality, reduction in forest carbon sink, and shifts on species and functional composition likely caused by on-going changes in climate. As temperature and the frequency of droughts are predicted to continue increasing in future is fundamental to understand how the water stress caused by these impacts will affect tree species in the Amazon. In this thesis I aimed to enhance the understanding of the sensitivity and vulnerability of Amazonian trees to drought by combining an extensive long-term tree monitoring database with in-situ experiments carried along a wide precipitation gradient. Firstly, I showed how tree hydraulic traits, therefore drought vulnerability vary across Amazonian forests, with site water availability, soil texture and biogeographic regions being the main contributors of this variation. Secondly, I showed that hydraulic traits are related with changes in aboveground biomass changes at community level (Chapter 2). In Chapter 3 I found that there is phylogenetic signal for embolism resistance, being Fabaceae an especially resistant clade. I further used this information to create a map of embolism resistance across 582 Amazonian tree communities distributed in the whole domain. Finally, I showed how embolism resistance and hydraulic safety margins are related to species biogeographical distribution, life history characteristics and drought induced mortality. Overall, this thesis assessed the variation of the hydraulic traits across Amazonian forests and among tree taxa, as well as validated the predictive power of Amazonian hydraulic traits over forest dynamics.

Contents

Acknowledgements	v
Abstract	ix
Contents.....	x
List of figures.....	i
List of tables	3
Appendices	4
Abbreviations.....	6
Chapter 1: General Introduction	8
1.1 Research rationale	8
1.2 Spatial variation of Amazonian forest composition and dynamics.....	9
1.3 Amazon climate under change and consequences	11
1.4 Plant hydraulic functioning	11
1.5 Mechanisms underpinning drought induced mortality.....	13
1.6 Xylem embolism resistance and Hydraulic safety margins.....	15
1.7 Methods to measure xylem vulnerability to drought	16
1.8 Thesis aims	19
1.9 Thesis objectives.....	19
Chapter 2: Variation in drought vulnerability across Amazonian forests	21
2.1 Introduction.....	22
2.2 Methods	25
2.3 Results and Discussion	32
2.4 Implications and Conclusions	40
Chapter 3: Evolutionary control of embolism resistance in Amazonian forests	42
3.1 Introduction.....	43
3.2 Methods	46
3.3 Results	49
3.4 Discussion	56
3.5 Implications and Conclusions	59
Chapter 4: Hydraulic traits are related to Amazonian species biogeographical distribution, tree performance and drought-induced mortality.....	61
4.1 Introduction.....	62

4.2 Methods	65
4.3 Results	70
4.4 Discussion	76
4.5 Implications and Conclusion.....	78
Chapter 5: Synthesis and Conclusions	80
5.1 Research synthesis and implications	80
5.2 Future research directions	85
5.3 Final remarks	89
References	89
Appendices	106

List of figures

Figure 1. 1 Illustration of water movement in plants from soil to atmosphere.	12
Figure 1. 2 Scanning electron micrographs showing a vessel with Non-vestured pits (A) and a vessel with vestured pit (B). pit membrane (PM). Figure from Jansen et al. 2004	13
Figure 1. 3 Hypotheses on tree mortality mechanisms under drought conditions.....	15
Figure 1.4 Schematic figure showing the pneumatic apparatus	17
Figure 1.5 Examples of vulnerability curves	18
Figure 2. 1 Sampled sites: spatial distribution and climatological variation	24
Figure 2. 2 Equipment use to construct the vulnerability curves.	29
Figure 2. 3 Hydraulic traits distribution across Amazonian tree taxa	33
Figure 2. 4 Hydraulic traits variation within and across Amazon forest types	34
Figure 2. 5 Relationship between tree community hydraulic traits and environmental variables	37
Figure 2. 6 Relationship between Aboveground net biomass and hydraulic traits.....	39
Figure 3. 1 Phylogenetic tree (Coelho de Souza et al., 2019) of Amazonian tree genera	50
Figure 3. 2 Embolism resistance variation across and within families with a wide occurrence in my dataset.....	52
Figure 3. 3 Difference in embolism resistance (Ψ_{50}) between Fabaceae and Non-Fabaceae across	53
Figure 3. 4 Map of Amazonian vulnerability to embolism	55
Figure 3. 5 Differences in embolism resistance among lineages with consistently present (Myrtales, Gentianales and Fabaceae) and absent (Ericales, Santalales and Sapindales) vestured pits.....	56

Figure 4. 1 Functional trait range of the 87 sampled species in the Western Amazon. Histograms of life-history related traits range of the sampled species in the Western Amazon (green) in relation to pan-Amazonian life-history range (grey) 66

Figure 4. 2 Climatological data when ψ_{\min} was sampled at each site in the Western Amazon.. 68

Figure 4.3. Relationship between hydraulic safety margins and Ψ_{\min} and embolism resistance across 79 Western Amazonian tree species..... 70

Figure 4.4 Relationship between water deficit affiliation and hydraulic traits 72

Figure 4. 5 Relationship between species mean key hydraulic traits and life-history strategy traits. 73

Figure 4.6 Relationship between species mean hydraulic traits and drought induced-mortality.. 74

Figure 4.7 Relationship between species mean wood density, Non-structural carbohydrates (NSC) at branch and leaf level with water deficit affiliation (WDA) and drought induced-mortality (Δm). 75

List of tables

Table 3. 1 Summary table of phylogenetic signal (PS) for embolism resistance of Amazonian trees.	50
-------------------------------------------------------------------------------------------------------	----

Appendices

Supplementary Information for Chapter 2.....	106
Figure A1. 1 Sites precipitation regime. Precipitation regime across the 11 sampled forest sites	106
Figure A1. 2 Sampled species functional trait range. Histograms of life-history related traits range of the sampled species (red) in relation to pan-Amazonian life-history range	107
Figure A1. 3 Hydraulic traits variation within and across Amazon forest types.....	108
Figure A1. 4 Hydraulic traits variation across Amazon forest sites	109
Figure A1. 5 Relationship between tree community hydraulic traits and environmental variables	110
Figure A1. 6 Climatological data when ψ_{\min} was sampled at each site	111
Table A1. 1 Sampling design summary: Site environmental characteristics.	112
Table A1. 2 Sampling design summary: Site biotic characteristics.....	113
Table A1. 3 Linear models relating Community weighted mean hydraulic traits and environmental variable.	114
Table A1. 4 Results of Kendall tau correlations among environmental variables.	119
Table A1. 5 Linear models describing the relationship between hydraulic traits and relative dominance per species per site.....	120
Table A1. 6 Summary of clusters and forest plots used to investigate changes in net biomass.	121
Supplementary Information for Chapter 3.....	123
Figure A2. 1 Phylogenetic tree (Coelho et al 2019) of Amazonian tree genera	123
Figure A2. 2 Map of phylogenetic signal at genus-level for Ψ_{50} (A) and Ψ_{88} (B).....	124
Figure A2. 3 Difference in embolism resistance (Ψ_{50}) among families across (A) and within (B) Amazonian forests and across tropical rainforests (C)	125
Figure A2. 4 Difference in embolism resistance (Ψ_{88}) between Fabaceae and Non-Fabaceae across (A) and within (B) Amazonian forests	125
Figure A2. 5 Community-weighted mean embolism resistance across Amazonian regions	126
Supplementary Information for Chapter 4.....	127
Table A3. 1 Summary of environments conditions of Western Amazonia.....	128

Table A3. 2 Models and respective values of the relationship between hydraulic safety margins and Ψ_{min} and embolism resistance for 79 Western Amazonian tree species.....	129
Figure A3. 1 Relationship between species mean Ψ_{50} and HSM ₅₀ and life-history strategy traits	130
Table A3. 3 Summary of standard maor axis (SMA) regressions between hydraulic traits and water deficit affiliation.	131
Table A3. 4 Drought induced mortality as a function of wood density at branch level and branch and leaves total non-structural carbohydrates concentrations.....	133
Table A3. 5 Relationship between drought induce mortality (ΔM) and hydraulic traits for common species of seasonal and aseasonal forest	135

Abbreviations

Δm	Drought Induced Mortality
AGB	Above Ground Biomass
AIC	Akaike Information Criteria
ALP-1	Allpahuayo plot 1
ALP-2	Allpahuayo plot 2
BCI	Barro Colorado Island plot
BM	Brownian Motion
CAX	Caxiuana plot
CRU	Climatic Research Unit
CWD	Cumulative Water Deficit
CWD	Climatological Water Deficit
CWM	Community Weighted Mean
DBH	Diameter at Breast Height
DSL	Dry Season Length
FEC	Fazenda Experimental Catuaba plot
HSM	Hydraulic Safety Margin
HSM50	Hydraulic Safety Margin related to Ψ_{50}
HSM88	Hydraulic Safety Margin related to Ψ_{88}
KEN-1	Kenia plot 1
KEN-2	Kenia plot 2
LMA	Leaf Mass per Area
MAN	Manaus plot
MAP	Mean Annual Precipitation
masl	Meters Above Sea Level
MCWD	Maximum Climatological Water Deficit
MCWD	Maximum Cumulative Water Deficit
NSC	Non-Structural Carbohydrates
NVX	Nova Xavantina plot
PAD	Percentage of Air Discharge
PLC	Percentage Loss of Xylem Conductance
PS	Phylogenetic Signal
P_{total}	Total Soil Phosphorus
RAINFOR	Amazon Forest Inventory Network
SMA	Standard Major Axis regressions
SUC	Sucusari plot
TAP	Tapajos plot
VPD	Vapour-Pressure Deficit
WDA	Water Deficit Affiliation
ψ_{50}	metric of embolism resistance at which 50% of the stem hydraulic conductance is lost

ψ_{88}

metric of embolism resistance at which 88% of the stem hydraulic conductance is lost

Chapter 1: General Introduction

1.1 Research rationale

Amazonian forests play a fundamental role in global biochemical cycles, being responsible for more than 10% of global net primary productivity (Zhao and Running, 2010) and housing over half of the remaining tropical rainforest in the world (Ter Steege et al., 2013). Several Global Circulation Models predict that climate change will increase the frequency, incidence and severity of droughts in tropical forests (Cox et al., 2008; Malhi et al., 2009). Increases in the frequency and duration of future drought events may reduce aboveground carbon storage by increasing tree mortality and reducing productivity of forests (Phillips et al., 2009). Ultimately, this may lead to a reduction of the Amazonian forest sink (Malhi et al., 2008; Malhi et al., 2009; Lewis et al., 2011) and act as a positive feedback on global warming (Cox et al., 2000; Rammig et al., 2010)

Drought-related tree mortality has been the focus of significant research over the past decade. In Amazonia, most studies of drought effects on forests have been descriptive in nature, focusing on quantifying the impacts of drought on forest growth and mortality (e.g. Phillips et al., 2009; Esquivel-Muelbert et al., 2018). To predict how forests will respond to future climate change and how future drought scenarios will affect forest structure and functional composition, it is necessary to understand the physiological mechanisms which drive drought impacts (Choat et al., 2012; Anderegg et al., 2012). Xylem embolism resistance and hydraulic safety margins have been recognized as key physiological traits that confer plant ability to cope with water stress and to be important predictors of drought-induced mortality (Tyree & Zimmermann, 2002; Anderegg et al., 2016; Choat et al., 2018).

Over the past years, great advances have been made on the understanding of hydraulic properties in Amazon forests (Rowland et al., 2015; Powell et al., 2017; Oliveira et al., 2018; Santiago et al., 2018; Brum et al., 2018; Fontes et al., 2018; Barros

et al., 2019). However, the studies have been restricted to local scales and a few species, being all studies realized in 4 forests in the Central-Eastern Amazon. A regional broad scale approach, covering a broad number of species and wide range of life-story strategies, is still lacking. The main question of this thesis is: How does vulnerability to drought vary across Amazonian forests?

This chapter introduces an overview about Amazonian forests and recent climatic changes and impacts faced by these forests. I also review plant hydraulic functioning and mechanisms underpinning mortality caused by drought. In the second chapter, I explore the spatial variation of hydraulic traits within and across Amazon forests, as well as test for the existence of relationship between tree community hydraulic traits and environmental characteristics and long-term community changes in aboveground biomass. In the following chapter, I evaluate within taxa variation of embolism resistance and assess the degree of phylogenetic conservatism this trait among Amazonian tree taxa. The fourth chapter investigates to what extent hydraulic traits are related to species water deficit affiliation, demographic traits and mortality caused by drought. The final fifth chapter provides a synthesis of my thesis findings and implications, as well as suggestions for future studies.

1.2 Spatial variation of Amazonian forest composition and dynamics

Amazonia is extremely diverse and heterogeneous, encompassing different forest types across broad range of precipitation regime and soil conditions. Spatially, species composition and dynamics highly vary across Amazonian forests. For example, Western Amazon has relatively higher soil fertility, lower wood density, higher forest productivity and higher forest turnover rates than Central-Eastern Amazon (Quesada et al., 2012; Malhi et al., 2015; Johnson et al., 2016). Across the basin, species composition is driven by two environmental main axis (Ter Steege et al., 2006). The first one is soil fertility related (north-eastern to south-western Amazon, poor to richer soils respectively) and the second is water availability related (north-western to south-eastern Amazon, wetter to drier environment, respectively). Burseraceae, Bignoniaceae and Rutaceae are families related to wet/dry gradient, showing greater abundance in drier environments. Moraceae, Myrtaceae, Urticaceae are more abundant in the more fertile Western Amazon, while

Chrysobalanaceae, Lecythidaceae have high abundance in phosphorus poor soil of Central-Eastern Amazon (Ter Steege et al., 2006). Fabaceae, the most abundant family in Amazonia has wide distribution across the basin, but with higher abundance in the Guiana Shield and Brazilian Shield (Ter Steege et al., 2006).

According to the physiological tolerance hypothesis (Janzen, 1967; Currie et al., 2004), the capacity of tree taxa to occur in a broad precipitation range is associated with physiological features that allow trees to withstand seasonal water shortage (Engelbrecht et al., 2007). Within Amazonia there is a positive relationship between tree diversity and water availability (Steege et al., 2003). Higher tree species diversity is found in very moist forest with low or null seasonal water deficit, while lower species diversity is found in highly seasonal or dry forests (Gentry, 1988; Clinebell et al., 1995; Steege et al., 2003). Esquivel et al. (2017a) demonstrated that seasonality of drought indeed constrains tree taxa distribution among the Western Neotropics, who based on taxa abundance across 531 widely distributed floristic plots generated an index of taxa Water Deficit Affiliation (WDA). Taxa with more negative WDA (dry affiliated taxa) are more adapted to overcome moist stress and its occurrence is widely spread in the Neotropics (Esquivel-Muelbert et al., 2017b). Dry affiliated taxa can also occur in wet places, while this does not hold true for most of Amazonian species, which are highly wet affiliated, with occurrence restricted to places with low or none seasonal moist stress (Esquivel-Muelbert et al., 2017a). Additionally, it has been demonstrated that WDA is related with mortality under drought at genus level, with wet affiliated genus having higher drought-induced mortality than genus dry affiliated (Esquivel-Muelbert et al., 2017b).

Besides of tree biogeographical distribution, tree growth rate, mortality rate and potential size (size that taxa can potentially reach) are fundamental ecological traits to understand forest structure, dynamics, and carbon dynamics (Phillips et al., 2009; Fauset et al., 2015; Brienen et al., 2015; Coelho de Souza et al., 2016). These traits compound the two major axes which describe life-history strategies among tropical trees. Additionally, they have been shown to be to some extent phylogenetically controlled across Amazonian tree taxa (Coelho de Souza et al., 2016).

Although it has been demonstrated that tree taxa distribution along a precipitation gradient is related to mortality induced by drought (Esquivel-Muelbert et al., 2017b), no tests relating biogeographical distribution and Amazonian tree physiological traits have

been yet attempted. Additionally, relationships between physiological traits and Amazonian tree species life-history strategy traits at a large scale still remains to be elucidated. Due to the especially high species diversity of Amazon forest, assessing which are the physiological mechanisms that reflect taxa ecological characteristics, distribution and drought induced mortality risk is essential to foresee shifts, forest composition and functioning under drying and warming future climate.

1.3 Amazon climate under change and consequences

Over the past two decades, Amazonian forests have experienced several of large-scale drought events (1998, 2005, 2010, 2015-16) (Aragão et al., 2007; Marengo et al., 2008; Phillips et al., 2009; Lewis et al., 2011; Jiménez-Muñoz et al., 2016), as well air temperature increases (Jiménez-Muñoz et al., 2013). These changes have been shown to substantially impact this environment, resulting in elevated tree mortality and decrease in forest productivity (Phillips et al., 2009) and possibly contributing for the decline of the long-term Amazon carbon sink (Brienen et al., 2015a). Additionally, studies have reported changes in floristic and functional composition, favouring taxa that affiliated to environments with high seasonality of water shortage and with wide occurrence along the precipitation gradient (Esquivel-Muelbert et al., 2018). Climate model projections foreseen enhanced water stress in Amazon rainforests in the future, due to the increase of frequency of extreme drought and substantial elevation of air temperature (Marengo et al., 2018). To improve our ability to predict how Amazon forests will respond to going and future changes in climate and, consequently, how forest structure and composition will be affected, it is necessary to understand the physiological mechanisms which drive drought impacts.

1.4 Plant hydraulic functioning

The ascension of water from root to leaves is a passive mechanism where water moves up in the soil-plant-atmosphere continuum as a solid liquid under high tension (Tyree & Zimmermann, 2002), due to Cohesion-Tension force (Dixon, 1914), across a water potential gradient (Fig 1.1). In the majority of angiosperms, water flows inside

vessels elements in the xylem. Mature vessels elements are generally dead lignified tissues to confer mechanistic support to cope with the the high tensioned water column through long distance water transport (Tyree & Zimmermann, 2002). This lignification process of xylem cells is an evolutionary plant adaptation to ensure the long-water-supply (Tyree & Zimmermann, 2002). Water moves from conduits lumens passing through adjacent pores (pit chambers) and their membranes (pit membranes)

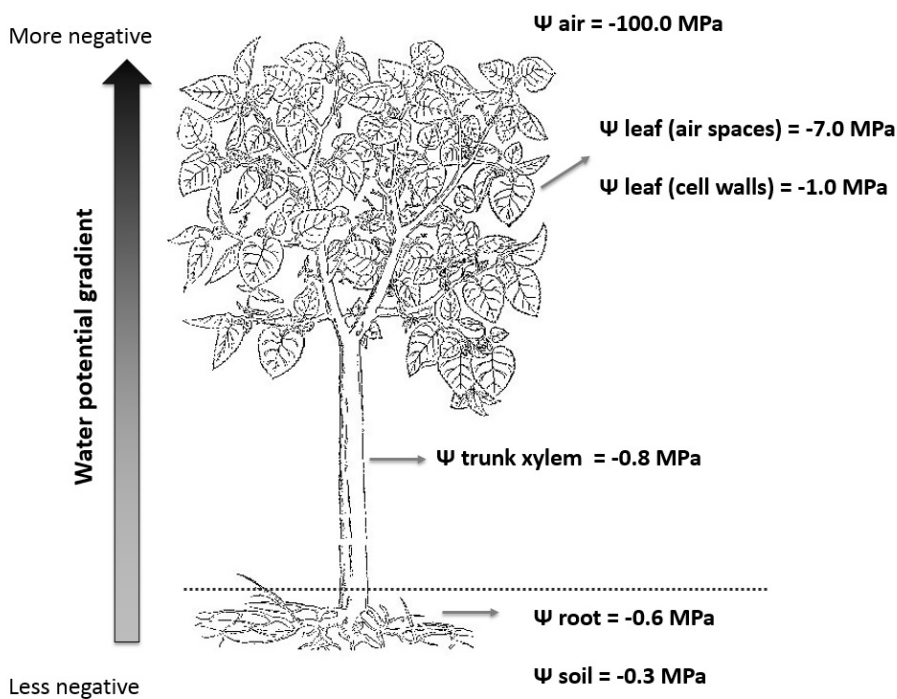


Figure 1. 1 Illustration of water movement in plants from soil to atmosphere. Water moves throughout a differential of water potential (less negative to more negative).

Thus Atmosphere vapour pressure deficit (VPD) and soil water availability are the key environmental features that drives changes in whole plant-functioning (Mencuccini, 2003; Mencuccini et al., 2015). Water column in the xylem is constantly under high tension, being at metastable state. Under high evaporative atmospheric demand and drying soil, the xylem tension can increase to such a point that triggers rapidly change from liquid water to vapour phase. This phenomenon is called cavitation. Straight after cavitation, air molecules from the surrounding tissues migrate to the empty space generated by cavitation. This process is known as xylem embolism. Once a given conduit is embolized (filled with air), embolism propagation across conduits happens

through air seeding (Tyree and Sperry, 1989; Tyree & Zimmermann, 2002). In this context, the pits (adjacent pores) works as inner valves restricting the propagation of embolism across vessels (Hacke et al., 2001), being fundamentally important to maintain the integrity of water transport (Sperry et al., 2006; Jansen et al., 2009). Pit membranes can be plain or vestured (Jansen et al. 2004, Fig.1.2). Vestured pits, structures from the secondary cell wall in the pit chambers, are recognized as particularly important features, conferring resistance to embolism by preventing pit membrane rupture or mechanically acting as a barrier against air seeding dispersal (Choat et al., 2004). It has been shown that vestured pits are phylogenetic conserved with trees belonging to Myrtales, Gentianales and non-basal Fabaceae invariably presenting vestured pits, while in Ericales, Santalales and Sapindales this feature is consistently absent (Jansen et al., 2003).

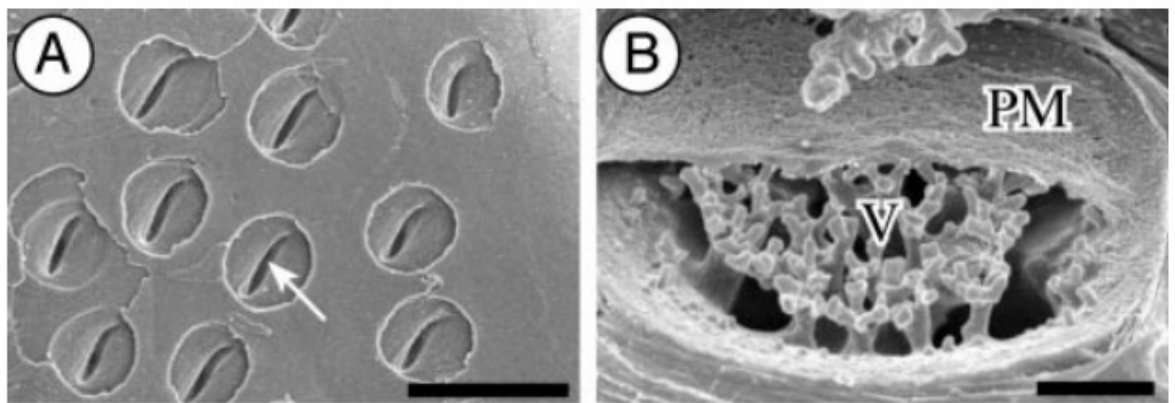


Figure 1. 2 Scanning electron micrographs showing a vessel with Non-vestured pits (A) and a vessel with vestured pit (B). Figure B show a pit chamber with the vestures (V) supporting the pit membrane (PM). Figure from Jansen et al. 2004

1.5 Mechanisms underpinning drought induced mortality

There has been considerable recent research on the mechanistic basis of tree mortality under drought conditions, with two major hypotheses being proposed: 1) hydraulic failure and 2) carbon starvation (Figure 1.3). The accumulation of embolism decreases the xylem hydraulic conductance (Tyree and Dixon, 1986; Sperry et al., 1988). Embolism caused by successive water stress can culminate in the blockage of water flow inside of xylem conduits by air bubbles, triggering hydraulic failure at tissue, branch or

whole plant level (Tyree and Sperry, 1989; Tyree & Zimmermann, 2002). Several studies have discussed embolism reversibility (Tyree et al., 1999; Sperry, 2013; Cochard and Delzon, 2013), but the overall results remain controversial. Nowadays, xylem refilling is thought to be unlikely and results indicate that plants could partially or totally recover from water stress by growing new tissues (Brodribb et al., 2010; Choat et al., 2018)

According to the Carbon starvation hypothesis proposed by McDowell et al. (2008), the stomata close in order to avoid the risk of high embolism in the xylem's conduits during dry periods. This closure causes a decrease in the stomatal conductance and, consequently, a decrease in carbon assimilation, causing photosynthetic C uptake to reduce to low levels. When the drought duration is significantly long, the storage of carbon reserves becomes lower than the amount of carbon maintenance demanded for metabolism and defence. Thus, the plant may 'starve' by running out of carbon (McDowell et al., 2008). Attacks from biotic agents would intensify both processes (McDowell et al., 2008). Despite of various possible plant responses to water shortage through adjustments of a complex range of factors, such as stomatal, leaf, stem and whole plant level adjustments (Martinez-Vilalta et al., 2019), hydraulic failure has been commonly related to mechanisms underpinning tree mortality under drought (Rowland et al., 2015; Anderegg et al., 2016; Adams et al., 2017).

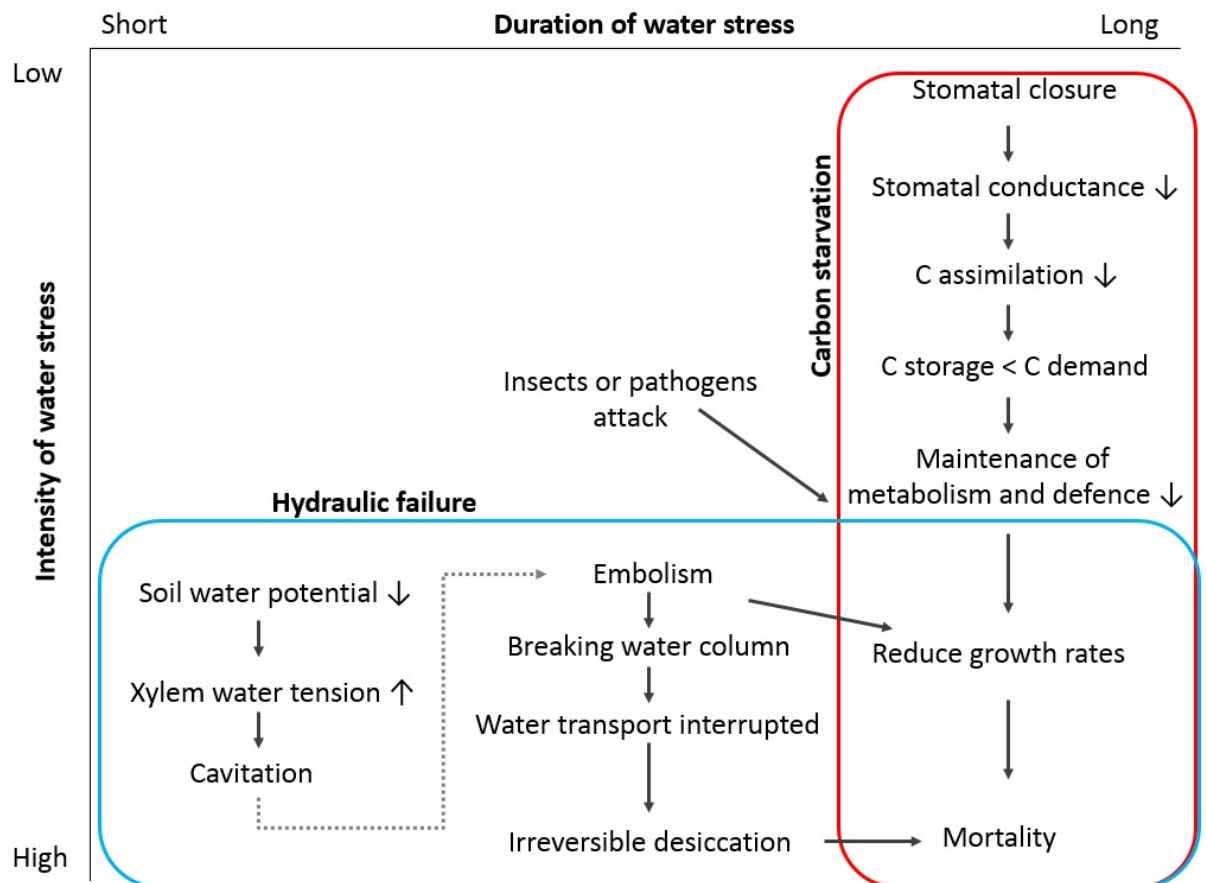


Figure 1. 3 Hypotheses on tree mortality mechanisms under drought conditions: Hydraulic failure vs. Carbon starvation. Physiological responses based on the relationship between duration of water stress (length of dry season) and intensity of water stress (continuous decrease in water availability). Adapted from (McDowell et al., 2008)

1.6 Xylem embolism resistance and Hydraulic safety margins

Hydraulic properties are central to current modelling efforts to mechanistically describe changes in vegetation function under drought (Christoffersen et al., 2016; Sperry et al., 2017; McDowell et al., 2018). Hydraulic traits integrate the whole plant performance, but the difficulty to measure them has called them “hard traits” and limiting our broad understanding of their variation across species and in a broad scale (Anderegg et al., 2016; Skelton et al., 2019)

The ability of plants to resist to water stress has been then commonly associated with embolism resistance (Ψ_{50} and Ψ_{88}) and the distance that the plants are to reach these thresholds (HSM – Hydraulic Safety Margins) (Delzon and Cochard, 2014; Rowland et

al., 2015; Anderegg et al., 2016; Choat et al., 2018; Barros et al., 2019). Frequently used metrics of xylem resistance to embolism are the xylem pressure at which 50% and 88% of conductivity is lost (Ψ_{50} and Ψ_{88} , respectively) (Sperry et al., 1988). Ψ_{88} represents more a lethal limit for angiosperm (Urli et al., 2013a; Choat et al., 2018). HSM, which is the difference between water potential in the peak of the dry season (Ψ_{\min}) and embolisms resistance (Ψ_{50} , Ψ_{88}), integrates whole-plant functioning and hydraulic strategies, as it integrates xylem tissue characteristics, environmental characteristics, rooting depth and stomatal control (Choat et al., 2012; Delzon and Cochard, 2014; Choat et al., 2018).

It has been suggested by a model based study that shown that plants tend to operate at water potentials close to the values causing xylem dysfunction (Tyree and Sperry, 1988). Indeed, a global meta-analysis has shown that worldwide, all biomes have equally narrow safety margins, indicating that Mediterranean and wet Tropical rainforest are equally vulnerable to drought (Choat et al., 2012). This finding could possibly explain the large global drought induced mortality. The knowledge of hydraulic properties of Amazonian trees expanded remarkably in the past few years (Rowland et al., 2015; Powell et al., 2017; Brum et al., 2018; Santiago et al., 2018; Oliveira et al., 2018; Fontes et al., 2018). However this increasing understanding is yet limited to a relatively few species from few locations in Central-Eastern Amazonia. A broader study which encompass the whole Amazon Basin and all its diversity, climate and geographical differences has been still needed

1.7 Methods to measure xylem vulnerability to drought

Xylem vulnerability curves are a commonly used approach to measure xylem vulnerability to embolism (Sperry et al., 1988, Cochard et al., 2013). These curves consist of the establishment of a relationship between xylem conductance loss and the dryness of xylem tissue, measured as the xylem water potential. There are many ways to generate xylem vulnerability curve, which vary in how embolism is induced and quantified.

Usual methods to induce embolism formation are the bench dehydration technique (Sperry et al., 1988), air injection (Cochard et al., 1992; Sperry & Saliendra, 1994) and centrifuge (Holbrook et al., 1995; Pockman et al., 1995). In literature, the most frequent method to assess embolism formation is the percentage loss of conductivity (PLC),

through hydraulic detection of embolism (Sperry et al., 1988). This technique has been widely used and directly measures xylem conductivity. However, it is time consuming, requires a vast amount of botanic material, as several stems have to be used for each curve (Choat et al., 2010), and to guarantee that the segment has two end walls, the sample has to be two times longer than the maximum vessel length.

Recently an alternative Pneumatic method has been developed (Pereira et al., 2016; Bittencourt et al., 2018). This method consists of measuring the air discharge from terminal branch ends, as the water stress increases (Fig.1.4 and Fig.1.5). The pneumatic method is an inexpensive, portable and very fast way to measure xylem emboli-formation and only one branch is used per curve, being a much less destructive approach than using flow meters, for example. Another advantage of this method is that the used branch does not need to be longer than the maximum tree vessel length, representing a good alternative for long-vesseled species. Pereira et al. (2016) tested for differences in air discharge of branches longer or shorter than the maximum vessel length and did not find differences. This method, which is an indirect measure of xylem conductivity, has been shown to have a good agreement with the used of flow meters for tropical (Bittencourt et al., 2016) and temperate species (Zhang et al. 2018).

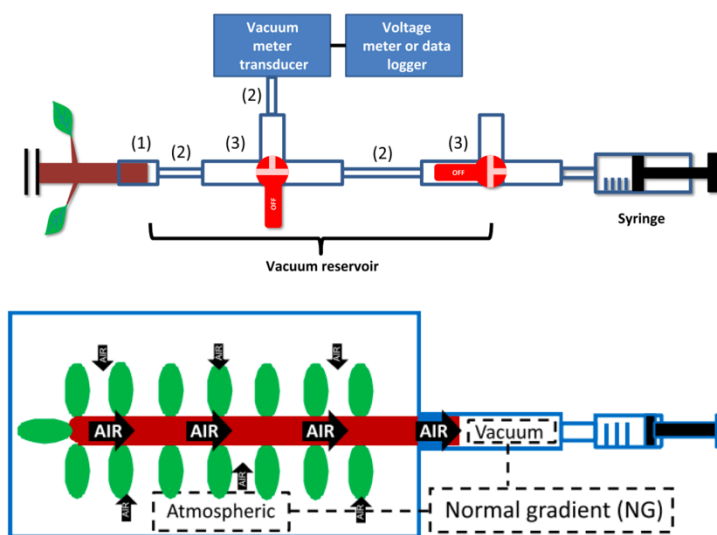


Figure 1.4 Schematic figure showing the pneumatic apparatus: which measures the amount of air discharge from a terminal branch end. At each dehydration state, the vacuum reservoir, created with a syringe, extracts the air formed inside the branch, as a result of embolised vessels. A vacuum meter transducer and voltage meter connected to the system then measures the amount of air discharge from the branch.

One unique branch is used in the entire process, since the most hydrated to the most dehydrated point (Figures from Pereira et al., 2016).

This technique represents a very good alternative to evaluate embolism resistance of trees in remote places with basic infra-structure. In this thesis, I therefore used this Pneumatic method combined with bench dehydration technique. In support to this choice, recent advances in the understanding of local scale Amazonian embolism resistance have been made using the same technique (Brum et al. 2018; Oliveira et al., 2018; Barros et al. 2019). A selection of xylem vulnerability curves is shown in the figure below (Fig. 1.5). The time spent to obtain each curve varied from three to eleven days, depending on the analyzed species and environmental conditions of each sites.

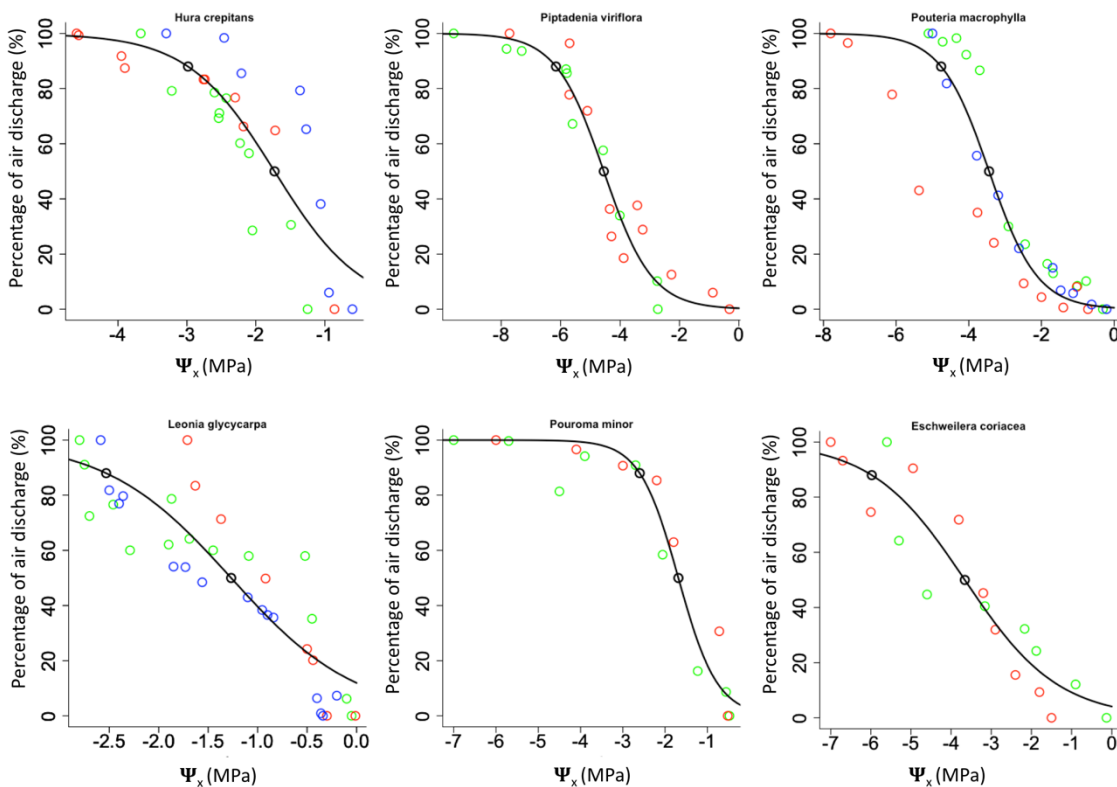


Figure 1.5 Examples of vulnerability curves. PAD represents the Percentage of air discharge as a function of xylem water potential decrease(Ψ_x). Different colours represent different individuals. Black open circles show the xylem water potential on which 50 and 88% of the conductance is lost (Ψ₅₀ and Ψ₈₈).

1.8 Thesis aims

The first chapter shows how heterogeneous Amazon forest is, how climate is changing over the past years and how drought events have impacted Amazon dynamics and compositions. This chapter has also shown the importance of tree hydraulic properties on integrating whole plant functioning and on underlying vulnerability to water stress worldwide. Despite of the importance of these properties, they are still poorly understood in the biggest and most diverse tropical forest on earth. The aim of this thesis is then to better understand the hydraulic sensibility and vulnerability across Amazonian forests.

1.9 Thesis objectives

Objective 1: Evaluate regional patterns of hydraulic traits variation across Amazonian forests.

1.1 Measure embolism resistance and minimum leaf water potential of Amazonian tree species across a broad precipitation and soil properties gradient.

1.2 Combine data collected during my PhD with data collected by collaborators and published data, which used the same standardized methodology, providing the first pan-Amazonian hydraulic traits dataset.

1.3 Investigate embolism resistance and hydraulic safety margins variation within and across Amazonian forests.

1.4 Test for relationships between community-weighted mean trait values and environmental variables (water availability, soil total phosphorus and soil texture)

1.5 Assess whether there is a relationship between hydraulic traits and aboveground biomass change at community level

Objective 2: Investigate within taxa (species/genus/species) variation of Amazonian tree embolism resistance

2.1 Investigate whether embolism resistance is phylogenetic conserved across in Amazonian tree taxa.

2.2 Test whether there are specific taxonomic group contributing more to the phylogenetic signal than others.

2.3 Assess embolism resistance variation across the most widely distributed families in our dataset.

2.4 Evaluate difference in embolism resistance among Fabaceae and Non-Fabaceae within and across Amazon forests and across tropical forests.

2.5 Using single censuses from forest plot inventories across Amazonia and the result from topic 2.1, calculate the community-weighted mean embolism resistance and construct a map of Amazonian embolism resistance.

2.6 Test for differences in embolism resistance between clades that normally present vestured pits and clades on which this structures are consistently absent.

Objective 3: Validate the predictive power of Amazonian tree species hydraulic traits to explain species biogeographical distribution, life-history strategy traits and drought induced mortality.

Investigate the extent on which embolism resistance and hydraulic safety margins are related to:

3.1 species bioclimatic affiliation (Water deficit affiliation –WDA) across Western Amazon tree species;

3.2 pan-Amazonian tree species life-history traits;

3.3 species mortality under drought.

Chapter 2: Variation in drought vulnerability across Amazonian forests

Abstract

Tropical forests face substantial climate risk due to increased drought frequency and elevated temperatures, yet our ability to predict their response to climate change is limited by poor mechanistic understanding of their capacity to resist water stress. Determining the thresholds at which plant xylem becomes blocked by gas bubbles (emboli), alongside how close plants operate to these thresholds under current climate conditions (hydraulic safety margins - HSM) is essential for quantifying hydraulic stress and drought-induced mortality risk. Remarkably little is known about if, how, and why these properties vary across Earth's largest and most biodiverse tropical forest. Here I present the first pan-Amazonian, fully standardized hydraulic traits data-set to assess variation in drought sensitivity across Amazonia. Whereas previous studies have highlighted convergence in drought vulnerability in forests globally, I document highly variable patterns in embolism resistance and HSM across Amazonian forests. Soil texture and biogeography play an important role in explaining this variation. Forests on clay soils and seasonal Central-Eastern forests have informed all of our mechanistic understanding to date about the drought risk to Amazon forests. Yet, our analyses show these forests are less vulnerable to drought and are better placed to cope with future climate than those on sandy soils and in Western and Southern Amazonia. Finally, I find that forests with low HSM are already gaining less biomass than those with higher HSM, suggesting that future climate-induced reductions in HSM may substantially reduce the Amazon carbon sink.

2.1 Introduction

Amazonia remains the most extensive, complex and diverse tropical forest in our planet. As a result, Amazon forests are critically important in the Earth System, housing approximately 16,000 species of trees (Ter Steege et al., 2013), storing >100 Pg of carbon in their biomass (Feldpausch et al., 2012) and regulating climate, by virtue of their substantial exchanges of carbon, water and energy with the atmosphere (Nobre et al., 2016). Amazon forests are, however, critically dependent on climate, particularly temperature and rainfall, and therefore likely to be especially vulnerable to climatic changes. Recently, recurrent drought events across Amazonia have resulted in substantially elevated tree mortality (Phillips et al., 2009) and may be partially responsible for the long-term decline of the Amazon carbon sink (Brienen et al., 2015). Water stress over Amazonian forests is likely to intensify under future climate as a consequence of increasing temperatures, altered rainfall regimes and increased frequency of extreme events (Duffy et al., 2015). Thus, an understanding of the hydraulic vulnerability of these forests is of paramount importance.

A large body of evidence points to hydraulic failure, defined as progressive loss of whole plant conductance due to embolism of xylem vessels, as a key mechanism underpinning drought-induced mortality (Rowland et al., 2015; Anderegg et al., 2016; Adams et al., 2017; Choat et al., 2018). The vulnerability of trees to hydraulic failure is closely related to their ability to resist xylem embolism formation and the proximity with which they operate to critical embolism thresholds (Adams et al., 2017; Choat et al., 2018). Commonly used metrics of embolism resistance include the xylem water potentials at which 50% and 88% of the stem hydraulic conductance is lost (ψ_{50} and ψ_{88}) (Choat et al., 2012; Anderegg et al., 2016; Choat et al., 2018). Hydraulic safety margins (HSM_{50} and HSM_{88}) integrate xylem resistance to embolism with stomatal responses to *in situ* atmospheric, soil water deficit, rooting depth and denote how close leaf water potentials in the field approximate ψ_{50} or ψ_{88} . These properties defining embolism resistance and hydraulic safety are central to current efforts to understand and mechanistically model changes in vegetation function under drought (McDowell and Allen, 2015; Christoffersen et al., 2016; McDowell, 2018).

A global meta-analysis has found convergence of hydraulic safety margins across forest biomes, suggesting that humid tropical rainforests are as vulnerable to

drought as dry forests in much more arid regions (Choat et al., 2012). In recent years, great advances have been made in understanding hydraulic properties of Amazonian trees (Rowland et al., 2015; Powell et al., 2017; Brum et al., 2018; Santiago et al., 2018; Oliveira et al., 2018; Fontes et al., 2018). However, these efforts have been limited to a relatively small number of taxa from four locations in Central-Eastern Amazonia, all within a broadly similar climate regime, and have been local in scale. A basin-wide perspective of how hydraulic properties vary across the breadth of Amazonian forests, which span the full range of geographic/climatic conditions and species composition, has thus far been lacking.

Here I assemble the first pan-Amazonian dataset of plant hydraulic properties, following a fully standardized methodology, and evaluate how vulnerability to drought varies across Amazonian tree taxa and forests. Our dataset includes hydraulic traits from 129 species across 11 sites in Western, Central-Eastern and Southern Amazonia, also including published data from one site (TAP) in Central-Eastern (Brum et al., 2018) (Fig. 2.1). Our sampling spans the entire Amazonian precipitation space and ranges from ecotonal forests at the biome edges experiencing <1200 mm of annual rainfall to aseasonal forests with close to 3000 mm of annual rainfall (Fig. A1. 1) and covers a range of soil conditions (Table A1. 1). In each site, our sampling effort was concentrated on adult dominant canopy and sub-canopy species. For each species at each site, I constructed xylem vulnerability curves, from which I calculated ψ_{50} and ψ_{88} , and measured minimum dry season leaf water potential (ψ_{\min} , $\psi < 0$), which was used to compute hydraulic safety margins ($HSM_{50} = \psi_{\min} - \psi_{50}$ and $HSM_{88} = \psi_{\min} - \psi_{88}$). Collectively, the species sampled account for ~24% of total Amazon tree biomass (Fauset et al., 2015) and encompass a wide array of life-history strategies (Coelho de Souza et al., 2016) (Fig. A1. 2). I use this dataset to test whether there is a pan-Amazonian convergence in drought vulnerability and assess the extent to which background water availability, biogeographic region and soil features drive variation in drought resistance.

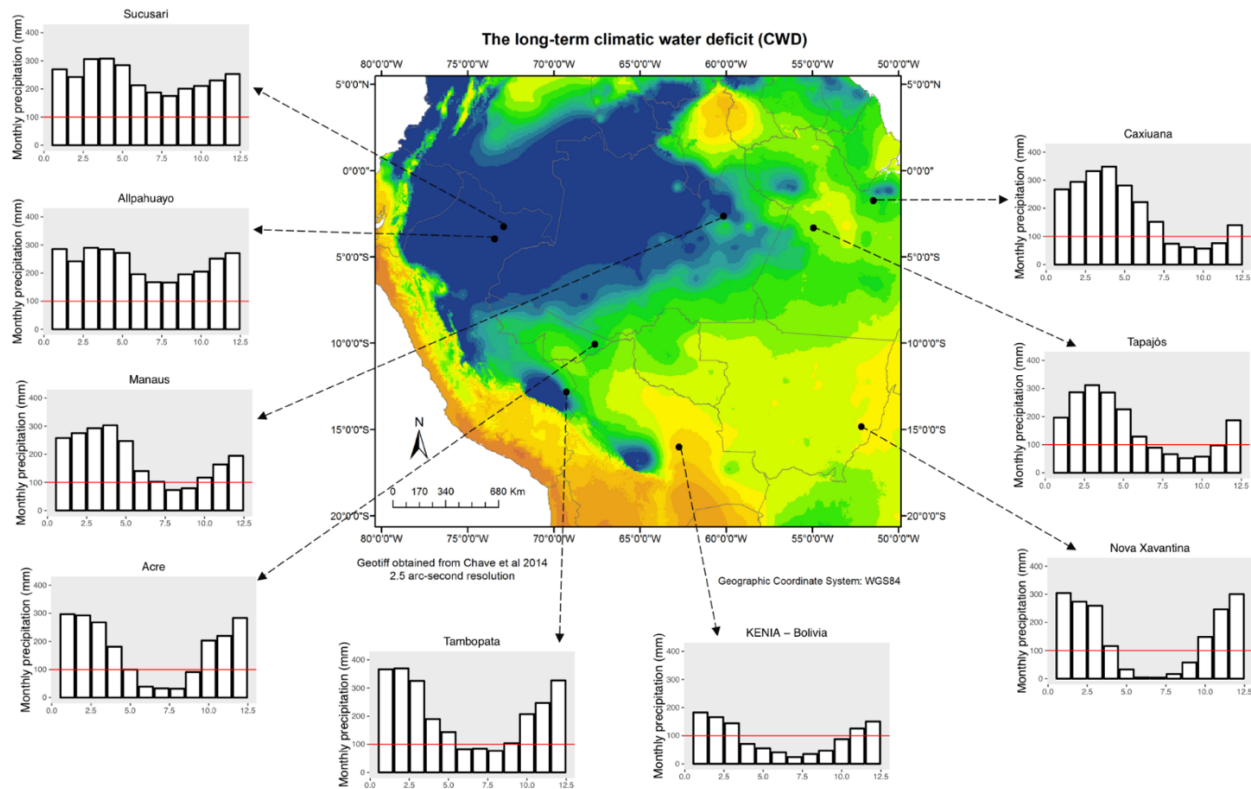


Figure 2. 1 Sampled sites: spatial distribution and climatological variation. Long-term climatic water deficit Geotiff obtained from (Chave et al., 2014) (2.5 arc-second resolution). Each graph shows the average of accumulated precipitation per month (1960-2015) per site. Precipitation data were obtained from CRU (Climatic Research Unit) at 0.5o spatial resolution. Western sites: Sucusari (SUC), Allpahuayo: (ALP-1 and ALP-2), Acre (FEC), Tambopata (TAM), Kenia (KEN-1 and KEN2); Southern site: Nova Xavantina (NVX); Central-Eastern sites: Tapajós (TAP), Caxiuana (CAX), Manaus (MAN).

We grouped plots into 3 forest types, based on their dry season length (DSL): (1) transitional/ecotonal forests with dry season length (DSL, equivalent to the number of consecutive months where long-term mean precipitation is less than 100 mm) ≥ 5 months, (2) seasonal forests with DSL ranging from 2 to 5 months and (3) aseasonal forests with no dry season (Fig. A1. 1) and tested for differences among them in embolism resistance and hydraulic safety margins. Based on previous global analyses (Choat et al., 2012), I expected xylem resistance to embolism formation to increase (*i.e.* I expected ψ_{50} and ψ_{88} to become more negative) from aseasonal to transitional forests but expected safety margins (HSM_{50} and HSM_{88}) to converge across forest types. Within individual forest types, I further tested for differences in embolism resistance and hydraulic safety margin between plots located in different biogeographical regions of the Amazon (Western Amazon vs. Central-Eastern Amazon for seasonal forests and Western Amazon vs. Southern Amazon for transitional forests). Additionally, to examine climate and soil controls on community-level embolism resistance and hydraulic safety margins, I constructed multiple regression models with maximum cumulative water deficit (MCWD – a well-established metric of background water availability), soil fertility status (total soil phosphorus - P_{Total}) and texture (% clay) as predictors. Finally, I explore whether hydraulic traits are related to long-term biomass change at community level, by combining hydraulic traits with forest dynamics data from the fully standardized RAINFOR forest inventory network within which our sampling is nested (Malhi et al., 2002).

2.2 Methods

2.2.1 Site description: I assemble the first pan-Amazonian data-set of the key hydraulic traits (ψ_{50} , ψ_{88} , HSM_{50} , HSM_{88}), including 129 species distributed across 11 forest sites. The sites are old-growth lowland forests (below 1,000 m of elevation), with no evidence of significant human disturbance, located in the Western, Central-Eastern and Southern Amazonia. They were specifically chosen to span the full Amazonian precipitation gradient and to encompass the major axes of variation in soil conditions and species composition in Amazonia. Mean annual precipitation varied from ~ 1100 to ~ 2900 mm yr⁻¹ and Mean Maximum Cumulative Water Deficit (MCWD) varied from -400 to -11 mm across sites. Soil texture varied sixfold across sites (from 16 to 90% Clay) and soil fertility varied 13-fold (P_{total} ranged from 37 to 478 mg kg⁻¹). Sites are classified

biogeographically using large-scale Amazon divisions (Lopez-Gonzalez et al., 2009; Lopez-Gonzalez et al., 2011). Summary information for all sites can be found in the supplementary material (Table A1. 1 and A1. 2).

2.2.2 Community representativeness: The sampling effort at each site varied from 7 to 25 species and sampled area, from 14% to 75% of the total basal area (Table A1. 2). The sites which I sampled less than 30% of the total basal area (ALP1, ALP2, SUC, CAX, MAN) are hyperdiverse forests and lack clear species dominance (*i.e.* where there are not few species contributing to most of the total basal area of the plot). The site on which ~14% of the total basal area was sampled is MAN in this dataset. It has been shown that for this 3.6 ha site, the sampled area basal coverage is likely to be representative of this community (Barros et al., 2019). Barros et al. (2019) has demonstrated community weighted mean (CWM) values are not likely to differ from community mean values if: (1) Species dominance is not driven by a few species, (2) traits have low dispersion around the mean (*ie.* low standard deviation compared the mean), (3) traits are randomly distributed across species dominance. In fact, Barros et al. (2019) incorporated to MAN site extra data of 28 species from another forest in Central-Eastern Amazon to test whether increasing the sample size would change CWM and mean values. Comparing the original and increased sample size, they find no significant differences in mean and CWM values were observed, indicating that the adopted sampling strategy was sufficient to represent that community. For the other 4 sites on which sampled coverage was less than 30%, these lack dominance by a few taxa (cumulative dominance of the 5 most dominant species at ALP-1 is 27.9%, ALP-1 26.2%, SUC 15.0% and CAX 10.7% (Table A1. 2). In terms of variance, for the referred sites, the standard deviations are 0.39-0.43 the P88 mean and 0.63-0.81 the HSM₈₈ mean (Table A1. 2). I also show that there is no relationship between species dominance and any hydraulic trait at any site (Table A1. 5). Thus, our CWM trait values found for the 11 sites are likely to well represent the evaluated communities.

2.2.3 Abiotic data: To characterize background water availability at each site, I calculated the Maximum Cumulative Water Deficit (MCWD), which is a measure of cumulative meteorologically-induced water stress experienced within an average year (Aragão et al., 2007). I firstly calculated the monthly water deficit (wd_n), as the difference between precipitation (P) and evapotranspiration (E) in each month n . Precipitation data

were obtained from the Climatic Research Unit (CRU TS 3.23) at 0.5° spatial resolution from 1960 to 2015 (Harris et al., 2014). Evapotranspiration was assumed at 100 mm per month, in line with previous studies (Aragão et al., 2007). MCWD was computed for each year as the maximum monthly cumulative water deficit (CWD) as follows:

$$\begin{aligned}
 wd_n &= P_n - E_n; && \text{Equation (1)} \\
 \text{if } CWD_{n-1} + wd_n &> 0; \\
 \text{then } CWD_n &= 0, \\
 \text{else } CWD_n &= CWD_{n-1} + wd_n
 \end{aligned}$$

As all our plots are in the southern hemisphere their hydrological year coincides with the calendar year, which allow us to start our MCWD calculations at the beginning of each calendar year. For statistical analyses, I use the mean MCWD calculated from 1960 to 2015 in the CRU TS 3.23 dataset.

Soil texture and fertility data for each site (Table A1. 1) were obtained from published sources (Ruivo et al., 2007; Quesada et al., 2010; Araujo-Murakami et al., 2014; Malhi et al., 2015) or via the ForestPlots.net database (Lopez-Gonzalez et al., 2011) (Quesada and Lloyd – unpublished data). More information is available in Table A1. 1.

2.2.4 Species selection and collection of plant material: To characterize drought sensitivity across a wide set of species and strategies, I sampled the most dominant adult canopy and sub-canopy tree species at each of the 11 sites. For one of these sites (TAP), I used published data which follows the same methodology of this study (Brum et al., 2018). One fully sun-exposed top canopy branch (or branch at the maximum height reachable by climbers) was collected from, on average, 3 individuals of each species at each site. Data collection was undertaken during the wet season, when forests were maximally hydrated. Branches (>1 m long) were harvested during predawn or very early in the morning, to capture a fully hydrated starting point. Immediately after collection, basal portions of branches were wrapped with a wet cloth and branches were placed in a humidified opaque plastic bag to avoid desiccation during transport. Bags were sealed and carried to the field station for determination of xylem vulnerability curves. For samples not collected during the predawn, branches were placed in a bucket, re-cut under water, covered with an opaque plastic bag and let to rehydrate for at least 5 hours.

2.2.5 Xylem embolism resistance (ψ_{50} or ψ_{88}): To quantify xylem resistance to embolism of Amazonian trees species, I focused on the water potentials associated with a 50 and 88% loss of hydraulic conductance (ψ_{50} or ψ_{88}), given the wide use of these metrics as critical embolism resistance thresholds (Urli et al., 2013a; Adams et al., 2017; Choat et al., 2018). To derive these parameters, I constructed xylem vulnerability curves by simultaneously measuring percentage loss of xylem conductance (PLC) and xylem water potential under progressive desiccation (Sperry et al., 1988). I estimated PLC using the pneumatic method of Pereira et al. (2016) (Pereira et al., 2016; Zhang et al., 2018; Bittencourt et al., 2018), which quantifies the air extracted from within branches at each stage of dehydration and expresses this as a percentage of the difference between the maximum amount of air removed under extreme dehydration (100% PAD) and the minimum amount removed under maximum hydration (0%PAD). The initial PAD measurement for each branch was made immediately after unbagging the branch from a sealed opaque plastic bag to ensure that vulnerability curves commenced from a maximally hydrated state. Subsequent measurements were then conducted successively throughout the desiccation process, with approximately 8-10 measurements per individual used to construct each curve. Branches were progressively dried through the bench dehydration technique (Sperry et al., 1988). The dehydration process varied from sites and species, varying from 10 -15 minutes for the most hydrated points to 60-180 minutes for the most dehydrated ones. Between each desiccation state, branches were bagged for a minimum of one hour to equilibrate leaf and xylem water potentials. Leaf water potential (used as a proxy for xylem water potential following equilibration) was measured with a pressure chamber (PMS 1505D and PMS 1000, PMS instruments).



Figure 2. 2 Equipment use to construt the vulnerability curves. **A:** Pneumatic apparatus to assess air discharge from the drying branch terminal end; **B:** Pressure chamber to assess leaf/xylem water potential.

We used the exponential sigmoidal function of Pammenter and Willigen (1998) to calculate ψ_{50} for each species at each site:

$$PAD = \frac{100}{1 + \exp\left[\frac{S}{25} (\psi_x - \psi_{50})\right]} \quad \text{Equation (2)}$$

where PAD = Percentage of air discharge (%); S = Slope of the curve; ψ_x = xylem water potential (MPa) and ψ_{50} is ψ_x corresponding to a PAD of 50%⁴⁴.

Following Domec and Gartner (2001), I computed ψ_{88} as:

$$\psi_{88} = \psi_{50} - \frac{2}{\left(\frac{S}{25}\right)} \quad \text{Equation (3)}$$

2.2.6 In situ leaf water potential and hydraulic safety margins (HSM₅₀, HSM₈₈): To calculate how close Amazonian trees operate to critical embolism thresholds in nature, I measured *in situ* minimum leaf water potential (ψ_{\min}). I sampled 2-6 top-canopy fully expanded and sun-exposed leaves per individual between 11:00-2:30. ψ_{\min} was measured with a pressure chamber (PMS 1505D and PMS 1000, PMS instruments) and the value averaged per individual. This method provides conservative estimates of plant water stress, because of pressure drops in transpiring leaves. Apart from aseasonal forests, which have no climatological dry season (monthly_{precip} < 100mm), data collection took place in the peak of dry season (Fig. A1. 6). For each species at each site I calculated the Hydraulic Safety Margins with respect to critical embolism thresholds (HSM₅₀, HSM₈₈), as the difference between species-level ψ_{\min} , taken as the minimum ψ_{\min} value of all individuals for that species, and ψ_{50} or ψ_{88} .

Due to logistical limitations, ψ_{\min} was measured as described above: as one point in time for each individual, in line with other studies (e.g. Choat et al. 2012, Brum et al., 2018, Barros et al., 2019). This lack of continuous measurements of *in situ* leaf water potentials is likely to underestimate the true minima for ψ_{\min} and, consequently, underestimate the hydraulic safety margins.

2.2.7 Statistical Analysis: To examine the distribution of hydraulic traits (ψ_{50} , ψ_{88} , HSM₅₀ and HSM₈₈ – Fig.1) across Amazonian tree taxa (N=129 species), trait values

were averaged for species occurring at multiple sites. I conducted statistical analyses to investigate differences in species-level hydraulic trait values among different forest types and geographical regions and also to evaluate controls on community-weighted mean hydraulic traits across the study sites. The field study sites consist of 11 forest sites across 3 different forest types, here classified according to their climatic regime. At one extreme, there are transitional/ecotonal forests, adapted long water shortage, with dry season length (DSL) equal or greater than 5 months, Mean annual precipitation (MAP) less than 1700 and a Maximum cumulative water deficit (MCWD) of less than -375mm. At the other extreme, there are aseasonal forests, which experience DSL ~ 0 months, MAP greater than 2800mm and MCWD greater than -15mm. In between, there are forests adapted to intermediary seasonality (seasonal forests), which experience DSL ranging from 5 to 2 months, MAP between 1980-2540mm and MCWD varying from -255 to -115mm (Table A1. 1).

To test for statistical differences in hydraulic traits across forest types, I performed one-way ANOVA, followed by Tukey HSD *post hoc* tests. ψ_{88} values were cubic-root transformed before statistical analysis to satisfy the assumption of normal distribution of residuals. To test for differences between biogeographical regions within seasonal (Western Amazonia vs. Central-Eastern Amazonia) and transitional forests (Western Amazonia vs. Southern Amazonia), I performed Wilcoxon rank sum tests. For all analyses, I assume a significance level of 0.05.

We used the community weighted mean (CWM) to describe the central tendency of tree community trait values at each site (Diaz et al., 2007). The CWM for each trait was calculated by weighting the trait value (X_i) of each species sampled (s) by its relative dominance (species basal area divided by the plot total basal area) in each study plot (W_i) (Pla et al., 2012):

$$CWM = \sum_{i=1}^s W_i * X_i \quad \text{Equation (4)}$$

To evaluate whether CWM hydraulic traits were related to maximum climatological water deficit (MCWD), soil texture (% Clay) or fertility (Total phosphorus), I performed simple and multiple linear regression models. Regression models were also conducted with mean annual precipitation (MAP) and dry season length

(DSL), instead of MCWD. I compared the different models based on their Akaike Information Criteria (AIC), smaller AIC values represent better model fit, model fit was considered different when they differ by more than 2 AIC units. Due to lack of P_{total} information, the southern Amazonian site of Nova Xavantina (NVX) was excluded from models which consider P_{total} as predictor. I used Kendall's tau correlation to test for correlations between predictors.

We performed standard major axis (SMA) regressions to investigate whether there is a relationship between hydraulic traits and long-term biomass dynamics at plot-cluster level. I analysed mean biomass net change of 8 clusters of forest plots from the RAINFOR network (Malhi et al., 2002) curated at ForestPlots.net database (Lopez-Gonzalez et al., 2011) and compare to CWM trait values. While each cluster includes the plots that I sampled directly for hydraulic traits, the combined RAINFOR sample spans a total of 46 long-term monitoring plots – all lacking a history of recent disturbance and with similar structure and composition to the sampling plots. Biomass data per plot per census were extract from ForestPlots.net database (Lopez-Gonzalez et al., 2009; Lopez-Gonzalez et al., 2011), using the Chave Moist equation to calculate biomass (Chave et al., 2014) and the Weibull equation at a regional level to calculate height following (Feldpausch et al., 2012).

We calculated the above ground biomass (AGB) annual net change per plot as ABG_{change} ($AGB_{\text{final census}} - AGB_{\text{initial census}}$) in Mg dry weight per hectare divided by $\text{Census}_{\text{length}}$ ($\text{Date}_{\text{final census}} - \text{Date}_{\text{initial census}}$) in years. I only considered plots with at least 5 years census interval. I then averaged annual net change and CWM traits values per cluster. I excluded KEN plots from this analysis because of fire event that reached the region in 2004 (Araujo-Murakami et al., 2014). Table A1. 6 shows the summary information per cluster.

2.3 Results and Discussion

Hydraulic trait distribution across Amazonian tree taxa

Xylem embolism resistance varies 15-fold across Amazonian rainforest species (ψ_{50} range: -5.02 to -0.33 MPa, ψ_{88} range: -7.14 to -0.52 MPa) but is negatively skewed, with >60% of all species having ψ_{50} between 0 and -2 MPa (Fig. 2.3). Hydraulic safety margins related to ψ_{50} also vary considerably across species (HSM₅₀: -2.52 to 3.41 MPa),

but are heavily clustered around zero. Approximately 40% of sampled taxa tolerate leaf water potentials beyond ψ_{50} (negative HSM_{50}) and a further 45% operate within a restricted HSM_{50} of 0 to 1 MPa.

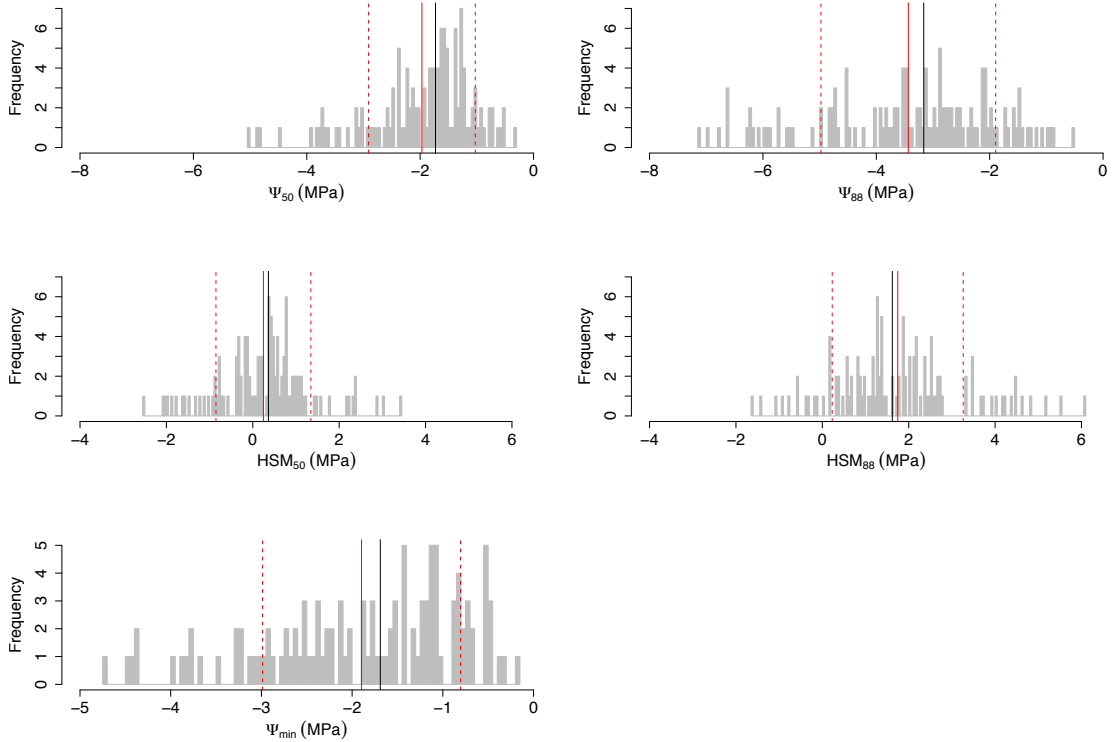


Figure 2.3 Hydraulic traits distribution across Amazonian tree taxa. a) and b): species mean xylem water potential at which 50% (ψ_{50}) and 88% (ψ_{88}) of the conductance is lost (N=129 tree species). c) and d): species mean hydraulic safety margins related to ψ_{50} (HSM_{50}) and ψ_{88} (HSM_{88}), respectively (N=113 tree species). Red, black and dashed lines show, respectively, the mean, median and standard variation value of each trait.

Furthermore, over two-thirds of all taxa operate within 1 MPa of the much more severe ψ_{88} threshold (mean HSM_{88} : 1.70 MPa, range: -1.64 to 6.08 MPa). Moreover, even with respect to this very risky threshold, I find that ~10% of taxa studied had negative HSM_{88} . I focus primarily on ψ_{88} and HSM_{88} as this is considered to represent a more lethal embolism threshold in angiosperms than ψ_{50} (Urli et al., 2013a; Choat et al., 2018). Results for ψ_{50} and HSM_{50} are broadly similar to those of ψ_{88} and HSM_{88} and are presented in the supplementary information.

Variation in Embolism Resistance across Amazonian Forests

My analyses suggest a strong overarching effect of background water availability on xylem resistance to embolism across Amazonian forests. Significant differences in species-level resistance to embolism are found across forest types (Fig. 2. 4). As expected, aseasonal wet forests have the least resistant xylem (least negative ψ_{50} and ψ_{88}), with seasonal and transitional forests having trees with more resistant xylem tissue (most negative ψ_{88}). Seasonal and transitional forests also display greater variation in embolism resistance, as indicated by their broader interquartile range in ψ_{88} , compared to aseasonal forests (1.4 MPa).

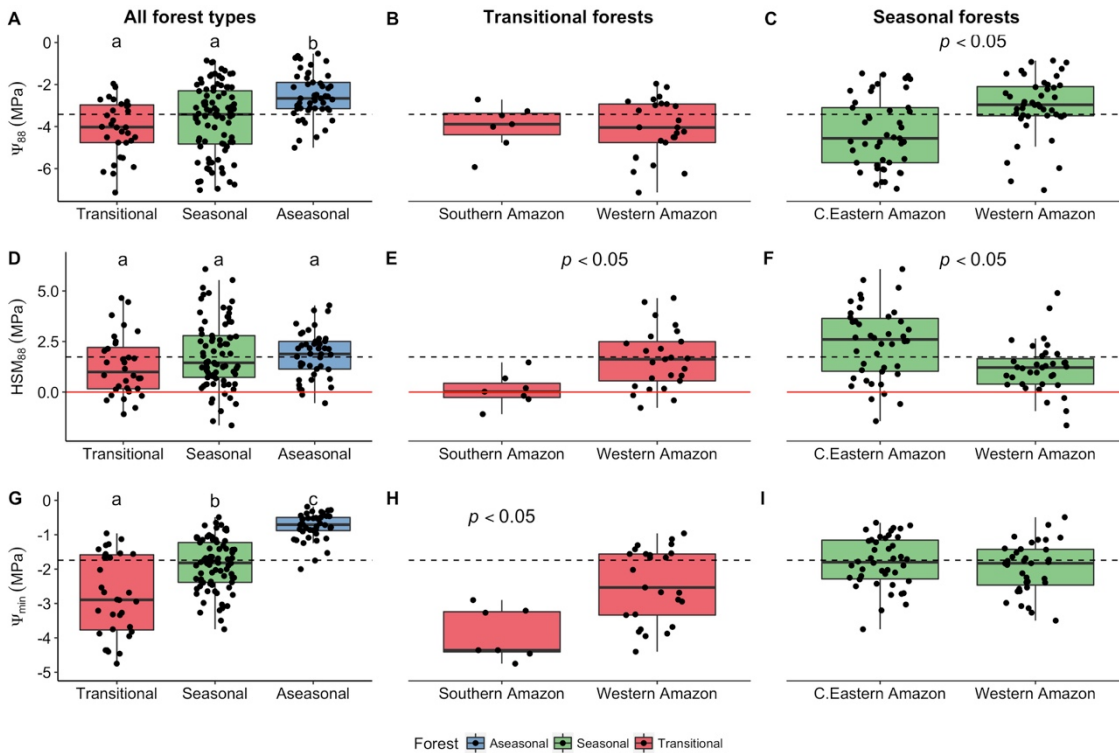


Figure 2. 4 Hydraulic traits variation within and across Amazon forest types. A, D) and G) Hydraulic traits variation across all three forest types, B), E) and H) Hydraulic traits variation within transitional forests (red). C), F) and I) Hydraulic traits variation within seasonal forests (green). A), B) and C) xylem water potential on which 88% (ψ_{88}) of the conductance is lost. D), E) and F) hydraulic safety margins related to ψ_{88} (HSM₈₈). G), H) and I) minimum leaf water potential (ψ_{min}) Dashed lines show the mean value of each trait across all tree taxa. Red line, the hydraulic safety margins equal to zero. Significant differences at $p < 0.05$ are shown by letters above each boxplot (panels A) and D): Anova and Tukey HSD *Pos Hoc*) or displayed on the figure (panels B), C), E), F): Wilcoxon rank sum tests). ψ_{88} values for were cubic-root transformed to meet the assumption of normal distribution of the errors (A). Each point represents one species per site.

Transitional, seasonal and aseasonal forests encompass 3, 5 and 3 forest sites, respectively.

Across all sites, community-weighted mean embolism resistance, which accounts for the relative basal area dominance of sampled tree taxa, is strongly related to MCWD (Fig. 2. 5). This alone explained 54% of the observed variation in ψ_{88} (and 68% of the variation in ψ_{50} , Table A1. 3). However, I find substantial variability in embolism resistance across seasonal forest sites, both in terms of species-level and community-weighted mean values. Despite similar background MCWD, species in seasonal Central-Eastern Amazon forests have markedly more resistant xylem than their Western Amazonian counterparts (Fig. 2. 4). Indeed, while resistance to embolism of seasonal forests in Western Amazonia ($\psi_{88} = -3.02 \pm 0.21$ MPa) is similar to that of aseasonal forests ($\psi_{88} = -2.55 \pm 0.15$ MPa), the seasonal forests in Central-Eastern Amazonia ($\psi_{88} = -4.28 \pm 0.25$ MPa) have the most resistant xylem of all forests in our database. Central-Eastern Amazonian forests also have very high within-site variability in embolism resistance – *e.g.* the Caxiuanã (CAX) and Manaus (MAN) sites are the most hydraulically diverse (the broadest ψ_{88} interquartile range) in the entire database (Fig. A1. 4).

Hydraulic Safety Margins across Amazonia

Statistically, there is no significant difference in HSM_{88} across climatically defined forest types (transitional, seasonal and aseasonal) (Fig. 2. 4). Furthermore, I find no relationship between community-weighted HSM_{88} and MCWD across forest plots (Fig. 2. 5). Similarly, no relationship is found between HSM_{88} and mean annual precipitation or dry season length (Table A1. 3). These overarching results are in line with previous findings from global meta-analyses which point to global convergence in drought vulnerability¹¹. However, they mask important differences within forest types. Seasonal forests in Central-Eastern Amazonia have considerably broader safety margins than those in Western Amazonia (Fig. 2. 4). Seasonal Central-Eastern Amazonian forests generally exhibit large within-site variation in hydraulic safety margins (Fig. A1. 4), as observed for embolism resistance metrics. For example, the Manaus site (MAN) effectively spans the entire range of hydraulic safety margins observed across the basin. Despite having similar embolism resistance, the transitional forests in our dataset diverge greatly in hydraulic safety margins (Fig. 2. 4). Transitional forests in Bolivia in the

western Amazon operate with a comparatively broad HSM_{88} ($HSM_{88}=1.63 \pm 0.28$ MPa). However, species-level HSM_{88} values for the only southern Amazonian transitional forest in our dataset (NXV, in the Brazilian state of Mato Grosso) centre around zero ($HSM_{88}=0.10 \pm 0.40$ MPa), with approximately half of the species measured operating at a negative HSM_{88} .

Across forest sites, I find soil texture to be a significant predictor of community-weighted HSM_{88} (Fig. 2. 5). A Kendall's tau test reveals no correlation among predictors (Table A1. 4). Thus, although variation in the measure of hydraulic architecture across Amazonia is largely governed by climate, the ultimate risk of hydraulic failure, as inferred from HSM_{88} is more influenced by soil conditions.

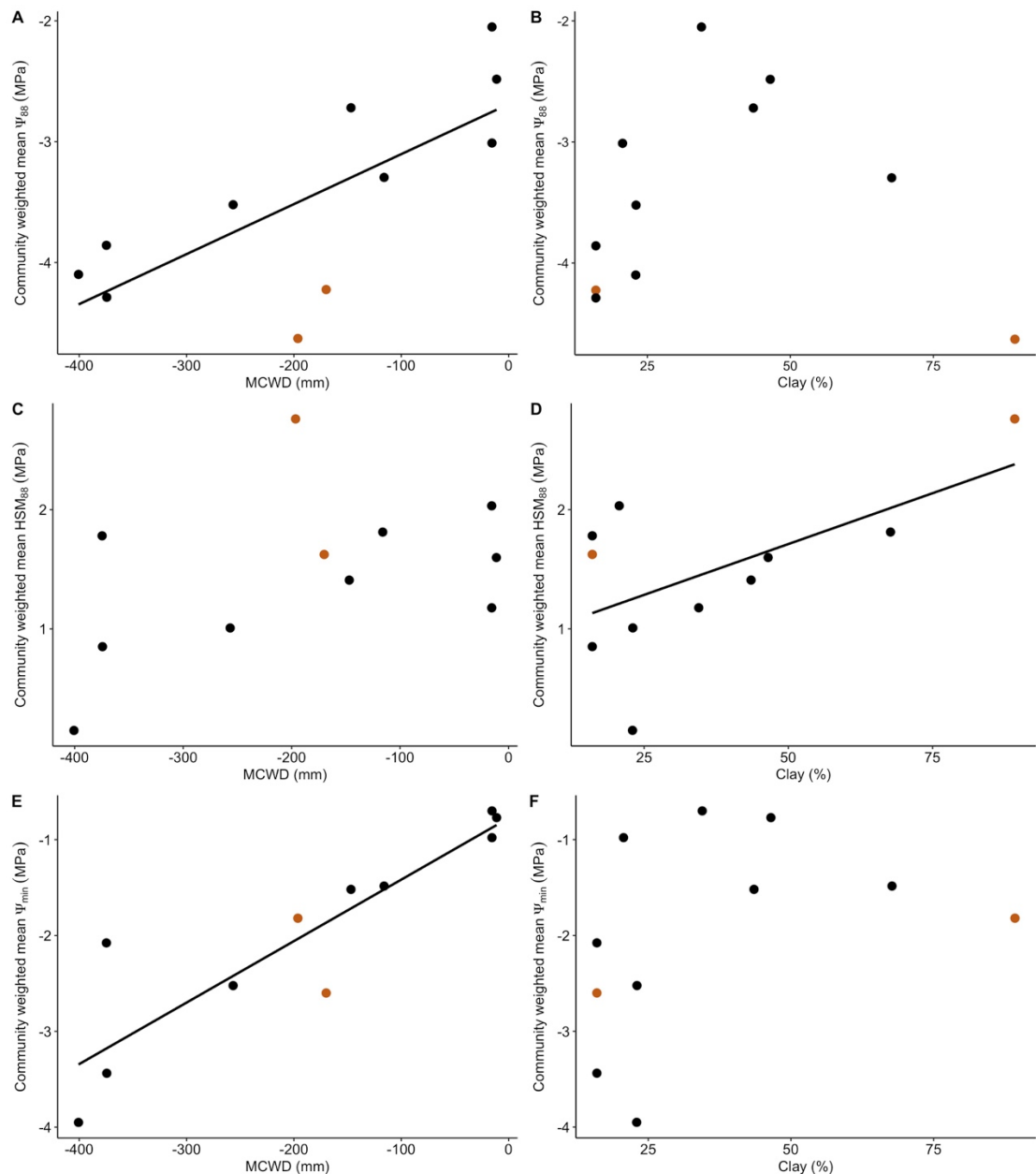


Figure 2. 5 Relationship between tree community hydraulic traits and environmental variables. A) and C) Community weighted mean ψ_{88} (xylem water potential on which 88% of the conductance is lost) and Community weighted mean HSM₈₈, respectively, in relation to Maximum Cumulative Water Deficit (MCWD), n=11; B) and D) Community weighted mean ψ_{88} and Community weighted mean HSM₈₈, respectively, in relation to Soil Clay Percentage, n=11. Significant linear relations are shown by regression line: A) R² = 0.54, p=0.01; D) R²=0.41, p=0.05 and E) R²=0.79, p<0.001. Further information available on Table A1. 3. Brown points show forest plots in drought experiment locations (TAP and CAX). Note that only data from control plots were used in these analyses.

Sites with high clay content have higher hydraulic safety margins. Amazonian clay soils have distinctly different water retention properties to their temperate

counterparts, being characterised by very low available water capacity (the amount of water released between soil matric potentials corresponding to field capacity and wilting point), despite absolute moisture content being relatively high (Hodnett et al., 1995; Hodnett and Tomasella, 2002; Oliveira Junior et al., 2010). For example, it has been previously shown that plant available water over the top 1m of soil in the sandy-soiled CAX site is over three times greater than in high-clay soil in the Manaus region (Fisher et al., 2008). My results suggest that this low plant available water in high clay soils has resulted in Amazonian plant communities with much more conservative water acquisition strategies and possibly tighter leaf water potential regulation than those found on soils with greater available water/lower clay content.

Plant communities with greater HSM might be expected to have more insurance against increasing climate stress than communities with lower HSM, as they are further away from critical embolism thresholds. Indeed, I find a strong positive relationship between HSM metrics and mean long-term aboveground biomass sink strength in clusters of forest plots across the Amazon (Fig. 2. 6, AGB_{sink} vs. HSM_{88} : $r^2 = 0.65$, $p=0.02$; AGB_{sink} vs. HSM_{50} : $r^2 = 0.72$, $p=0.008$). Thus, forests characterized by low community-level HSM are gaining less biomass than those with high HSM. No relationship is found between metrics of xylem embolism resistance and long-term AGB dynamics, suggesting that the ultimate control on forest sink capacity under changing climate is HSM and not embolism resistance *per se*.

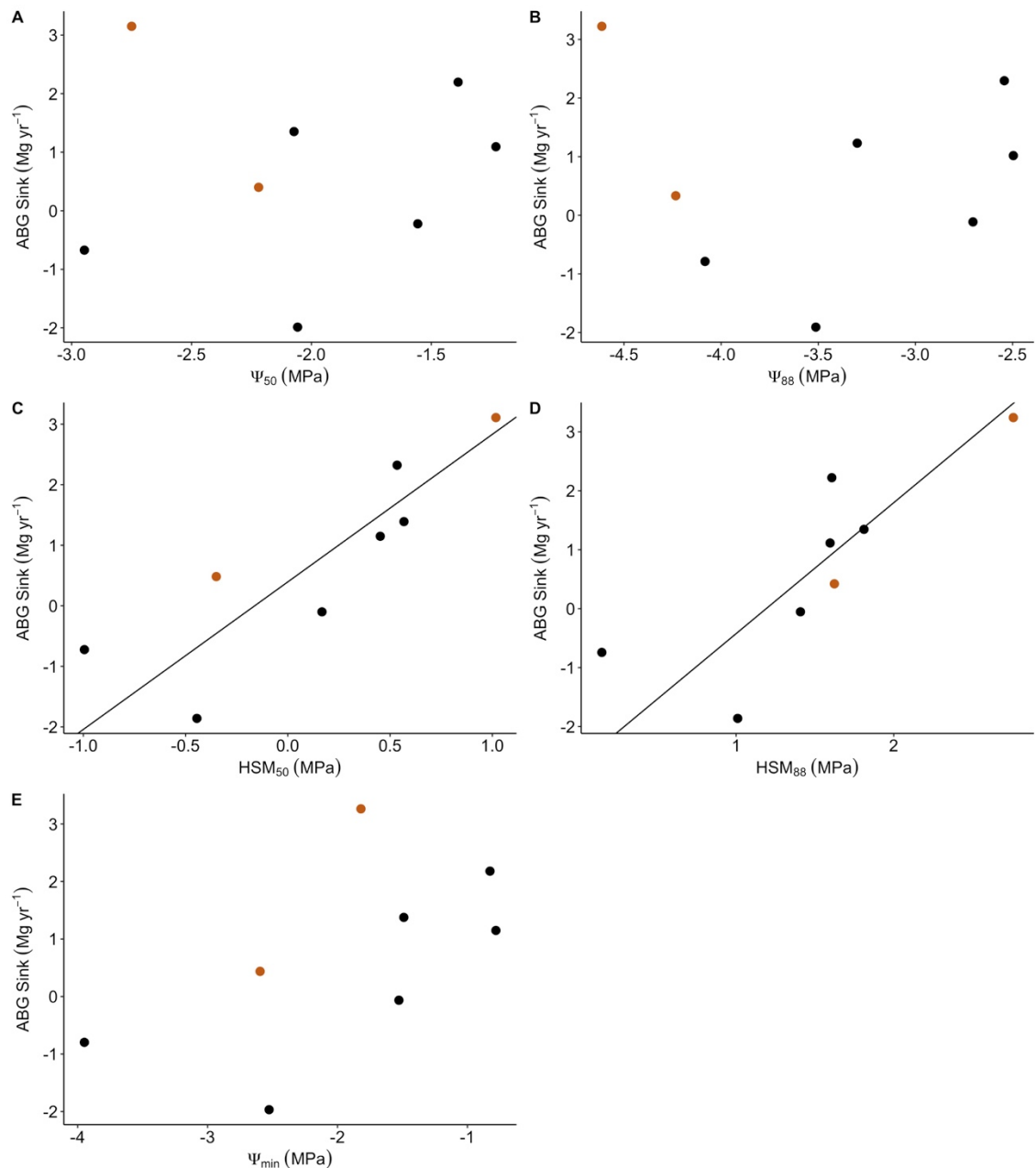


Figure 2. 6 Relationship between Aboveground net biomass and hydraulic traits. Cluster mean biomass net change in relation to: A) and B) cluster mean CWM ψ_{50} and CWM ψ_{88} (xylem water potential on which 50 and 88% of the conductance is lost, respectively); C) and D) cluster mean CWM HSM₅₀ and CWM HSM₈₈. Significant standard major axis regression (SMA) are shown by solid lines: C) $R^2 = 0.71$, $p=0.009$ and D) $R^2=0.61$, $p=0.02$. Each point represents a cluster of forest plots. Brown points show clusters in drought experiment locations (TAP and CAX). Note that only data from control plots were used in these analyses. Further cluster information available on Table A1. 6.

It is important to notice that in this study minimum leaf water potential was measured as one point in time, on which I tried to capture the pick of the dry season (Fig

A1.6). As it was not possible to measure ψ_{\min} continuously and across several dry seasons, the values presented in this study could perhaps not represent the true minima faced by the plants in each site. Consequently, the hydraulic safety margins shown here are possible underestimated.

2.4 Implications and Conclusions

Our results provide important new insights into how vulnerability to drought varies across Amazonian forests. The combination of markedly resistant xylem and wide safety margins indicates that seasonal Central-Eastern Amazonian forests are likely to be the least vulnerable forests to drought in the Amazon Basin. This may be associated with the periodic occurrences of ENSO events and generally greater climate variability in this region relative to the Western Amazon (Yoon and Zeng, 2010; Ciemer et al., 2019), which may have created selection pressure for more drought-adapted taxa. Data from the Eastern Amazon have informed most of this understanding to date of drought impacts on Amazonian forests as the only two ecosystem-scale throughfall exclusion experiments in Amazonia have been installed there (Nepstad, 2002; da Costa et al., 2010; Meir et al., 2015). Remarkably, of the eleven sites encompassed by my study, the forests in these two drought experiment locations (TAP and CAX) have the most resistant ψ_{88} while TAP also has the most positive HSM_{88} values, and, along with another plot in Manaus, the widest HSM_{88} values (Fig. A1. 4). Our results indicate that upscaling of drought sensitivity inferred from these forests to the whole biome might therefore underestimate Amazonian vulnerability to climate change.

These results suggest that Amazon forests cease to act as aboveground biomass sinks when community-level $HSM_{88} < 1.0$ or $HSM_{50} < 0.0$. Hydraulic safety margins of Amazonian species have been shown to decline markedly in response to increases in temperature and VPD (Fontes et al., 2018). Continued increases in temperature and VPD, as predicted by all climate models, will likely reduce safety margins across Amazonian forests and so further reduce the already-declining Amazon carbon sink (Brienen et al., 2015b). Our results suggest that these effects will be most marked in Western Amazonian forests on sandier soils.

In addition, the most vulnerable site in our study is in the southern fringe of the Amazon, which has faced the greatest recent climatic changes (Nobre et al., 2016; Fu et

al., 2013) of all Amazonian regions. The very low hydraulic safety margins observed in this site point to substantial hydraulic stress and may indicate that this region of the Amazon is most imminently at risk of suffering with drought induced mortality. Further studies are, however, required to confirm the generality of this pattern.

Chapter 3: Evolutionary control of embolism resistance in Amazonian forests

Abstract

Over the past decades Amazon rainforest has been facing changes in climate, including increase of air temperature and intensification of large drought events. Tropical trees ability to persist under these observed and predicted climate changes, strongly depends on their capacity to cope with water stress. Embolism resistance, defined as plant capacity to resist the disruption of water flow by air formation (emboli) is a then a fundamental tree trait to be investigated. It remains still unknown whether this trait is phylogenetically controlled across Amazonian tree taxa. Addressing this question is critically important for predicting how the vast Amazonian species diversity and its composition will respond to changes in climate. If heritability plays a major role on determining species embolism resistance, species may not be able to change their embolism resistance and adapt to future changes in water availability. While, the opposite is expected if embolism resistance is widespread across the phylogeny. Here I show that embolism resistance is more similar among Amazonian closely related tree taxa than expected by chance, with hydraulic conservatism preserved at family level. Fabaceae has especially high embolism resistance, among families in our dataset, and it is consistently more emboli-resistant than non-Fabaceae within Amazonia and other tropical rainforests. Based on the phylogenetic signal found in our dataset and on species distributions from 582 inventory forest plots widely distributed across Amazonia, I map the Amazonian embolism resistance. Our study reveals that Brazilian and Guyana Shield tree communities' composition are particularly embolism resistant. In contrast, tree communities of Western Amazon have generally embolism vulnerable species composition, indicating low ability of this region to withstand future warming and drying conditions.

3.1 Introduction

The Amazon region is home to the largest and most diverse tropical forest in the world and plays an important role in planetary biogeochemical cycles. Recent findings have documented substantial changes in floristic and functional composition (Esquivel-Muelbert et al., 2018), structure and dynamics (Phillips et al., 2009; Brienen et al., 2015) across Amazonian forests, potentially associated with ongoing changes in climate and atmospheric composition. In recent decades, the Amazon has been subjected to a sequence of large-scale drought events (1998, 2005, 2010, 2015-16) (Aragão et al., 2007; Marengo et al., 2008; Phillips et al., 2009; Lewis et al., 2011; Jiménez-Muñoz et al., 2016), as well as progressively increasing air temperatures (Jiménez-Muñoz et al., 2013). Climate model projections suggest that the frequency of extreme drought events will continue to increase in the future (Marengo et al., 2018) and that temperatures will likely rise to levels without historical analogues. Together, these climatic changes are expected to enhance water stress in Amazon rainforests.

A mechanistic understanding of Amazonian tree capacity to withstand water shortage is needed to predict the future impacts of climate change on these forests. Xylem embolism resistance is a key structural trait that underpins plant ability to tolerate water stress. This is because water stress is associated with increasingly negative xylem water potential which may cause embolism and xylem damage (Tyree & Zimmermann, 2002). Typically, embolism resistance is quantified as the xylem water potential at which a tree's hydraulic conductivity declines to 50% (ψ_{50} (MPa)) or 12% (ψ_{88} (MPa)) of its maximum value (Sperry et al., 1988). In Amazonia, these traits (ψ_{50} and ψ_{88}) have been shown to explain transpiration and canopy conductance responses to extreme drought (Fontes et al., 2018; Barros et al., 2019), as well as local patterns of species distribution (Oliveira et al., 2018) and differential mortality patterns under imposed drought (Powell et al., 2017).

In recent years, great advances have been made in understanding local (Rowland et al., 2015; Powell et al., 2017; Santiago et al., 2018; Brum et al., 2018; Oliveira et al., 2018; Clarissa G Fontes et al., 2018; Barros et al., 2019) and broad-scale (see Chapter 2) patterns of embolism resistance across Amazonian forests. Vulnerability to embolism varies widely across the Amazon Basin, being mainly associated with climatological average water availability, with forest communities in the Western Amazon possessing particularly vulnerable hydraulic architecture (see Chapter 2). However, the extent to

which taxa will be able to adapt their xylem architecture in the face of increasing water stress remains unknown.

Insights into adaptation capacity can be obtained by examining the extent to which embolism resistance is phylogenetically controlled. Present-day trait values are the result of millions of years of evolutionary processes. The extent to which traits are phylogenetically controlled depends on a range of evolutionary and ecological processes, including heritability, convergent evolution and divergent selection (Crisp et al., 2009). Global xylem anatomy studies have found that closely related lineages possess markedly similar xylem anatomical traits, especially pit membrane characteristics, which are membranes between pores that connect adjacent vessels (Jansen et al., 1998; Jansen et al., 2001; Jansen et al., 2003). These pit membrane characteristics have been hypothesised to be intrinsically related to embolism resistance (Choat et al., 2008; Jansen et al., 2009). Projections of the secondary cell wall in the pit chambers, called vestured pits, are thought to be particularly important in conferring embolism resistance by preventing pit membrane rupture or mechanically acting as a barrier against air seeding dispersal (Choat et al., 2004). The presence/absence of vestured pits varies greatly across angiosperm clades (Jansen et al., 2003; Medeiros et al., 2018), being, indeed, most prevalent in angiosperm taxa occurring in warm and seasonally dry habitats (Jansen et al., 2004). In tropical seasonal woodlands, for example, vestured pits are reported to be found in up to 50% of tree species, compared to only 30% of species in moister forests (Jansen et al., 2004).

As well as vestured pits, if embolism resistance have evolved little from their ancestor state, species may not be able to adapt. Because, through time, the consequences of climate change on species persistence in the environment is a result of how fast species respond and whether they can adapt to these changes evolutionarily (Lavergne et al., 2010; Quintero and Wiens, 2013). In contrast, if embolism resistance is randomly spread across phylogeny, species may be able to adapt to future changes in water stress. Understanding whether plant hydraulic traits exhibit phylogenetic conservatism, indicated by significant phylogenetic signal, is thus important for predicting how the Amazonian species diversity and composition may respond to climate change. Furthermore, the existence of phylogenetic conservatism would enable us to predict community-level patterns of embolism resistance based on compositional data alone.

To explore the extent to which embolism resistance across Amazonian tree taxa is phylogenetically controlled, I combined the first fully standardized pan-Amazonian hydraulic trait database (see Chapter 2) with the most up-to-date Amazonian molecular-genus-level phylogenetic tree (Coelho de Souza et al., 2019). I aimed to (1) test for the presence and quantify the strength of phylogenetic signal (PS), (2) explore the influence of potentially key families and clades, and (3) use our results in combination with extensive floristic sampling to predict community hydraulic resistance across the whole Amazonian domain. As xylem embolism resistance is a structural trait intrinsically related to plant survival (Rowland et al., 2015; Anderegg et al., 2016; Adams et al., 2017), I hypothesized that both ψ_{50} and ψ_{88} are phylogenetically conserved. Additionally, based on the hypothesized by previous studies, I expect that clades which conserve vestured pits are more embolism resistant than those where this feature is absent.

Our embolism resistance database encompasses 129 species spread within 88 genera, 36 families and 14 orders occurring across 11 sites spanning a wide range of precipitation, soil properties and life history strategies (see Chapter 2). The most common families across our sites, in terms of geographic occurrence are: Fabaceae (10 sites), Burseraceae (9 sites), Euphorbiaceae, Moraceae, Sapotaceae and Lecythidaceae (8 sites) and Lauraceae (6 sites). These are amongst the most abundant families in the Amazon in terms of numbers of stems (Ter Steege et al., 2006; Ter Steege et al., 2013) and aboveground biomass and wood productivity (Fauset et al., 2015).

As well as testing whether embolism resistance (ψ_{50} and ψ_{88}) across Amazonian tree taxa is constrained over the evolutionary scale, I also evaluated whether there are specific taxonomic groups strongly contributing to this signal. Additionally, I tested for differences in embolism resistance across the major Amazonian families, not only for our newly-assembled dataset, but also in other available published datasets (Choat et al., 2012; Santiago et al., 2018). Finally, these results permitted us to infer embolism resistance / vulnerability patterns across a large network of floristically identified and consistently measured forest plots (RAINFOR (Malhi et al., 2002)), consisting of 582 local forest community samples spanning the entire Amazonian domain.

3.2 Methods

3.2.1 Amazonian tree embolism resistance (ψ_{50} and ψ_{88}) dataset

In this study, I used species or genus mean values of ψ_{50} and ψ_{88} from 129 species, 88 genus, belonging to 36 families and 14 orders obtained from the previous chapter. In Chapter 2 I provided the first pan-Amazonian hydraulic traits dataset, on which, embolism resistance was characterized by constructing xylem vulnerability curves for 129 species among 11 sites in the Western, Eastern and Southern Amazon and encompassing a broad climatological and soil gradient. Xylem vulnerability curves quantify xylem embolism formation as a function of branch dehydration (Sperry et al., 1988). Pneumatic method, which consists on measuring the air discharge from terminal branch ends, was used to assess embolism formation (Pereira et al., 2016; Zhang et al., 2018; Bittencourt et al., 2018) and bench dehydration technique (Sperry et al., 1988) was used to induce water stress in a given branch. More information is described in Chapter 2.

3.2.2 Data analysis

Phylogenetic signal: I used the most up to date Amazonian tree genus-molecular base phylogenetic tree (Coelho de Souza et al., 2019), to explore the existence of phylogenetic signal (PS) in Ψ_{50} and Ψ_{88} across different Amazonian genera (N=88 genera, 36 families, 14 orders). To quantify the strength of PS, I used Blomberg's k . ' k ' values provide a measure of the strength of phylogenetic signal based on comparing the observed variance for a given trait against the variance that would be expected under a Brownian motion (BM) model of trait evolution (Blomberg et al., 2008). ' k ' values close to zero imply evolutionary independence (random trait distribution among the branches of the phylogenetic tree), while values close to one denote phylogenetic non-independence, indicating high trait similarity among closely related clades. The significance (p value) of k was estimated through a randomization exercise in which tips of the phylogenetic tree were randomized 1000 times and the resulting distribution of k values compared to my observed value of k . k values were taken to be significant if they fell outside the 2.5-97.5 percentile range of the simulated distribution. Blomberg's k test has been shown to be able to detect PS on trees with at least 20 observations and is thus appropriate for the size of my dataset (Blomberg et al., 2003). I further tested the

sensitivity of the observed phylogenetic signal (PS) by repeating the analyses on restricted subsets of my dataset. As the dataset spanned dry-adapted transitional forests as well as core Amazon forests, I re-ran the analyses excluding transitional forests to verify that observed PS patterns were not driven simply by differential sampling of genera across different climate regimes. Secondly, to account for unbalanced sampling, I also re-ran the analyses excluding the most abundant family in our database, the Fabaceae, which accounted for ~15% of our sampled genera. Data were transformed to meet the normality criteria of the test, when necessary (Table 3. 1). To test which specific taxonomic groups may strongly contribute to PS, I employed the randomization approach of Dexter et al. (2016). In brief, the approach consists of first estimating the ancestral value for each node in the phylogeny using ancestral state reconstruction and then randomizing the tips of the phylogeny 1000 times to generate a random distribution of ancestral nodes which are compared to the observed reconstructed node value.

Complementarily, to better understand the variation in Ψ_{50} and Ψ_{88} explained by different taxonomic levels (species, genus, family), I performed a nested ANOVA [family/genus/species]. This analysis was limited to genera for which I had data from more than one species and to species which I sampled in more than one site. Data were square root transformed to meet the normal distribution criteria of the test.

Embolism resistance variation across families: To evaluate embolism resistance variation across widely occurring families in my dataset, I performed one-way ANOVA followed by Tukey honest significant difference (HSD) tests. In this analysis, I selected only families that occurred in at least 6 sites along a wide mean MCWD (Maximum Climatological Water Deficit) gradient.

Given the importance of the Fabaceae both in this dataset and across Amazonian forests more generally, I also investigated whether there were differences in embolism resistance between the Fabaceae and non-Fabaceae by performing Wilcoxon rank sum test with continuity correction. I did this across the entire dataset but also for specific forest types (aseasonal, seasonal, transitional), following the information at the previous chapter. To assess whether the pattern found for Amazonia was also observed across other lowland tropical rainforests (<1000 masl), I collated published ψ_{50} data for tropical Angiosperms trees (Choat et al., 2012; Santiago et al., 2018) and also used these data to test for differences between Fabaceae and non-Fabaceae (Wilcoxon rank sum test).

Winteraceae were excluded from this analysis due to absence of vessels in this family. Species, Genus and Family names were checked using The Taxonomic Name Resolution Service (Boyle et al., 2013).

Map of Amazon embolism resistance: Based on the phylogenetic signal observed in my database, I computed community-weighted mean ψ_{50} and ψ_{88} for a further 582 Pan-Amazonian plots from the RAINFOR inventory network (Malhi et al., 2002). Tree by tree data for each plot were obtained from the ForestPlots.net database (Peacock et al., 2007; Lopez-Gonzalez et al., 2009; Lopez-Gonzalez et al., 2011). I selected best identified single censuses at species level for each structurally mature lowland tropical forest plot from Extended Amazonia, thus excluding dry forests, swamp forests, and plots with elevation > 1000 m above sea level, as well as those affected by direct human disturbance. As the results of my nested ANOVA analyses suggested a strong family control on embolism resistance, I restricted the mapping exercise to plots that shared at least 60% of their dicotyledonous arboreal family composition, in basal area terms, with my trait database.

We gap-filled missing data following the methods of Esquivel-Muelbert (2018), whereby I used values for the next available taxonomic level. For example, for species for which I had not measured ψ_{50} , I used genus-level means when available and family-level means when genus-level data was not available. When family-level data were not available, I used the plot mean value. I used the community weighted mean (CWM) to describe the central tendency of tree community trait values at each site. The CWM for ψ_{50} and ψ_{88} was calculated by weighting the trait value (X_i) of each species (s) by its relative dominance (species basal area divided by the plot total basal area) in each study plot (W_i):

$$CWM = \sum_{i=1}^s W_i * X_i \quad \text{Equation (1)}$$

Vestured pits: I tested for differences in embolism resistance among taxa with consistently present versus consistently absent vestured pits (Jansen et al., 2003), by conducting a Wilcoxon rank sum test with continuity correction. I used Jansen et al (2003) classification to subset and group my dataset between presence and absence of this characteristic: Myrtales (Vochysiaceae, Melastomataceae, Combretaceae), Gentianales

(Rubiaceae, Apocynaceae) and Fabaceae invariably exhibiting pit vestures and Ericales (Lecythidaceae, Sapotaceae), Santalales (Olacaceae) and Sapindales (Meliaceae, Burseraceae, Simaroubaceae, Anacardiaceae), exhibiting no vesturing in their pit chambers.

3.3 Results

Evidence of phylogenetic control on embolism resistance of Amazonian trees

I find evidence of strong phylogenetic signal for embolism resistance of Amazonian trees (Fig. 3. 1, Tab. 3. 1), as demonstrated by a value of Blomberg's k of 0.49 ($p=0.01$) for ψ_{50} , across the entire dataset. This value is at the top-end of reported k values for tropical forest tree traits (Coelho de Souza et al., 2016). The observed PS remained similar when accounting for environmental variation (i.e. excluding dry transitional forests) (Fig 3.1B, Tab1) and unbalanced sampling (i.e. excluding Fabaceae, the most abundant family in our dataset) (Fig 3.1C, Tab1). Nested analysis of variance further revealed that family ($F=2.74$, $p=0.02$) is a stronger predictor of ψ_{50} than genus ($F=1.88$, $p=0.07$) or species ($F=1.1$, $p=0.4$), implying that these hydraulic properties evolved early in the history of the Amazonian tree flora.

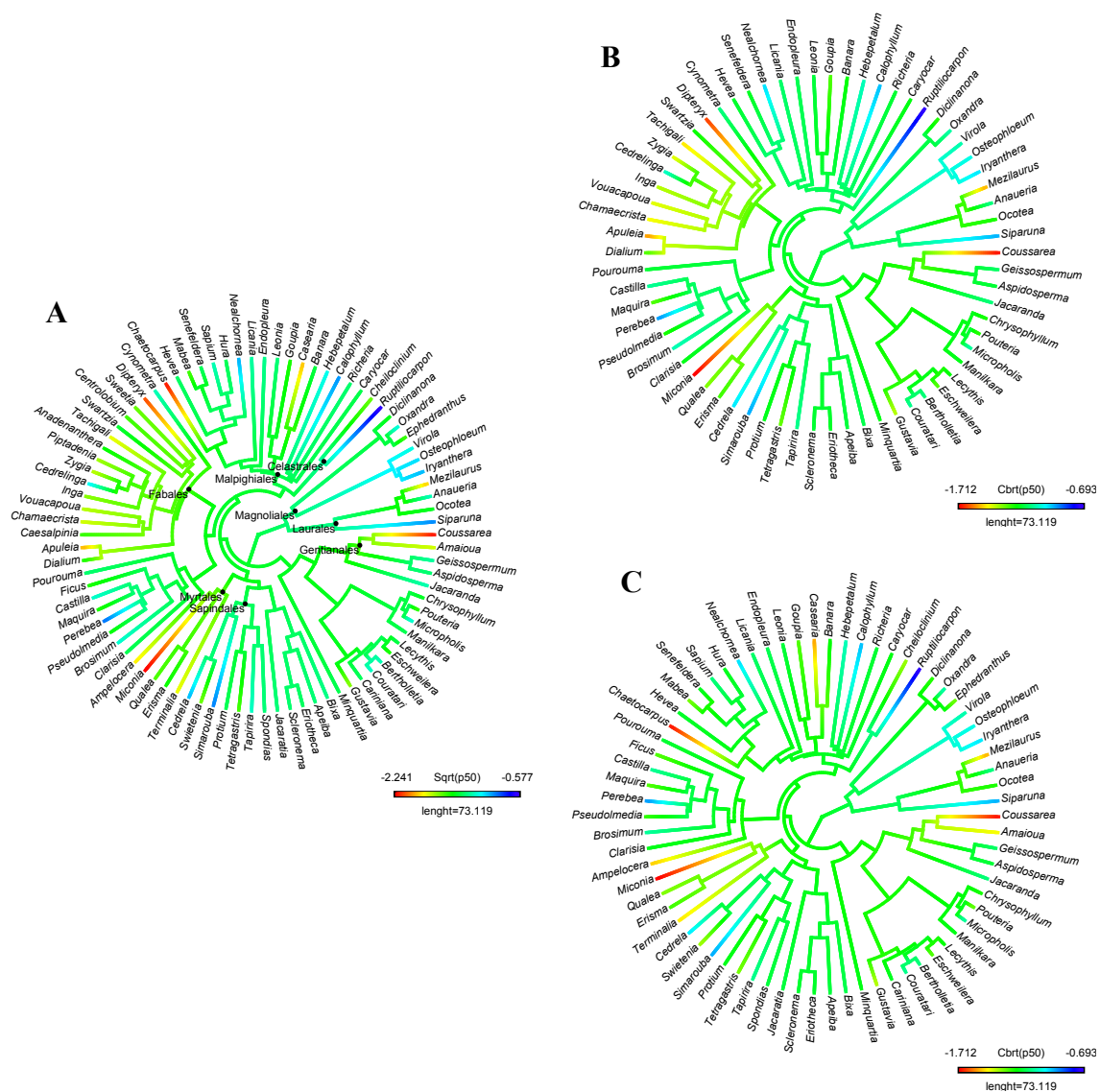


Figure 3. 1 Phylogenetic tree (Coelho de Souza et al., 2019) of Amazonian tree genera with branches coloured as: absolute mean ψ_{50} value per genus, $n = 87$ genera (A), Phylogenetic signal for ψ_{50} account for environmental variation: excluding transitional forests, $n = 67$ genera (B) and for unbalanced sampling: excluding Fabaceae, the most abundant family in the dataset, $n = 71$ genera (C).

Table 3. 1 Summary table of phylogenetic signal (PS) for embolism resistance of Amazonian trees. PS measured by Blomberg's K and significance values for absolute Ψ_{50} and Ψ_{88} values (all dataset) and sensitivity analyses: excluding transitional forests and excluding Fabaceae (to account for unbalance sample). Transformation: type of transformation applied on the data to meet normality assumption of the test.

Sampling	Transformation	Embolism resistance (MPa)	PS (K)	pvalue
All dataset	Square root (Sqrt)	ψ_{50}	0.49	0.01
		ψ_{88}	0.44	0.02
Transitional forest excluded	Cube root (Cbrt)	ψ_{50}	0.53	0.007
		ψ_{88}	0.39	0.09
Fabaceae excluded	Cube root (Cbrt)	ψ_{50}	0.46	0.02
		ψ_{88}	0.41	0.06

Fabaceae have particularly high embolism resistance

A phylogenetic randomization analysis (Dexter and Chave, 2016) revealed that two plant orders, Myrtales and Fabales, were particularly important in driving the extent of phylogenetic signal in the database, both of which exhibit marked resistance to embolism. When I performed my family-level analysis but constrained it only to those families occurring across a majority of the sites, among-family differences in embolism resistance were also detected ($F=2.45$, $DF=6$, $p=0.05$), with the Fabaceae standing out as having especially low values of Ψ_{50} and Ψ_{88} (Fig. 3. 2). The Fabaceae are the most diverse of Angiosperm families (Christenhusz and Byng, 2016) and the most abundant and ecologically dominant plant family in Amazonia (Ter Steege et al., 2013; Fauset et al., 2015), as well as being broadly distributed and dominant across most of the world's tropical forests (Gentry, 1988).

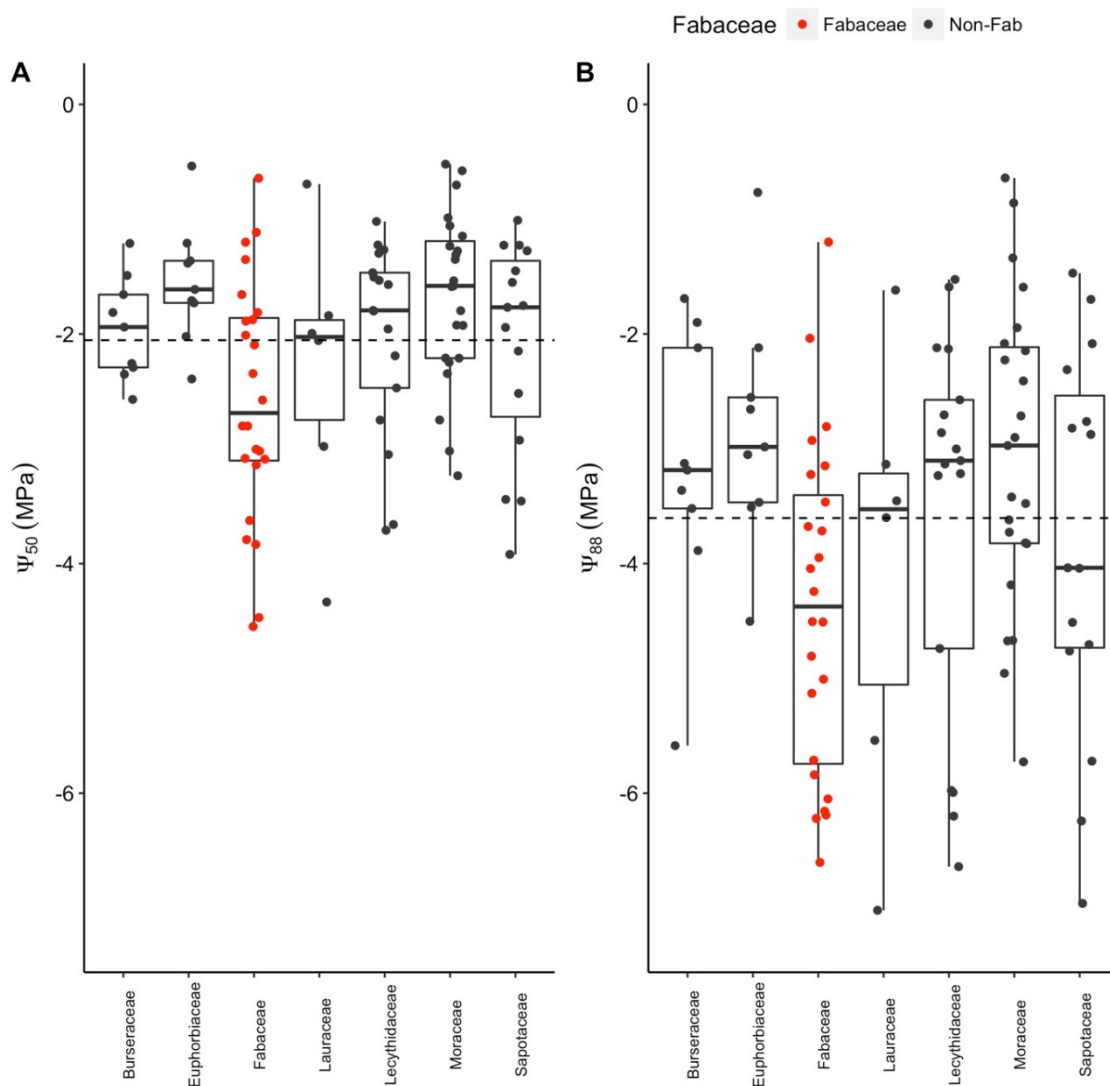


Figure 3. 2 Embolism resistance variation across and within families with a wide occurrence in my dataset. Boxplots of Ψ_{50} (A) and Ψ_{88} (B) variation across families. Dashed horizontal lines show mean trait value across families (only considering those with wide occurrence). Anova and Tukey HSD *Pos Hoc* at 0.05 significance level were performed and significant differences are displayed on the figure.

Given their overarching importance, I then tested whether the Fabaceae are on average more emboli-resistant than non-Fabaceae within tropical forests, using my standardized dataset, and across tropical rainforests, using other published databases (Choat et al., 2012; Santiago et al., 2018). I find that Fabaceae (mean ψ_{50} : -2.6 ± 1.0 , ψ_{88} : -4.4 ± 1.4) have significantly more resistant xylem than non-Fabaceae (mean ψ_{50} : -1.8 ± 0.8 , ψ_{88} : -3.3 ± 1.5) across Amazonian forests (Fig. 3. 3), with the difference being

especially marked in seasonal Amazonian forests (Fig. 3. 3.), which occupy most of the Amazon basin. Embolism resistance did not differ significantly ($p=0.2$ for ψ_{50} , $p=0.08$ for ψ_{88}) between Fabaceae and non-Fabaceae in aseasonal forests, where the number of Fabaceae sampled was very low, but general patterns appeared to be similar to seasonal forests. In transitional dry forests, where species are more adapted to water stress, Fabaceae and non-Fabaceae have equally resistant xylem (Fig 3. 3). Analysis of the broader published data from tropical forests also yields similar results, with Fabaceae having significantly more resistant xylem than non-Fabaceae ($W=539$, $p=0.02$).

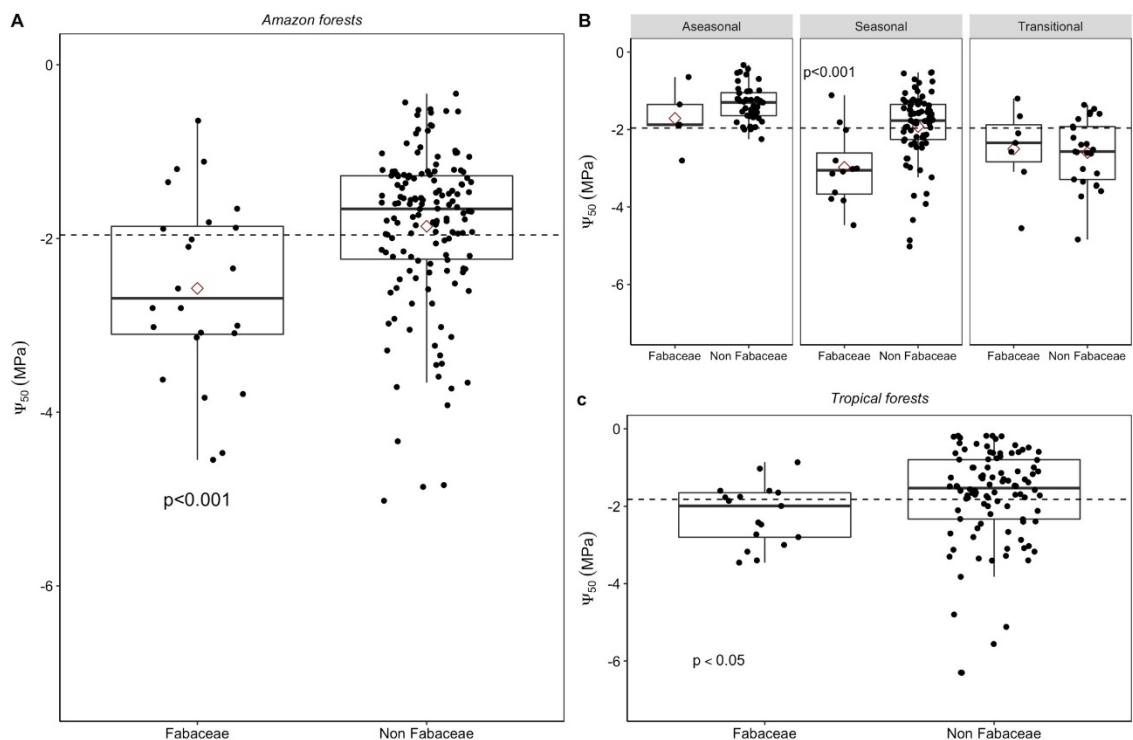


Figure 3. 3 Difference in embolism resistance (Ψ_{50}) between Fabaceae and Non-Fabaceae across (A) and within (B) Amazonian forests and across tropical rainforests (C). Dashed vertical lines show mean trait value across pan-Amazonian dataset (A, B) and compiled dataset (C). Statistical differences at $p < 0.05$ using Wilcoxon rank sum tests are displayed on the figure.

Embolism resistance of Amazonian tree communities

Based on the phylogenetic signal observed in my database, I computed community-weighted mean ψ_{50} and ψ_{88} for a further carefully identified and measured

582 permanent plots across Amazonia curated at ForestPlots.net (Lopez-Gonzalez et al., 2011). Because these are geographically extensive and each include information on species composition, abundance, and the size of each tree, they allow me to map embolism resistance across Amazonia for the first time, accounting for the relative local dominance of each taxon. Our resultant maps (Fig 3. 4) of community-weighted mean ψ_{50} and ψ_{88} show that forests in the Brazilian and Guyana shields have species communities with particularly high embolism resistance. Western Amazon forests, on the other hand, generally have the least resistant xylem in the Amazon Basin. For example, mean ψ_{50} and ψ_{88} were -0.22 and -0.41 MPa lower across western Amazonian plots than in the Brazilian shield respectively (Fig A2. 5).

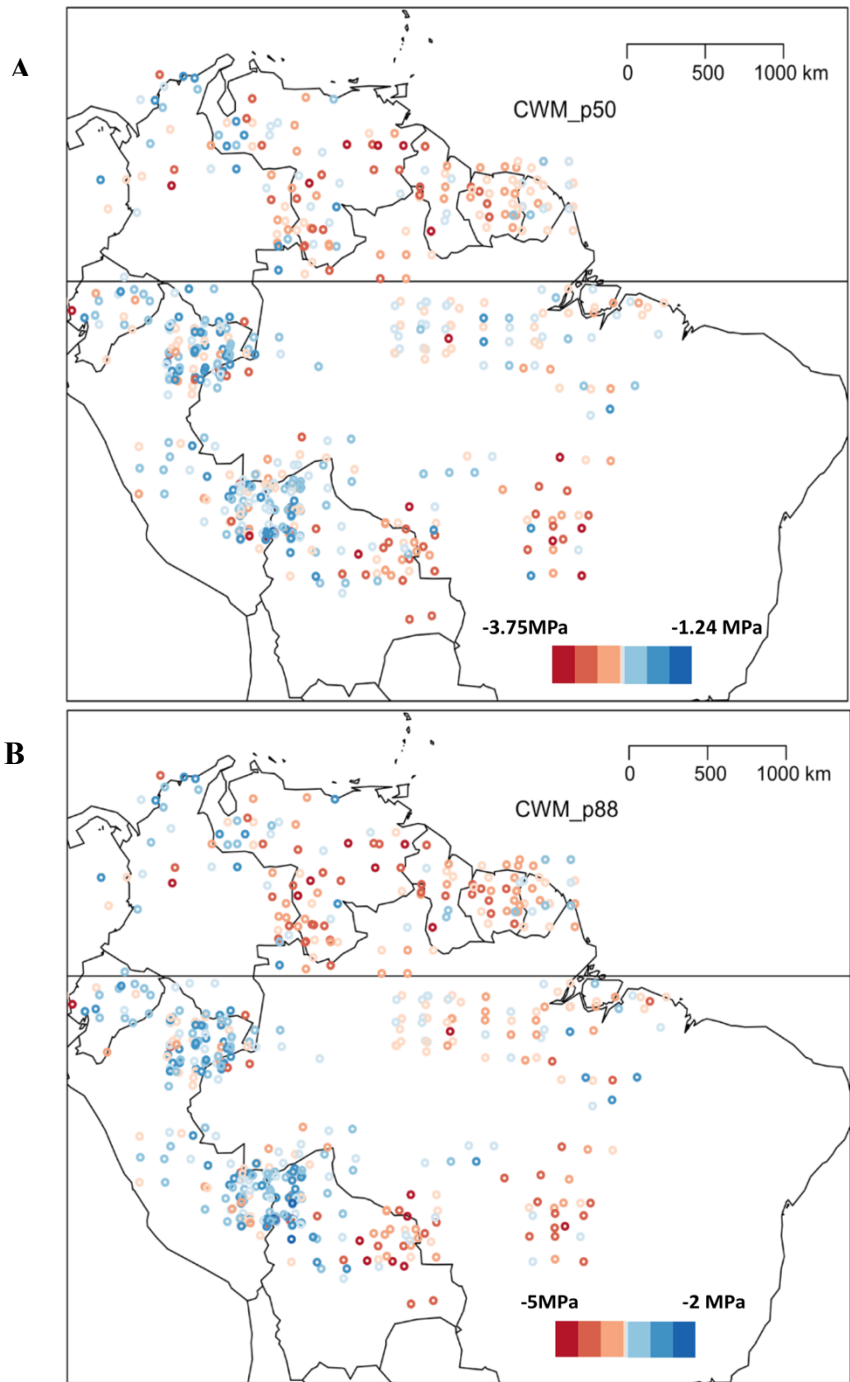


Figure 3. 4 Map of Amazonian vulnerability to embolism. Each point represents the community weighted mean value of Ψ_{50} (A) and Ψ_{88} (B) for 582 inventory forest plots widely distributed across Amazonia. The colours are a continuum of xylem embolism vulnerability, where dark red indicates the less vulnerable and dark blue the more vulnerable plant communities.

Lineages with vested pits have higher embolism resistance

Additionally, I evaluated whether there is difference in embolism resistance between lineages with and without pit vestures. The results show that Myrtales, Gentianales and Fabaceae, which are the lineages in my dataset that invariably exhibit vesturing in their pit chambers (Jansen et al., 2003) are more emboli resistant than Ericales, Santalales and Sapindales, which do not exhibit this characteristic (Fig. 3.5).

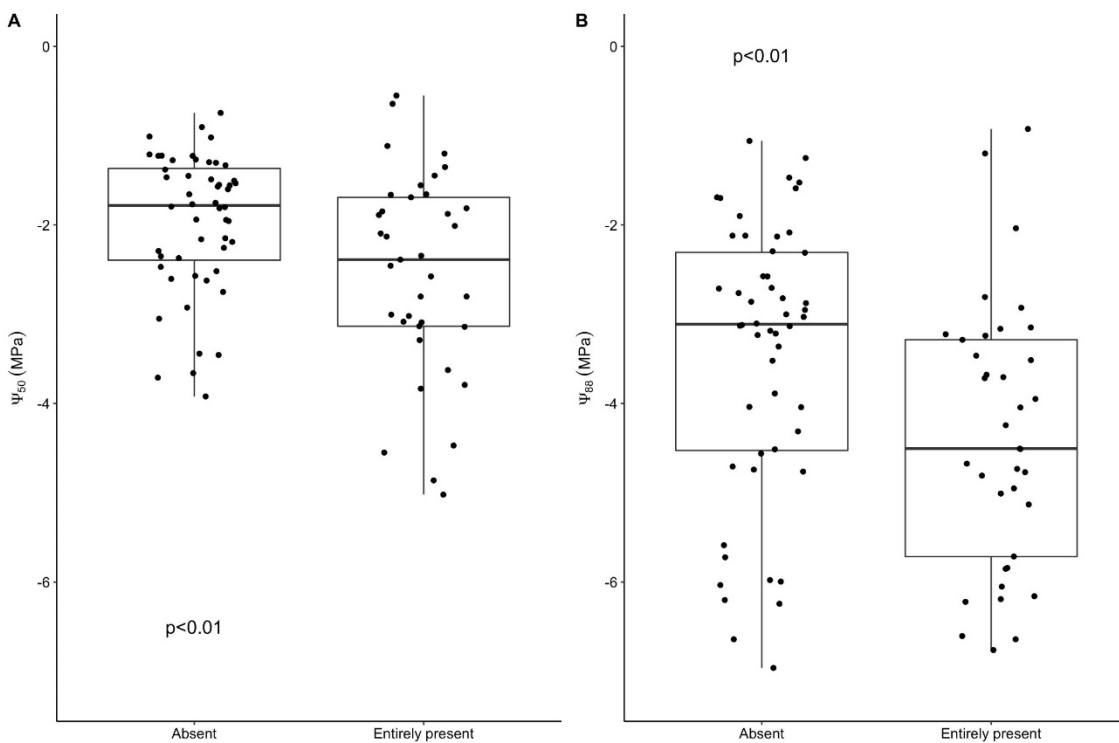


Figure 3. 5 Differences in embolism resistance among lineages with consistently present (Myrtales, Gentianales and Fabaceae) and absent (Ericales, Santalales and Sapindales) vested pits: Ψ_{50} (A) and Ψ_{88} (B). Species are indicated by the black points. Significant differences at $p < 0.05$, using Wilcoxon rank sum tests are displayed on the figure. The presence and absence of vested pits follows Jansen et al., 2003.

3.4 Discussion

My analyses suggest that closely-related taxa have more similar embolism resistance than would be expected by chance. However the signal is substantially weaker

than expected under a Brownian motion (BM) model of evolution. Under the null BM model, traits evolve by gradual non-directional changes over time and evolutionary related taxa would have a high similarity because trait values have had less time to diverge (Blomberg et al., 2003; Losos, 2008; Revell et al., 2008). Levels of phylogenetic signal that are lower than expected under BM, indicate that a wide range of other processes may also be important (Crisp & Cook 2012). For example, convergent evolution in distantly related lineages, or divergent selection among closely related species tend to reduce levels of phylogenetic signal compared to a BM model. Another process that may affect patterns of phylogenetic similarity is dispersal limitation. However, in the Neotropics, most lineages are widespread (ter Steege *et al.* 2006), suggesting that at least at the genus-level these forests are not dispersal limited (ter Steege *et al.* 2006). Overall, the extent of signal that I found here, shows that heritability plays an important role in determining hydraulic traits, but it also highlights that convergent evolution and divergent selection in some groups may have also played an important role in the evolution of the variation we see today in hydraulic strategies.

The heritability of this characteristic represents the maintenance of a fundamental survival-related trait within clades through evolutionary history. Indeed, embolism-resistance has been proposed to be a “super-trait” (Brodribb, 2017; Larter et al., 2017), as it integrates whole plant performance (Tyree & Zimmermann, 2002; Anderegg et al., 2016; Choat et al., 2018). The strength of PS found in our study is higher than PS found for a broad variety of traits in tropical forests. For example, Coelho de Souza et al. (2016) compiled Blomberg k values spanning ~20 functional traits, with the range in k varying from 0 to ~0.5. My reported k values of 0.49 and 0.44 for ψ_{50} and ψ_{88} respectively are at the high end of this range. Although the number of taxa in this analysis is not as high as in some of these studies, the high k value I find clearly supports the idea that embolism resistance traits are strongly related to plant fitness. Thus far, the evidence of phylogenetic signature across tropical tree species has focused largely on easily measurable ‘soft’ traits related to leaf economics (*e.g.* LMA), plant structure (*e.g.* wood density) and other specific aspects of plant function. Such traits are typically not directly related to survival and thus might be expected to be more labile than ‘hard’ traits fundamentally related to survival such as embolism resistance.

As well as embolism resistance, vestured pits have been shown to be crucially related to plant ability to withstand water stress. While divergent selection of this characteristic is found across many lineages, such as Malvales, Solanales and Rosaceae, trees belonging to Myrtales, Gentianales and non-basal Fabaceae have been invariably shown the presence of vestured pits. In other orders, such as Ericales, Santalales and Sapindales, vestured pits appear to be completely absent (Jansen et al., 2003). For example, 93% of Fabaceae species (121/130) and 100% of species (56/56) belonging to Myrtales in a recently compiled database by Medeiros et al. (2019) have vestured pits, compared to 0% of species belonging to Sapindales (0/22). My results demonstrate at a large –scale for the first time, that plant lineages which are known to almost always possess vestured pits (Myrtales, Gentianales, Fabaceae) were found to have markedly more robust xylem architecture (more negative ψ_{50} and ψ_{88}) than those lineages where vestured pits are known to be always/almost always absent (Ericales, Santalales, Sapindales).

This finding that tropical Fabaceae exhibit substantial resistance to embolism in comparison with non-Fabaceae taxa is particularly noteworthy, given the status of Fabaceae as the most dominant Neotropical angiosperm tree family (Gentry, 1988). Several factors have been proposed to explain the success of the Fabaceae across Amazonia. In primary forests, Fabaceae has been suggested to be more successful in low-dynamic environments, showing higher shade tolerance than other families in poor soils, not only due to the ability to fix N but also due to their higher seed mass (Ter Steege et al., 2006). In secondary forests, the combination of the ability to fix nitrogen and their reduced leaflet size, which together result in enhanced nutrient use efficiency and drought tolerance, are key factors explaining the ecological success of this group in regrowth areas (Batterman et al., 2013; Gei et al., 2018). This study suggests that enhanced drought tolerance, as inferred from their high xylem embolism resistance, may also help to explain the remarkable abundance, dominance, diversity and extensive distribution of Fabaceae in primary forests in Amazonia and in tropical forests more generally.

The phylogenetic signal found in our database combined with the vast forest inventory information across the Amazon, allowed me to provide the first pan-Amazonian map of vulnerability to embolism. The resultant map of community-weighted mean embolism resistance across Amazonian forests does not simply reflect the precipitation

map for the Basin. In addition to the known precipitation gradient from northwestern to southern Amazon reflected in vulnerability distribution, I also find markedly high embolism resistance across the Brazilian and Guyana Shields, which comparatively have low and high precipitation regimes (Johnson et al., 2016). The observed high community-level embolism resistance in these areas is likely to be driven by the high abundance of Fabaceae in both the Guyana Shield (CWM50: $F=68.4$, $p<0.0001$; CWM88: $F=94.4$, $p<0.0001$) and Brazilian Shield (CWM50: $F=15.5$ $p<0.0001$; CWM88: $F=21.0$ $p<0.0001$) (Ter Steege et al., 2006). If I used only rainfall patterns to produce the map, instead of considering differences in forest composition, Guiana Shield would be expected to have low community mean embolism resistance. My regional phylogenetic mapping further confirms, in line with the Chapter 2 of this thesis, that tree communities in the Western Amazon are characterized by markedly less resistant xylem than those in Central and Eastern Amazonia.

3.5 Implications and Conclusions

The finding that resistance to water stress is phylogenetically constrained suggests that species may have limited potential to adapt to current and future climatic changes. This is because over the evolutionary history lineages tend to retain their ancestor characteristic, under climate change they may not be able to change their trait fast enough to cope with new conditions. Nevertheless, under a warming and drying climate, the species composition of Amazon forests would be expected to shift towards more embolism resistant taxa. Indeed, recent findings from Ghana support this expectation, as multi-decadal long-term drought has been found to substantially alter community composition (Aguirre-Gutiérrez et al., 2019), which includes moderate increase in Fabaceae abundance. My pan-Amazonian mapping of embolism resistance suggests that intensified water stress would result in greater floristic filtering in the western Amazon, where the current community composition is particularly vulnerable to embolism. In this region, a continued increase in drought frequency would thus be expected to lead to more pronounced compositional shifts and ultimately to loss of biodiversity since the large majority of Amazon arboreal diversity is strongly mesophilic (Esquivel-Muelbert et al., 2017a). Furthermore, as lineages which are more embolism

resistant are clustered rather than over-dispersed in the phylogeny, it is possible that entire clades face the prospect of being lost from Amazonian landscapes under future high water stress scenarios.

It is important to notice that this chapter explores the phylogenetic signal observed for embolism resistance (Ψ_{50} and Ψ_{88}), which reflects the ability of the xylem to withstand water tension. In a subset of 75 genera and 112 species, no phylogenetic signal was found for hydraulic safety margins (HSM_{50} and HSM_{88}) at genus level. This could be due to lower sample size (for HSMs), or indicate that the ability of plants to control the margin between Ψ min and Ψ_{50} and Ψ_{88} at which they operate is conserved at species level. Alternatively, the absence of phylogenetic signal for HSMs could possibly due to high intra specific variation across sites, indicating that plants could adapt this characteristic under future climatic conditions.

Chapter 4: Hydraulic traits are related to Amazonian species biogeographical distribution, tree performance and drought-induced mortality

Abstract

Xylem resistance to embolism and hydraulic safety margins are critically important to characterize tree functioning under water stress. Great advances have been made in understanding how these hydraulic traits vary across Amazon rainforest plots and tree taxa. In a recent analysis, I have shown that community-level hydraulic safety margins reflect aboveground biomass sink strength over the past decades across Amazonian plots. However, the extent to which hydraulic traits are related to performance at the species level in Amazonia has been little explored. Using a standardized hydraulic traits (embolism resistance, hydraulic safety margins) dataset for 87 species across Western Amazonia, I explored the extent to which hydraulic traits relate to species biogeographical distribution, life history characteristics (species-level mean growth and mortality rates) and mortality induced by drought. I find that embolism resistance reflects the biogeographical distribution (in terms of climate space) of forest species across Amazonia in that wet-affiliated species have less resistant xylem than dry-affiliated species. I also find evidence that hydraulic traits are related to life history characteristics. More specifically, I find that pan-Amazonian species mean growth rates are weakly negatively correlated to hydraulic safety margins. Meanwhile pan-Amazonian species mean mortality rates, at least in environments with some degree of seasonality, are strongly correlated with xylem embolism resistance such that species with more resistant xylem have lower mortality rates. As might be expected *a priori*, species characterised by low hydraulic safety margins were found to suffer greater mortality in Amazonian drought experiments. In contrast, branch wood density and non-structural carbohydrates at leaf and branch level are not related to species biogeographical distribution and response to drought. These findings highlight the important role of hydraulic traits in explaining Amazonian biogeography, ecology and responses to drought, and suggest they are highly important for better predicting changes in vegetation structure and dynamics under climate change.

4.1 Introduction

Amazonia is the most biodiverse and extensive tropical forest on Earth, housing more than 16000 tree species (Ter Steege et al., 2013) and stocking approximately 100 Pg of carbon in its biomass (Feldpausch et al., 2012). Changes in this ecosystem are likely to impact global climate, due to its important role in large-scale exchanges of water and carbon with the atmosphere (Nobre et al., 2016). Recent decades have seen an increase in the frequency of extreme drought events and progressive increases in air temperature across Amazonia (Aragão et al., 2007; Marengo et al., 2008; Phillips et al., 2009; Lewis et al., 2011; Jiménez-Muñoz et al., 2013; Jiménez-Muñoz et al., 2016) and climate model projections suggest these trends will continue in the future (Marengo et al., 2018). Over the past 3 decades Amazonian forests have also experienced changes in floristic and functional composition likely due to on-going changes in climate and atmospheric CO₂, favouring taxa that are more affiliated to drier environments and that occur along a wide precipitation gradient (Esquivel-Muelbert et al., 2018). Similar patterns have been reported in response to El Niño induced drought in Panama (Feeley et al. 2011) and to long-term drought in Ghana (Fauset et al., 2012; Aguirre-Gutiérrez et al., 2019). Understanding the mechanisms which underpin such compositional shifts in response to drought is crucial for an improved ability to predict the response of tropical forests to climate change.

Hydraulic traits, such as embolism resistance and hydraulic safety margins are physiological traits intrinsically related to plant ability to withstand water shortage (Tyree & Zimmermann, 2002; Anderegg et al., 2016; Choat et al., 2018) and have been found to be important predictors of drought-induced mortality in experimental studies, mainly on saplings and seedling of temperate tree species (Adams et al. 2017). Under drought, drying soil and increasing atmospheric demand progressively increase xylem tension, which may cause embolism and blockage of water flow (Tyree & Zimmermann, 2002). Xylem embolism resistance metrics describe the ability of the xylem to maintain functionality under increasingly negative water potentials (ψ_{50} and ψ_{88} (MPa)) and are commonly quantified as the water potentials resulting in 50 (ψ_{50}) and 88% (ψ_{88}) of xylem conductance loss (Sperry et al., 1988; Choat et al., 2012). Hydraulic safety margins (HSM_{50} and HSM_{88}), defined as the difference between leaf water potential at the peak

of the dry season (ψ_{\min}) and ψ_{50} or ψ_{88} , integrate soil and atmospheric water stress and stomatal regulation (Delzon and Cochard, 2014). This metric quantifies the *in situ* proximity (or even exceedance) of leaf water potential to critical embolism thresholds (Choat et al., 2012; Choat et al., 2018).

Embolism resistance has been shown to vary spatially across Amazonian forests (see Chapter 2), with seasonal Western Amazon forest having lower embolism resistance and narrower safety margins than seasonal Central-Eastern Amazon forests. Furthermore, embolism resistance has been demonstrated to be phylogenetically conserved among Amazonian clades (see Chapter 3) and that certain plant families (*e.g.* Fabaceae) are markedly resistant to embolism. At local scales, embolism resistance has been shown to drive Amazonian species distribution along a topographical gradient (Oliveira et al. 2018) and local niche segregation (Brum et al. 2018). Consistent with drought affecting more large trees (Bennett et al., 2015), xylem resistance to embolism has been shown to also relate to tree size, with large trees having more vulnerable xylem than small trees (Rowland et al., 2015). Finally, it has been found that two species which exhibited lower mortality in Amazonian drought experiments had more negative ψ_{50} values than two species which were more sensitive to drought (Powell et al., 2017). However, all of these studies have been localised in nature and largely restricted to single sites.

Hydraulic safety margins have been shown to decrease during intensive drought in the Central-Eastern Amazon, in tandem with drops in sap velocity and in whole tree hydraulic conductance (Fontes et al., 2018). These results indicate the potential of hydraulic safety margins to reflect tree drought responses, ultimate risk of hydraulic failure and to affect forest functioning. Consistent with these findings, across the Amazon basin, hydraulic safety margins, and not embolism resistance (ψ_{50} and ψ_{88}), reflect long term biomass changes at community level, with communities which have narrow safety margin showing reduced biomass sink strength in the past decades (see Chapter 2). Additionally, hydraulic safety margins and embolism resistance have been also shown to be strongly correlated with species-level aboveground biomass gain increments in a cloud forest in Atlantic forest region (Eller et al., 2018). However, the role of hydraulic safety margins in explaining species-level ecology and response to drought across large tropical domains remains unknown.

Here I use a unique data-set of hydraulic traits (ψ_{50} , ψ_{88} , HSM_{50} , HSM_{88}) consistently measured across 87 tree canopy and subcanopy species in the Western Amazon, spanning a broad precipitation gradient, to evaluate to what extent hydraulic traits are related to pan-Amazonian species biographical distribution (Esquivel-Muelbert et al., 2017a), life-history strategies traits (Coelho de Souza et al., 2016), and drought-induced mortality (Esquivel-Muelbert et al., 2017b). I further compare the predictive power of hydraulic traits in explaining the biogeography, life history strategies and resistance to drought of Amazonian tree species with the predictive power of two other traits believed to have important functional significance: wood density and non-structural carbohydrate (NSC) concentrations. Wood density is often thought of as one the traits that best reflects the classical growth-survival ecological trade-off and has been shown to be a significant predictor of both growth rate and mortality rates in Amazonian forests (Chao et al. 2008). NSCs are important for several metabolic functions (Martinez-Vilalta et al. 2016), and have also been suggested to enhance the resistance of plants to drought stress (O'Brien *et al.* 2014).

Esquivel-Muelbert et al. (2017) demonstrated that seasonality of drought constrains tree taxa distribution in the Western Neotropics, and that tree taxa have fundamentally different Water Deficit Affiliations (WDA). Taxa with more negative WDA (dry affiliated taxa) are more adapted to overcome moisture stress and are widely spread in the Neotropics (Esquivel-Muelbert et al., 2017a). Although dry affiliated taxa can also occur in wet places, this is not true for most Amazonian species, which are highly wet affiliated, and whose occurrence is restricted to places with low or no seasonal moisture stress (Esquivel-Muelbert et al., 2017a). Additionally, it has been demonstrated that WDA is related to mortality under drought at genus level, with wet affiliated genera having higher drought-induced mortality than dry affiliated genera (Esquivel-Muelbert et al., 2017b). In this chapter, I formally evaluate the relationship between hydraulic traits and WDA. I also consider the extent to which hydraulic traits relate to fundamental life history strategy traits. Previous work has shown that three traits encompass the major axes of life history variation in Amazonia: tree growth rate, mortality rate and potential size (size that taxa can potentially reach). Thus, I focus on these traits, which have been shown to be to some extent phylogenetically controlled across Amazonian tree taxa (Coelho de Souza et al., 2016). I also relate hydraulic traits to species-level differential

survival under sustained drought (Esquivel-Muelbert et al., 2017b) and thus evaluate the linkage between hydraulics and drought-induced mortality in the Tropics in much more depth than has hitherto been possible (*e.g.* the analysis of Powell et al. (2017) was restricted to four species). Based on findings that show embolism resistance modulating local distribution of species and niche segregation (Oliveira et al., 2018; Brum et al., 2018), I hypothesize that embolism resistance will be related to large-scale species biogeographical distributions, with dry affiliated species having more negative ψ_{50} and ψ_{88} than wet affiliated species. I also hypothesize that species potential size will correlate with resistance to embolism. Additionally, I predict that species growth rate will be related to both embolism resistance and hydraulic safety margins but that drought induced mortality risk will only be related to hydraulic safety margin.

4.2 Methods

4.2.1. Plot characteristics

The analyses presented in this chapter use trait data from 87 species measured in 7 permanent forest plots distributed across the Western Amazon (Table A3.1). The plots are part of the RAINFOR forest inventory network (Malhi et al., 2002) curated by the ForestPlots.net database (Peacock et al., 2007; Lopez-Gonzalez et al., 2011). All plots are lowland, *terra-firme*, structurally intact forests. In all seven plots, 100% of tree stems with DBH of at least 10 cm were identified to species level. The plots encompass a wide environmental range, with mean annual precipitation varying from 1127 to 2880 mm, soil texture from 16 to 46 Clay percentage and soil fertility from 110 to 478 mg.kg⁻¹ of P_{total}. In general, compared to other parts of Amazon Basin, the Western Amazon is characterized by its relatively soil fertility, high forest productivity and high forest turnover rates (Quesada et al., 2012; Malhi et al., 2015; Johnson et al., 2016).

4.2.2. Species characteristics

To select species for sampling, I accessed single census inventory data of each plot from ForestPlots.net database (Lopez-Gonzalez et al., 2009; Lopez-Gonzalez et al., 2011), calculated species relative dominance in basal area terms, and then selected the most dominant species at each plot. Selection was restricted to dicotyledonous trees with

DBH>10 cm. The set of 79 selected species spans a broad spectrum of life-history characteristic traits (Fig 4.1) and includes most hyperdominant Amazonian species in terms of number of tree stems (Ter Steege et al., 2013) and woody productivity (Fauset et al., 2015).

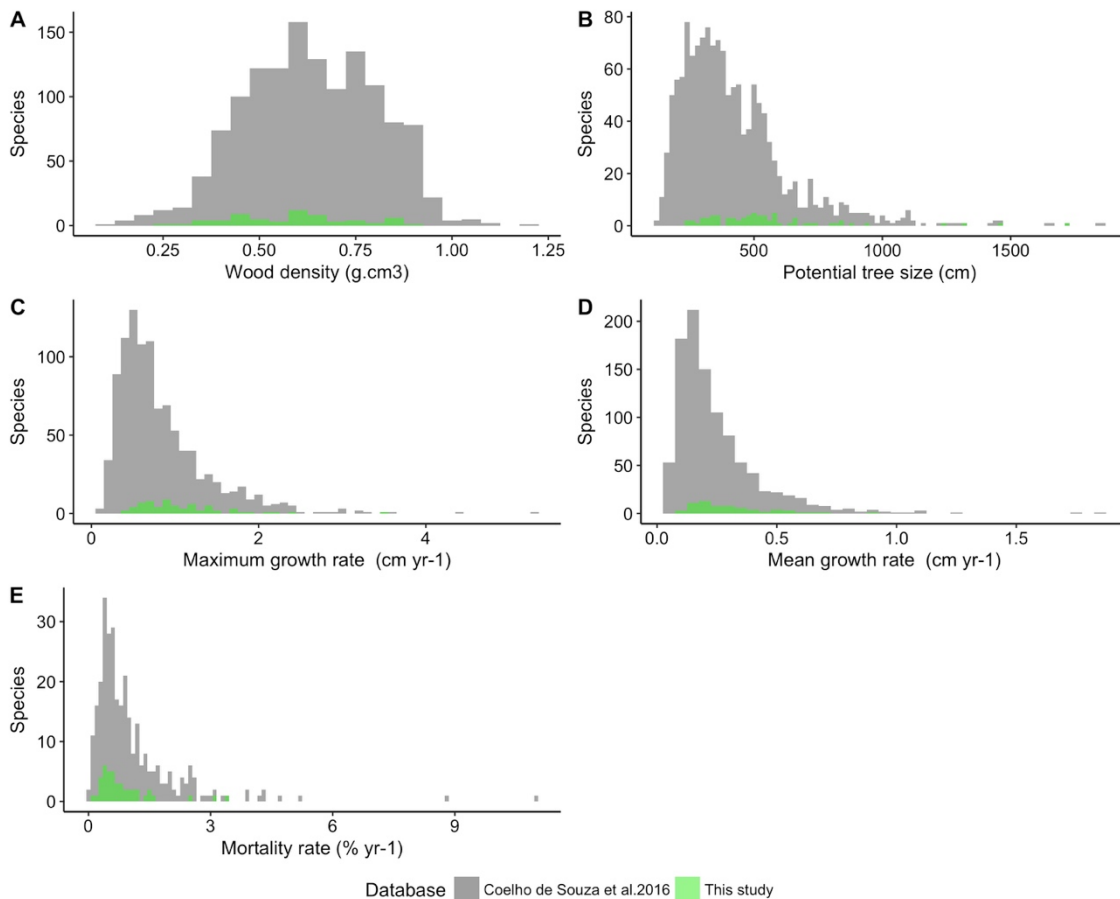


Figure 4. 1 Functional trait range of the 87 sampled species in the Western Amazon. Histograms of life-history related traits range of the sampled species in the Western Amazon (green) in relation to pan-Amazonian life-history range (grey). A) Species mean wood density (g.cm^3) (Zanne et al., 2009; Chave et al., 2014); B) Species Potential size, calculated as the 95th percentile of diameter distribution (cm); C) Species Maximum growth, calculated as the 95th percentile of growth rates distribution (cm yr^{-1}); D) Species Mean growth rate (cm yr^{-1}); E) Species mortality rate ($\% \text{ yr}^{-1}$). All trait data shown in this figure were extracted from Coelho de Souza et al. (2016). Note that in this chapter I am using only the species sampled in the Western Amazon, representing then a subset from the database shown in the chapters two and three.

4.2.3. Traits

Measured Traits

Embolism resistance, wood density and total non-structural carbohydrates were measured from most basal area dominant canopy and sub canopy tree species (~3 individuals per species) in each site. Top canopy fully sun-exposed branches and leaves (or maximum height possible to be reached by the tree climbers) were collected for all the measured traits. Data collection of these three traits was carried out during predawn in the wet season, to assure maximum hydration of the forests.

To avoid dehydration during transport from the plot to the field laboratory, branches used to measure embolism resistance and wood density had their basal portion wrapped in a wet cloth and were placed into an opaque wet plastic bag, immediately after collection. Xylem embolism resistance was quantified by measuring the amount of air formed inside the branch (Pereira et al., 2016; Bittencourt et al., 2018) due to progressively increase in dehydration (Sperry et al., 1988). Detailed method description is available in the section 2.2.5 of this thesis.

To quantify total non-structural carbohydrates, immediately after collection, branches and leaves were bagged using Ziplocs, placed into cooling boxes filled with ice and then transport from the site to the field laboratory. The samples were transferred to paper bags and put into microwave at the maximum power for 3min. Afterwards, the samples were dried in oven for at least 48 hours at approximately 65 °C and then sent to the UNICAMP university to be analysed following (Sevanto et al., 2014).

To assess species hydraulic safety margins ($HSM_{50} = \psi_{min} - \psi_{50}$ and $HSM_{88} = \psi_{min} - \psi_{88}$), I measured minimum leaf water potential (ψ_{min}) from 2-6 top mature, healthy and fully sun-exposed leaves from top-canopy branches from the same individuals I measured the other traits. Data collection was done from 11:00 am-2:30 pm during the peak of dry season apart from aseasonal forests, which on average have no months with precipitation < 100mm.

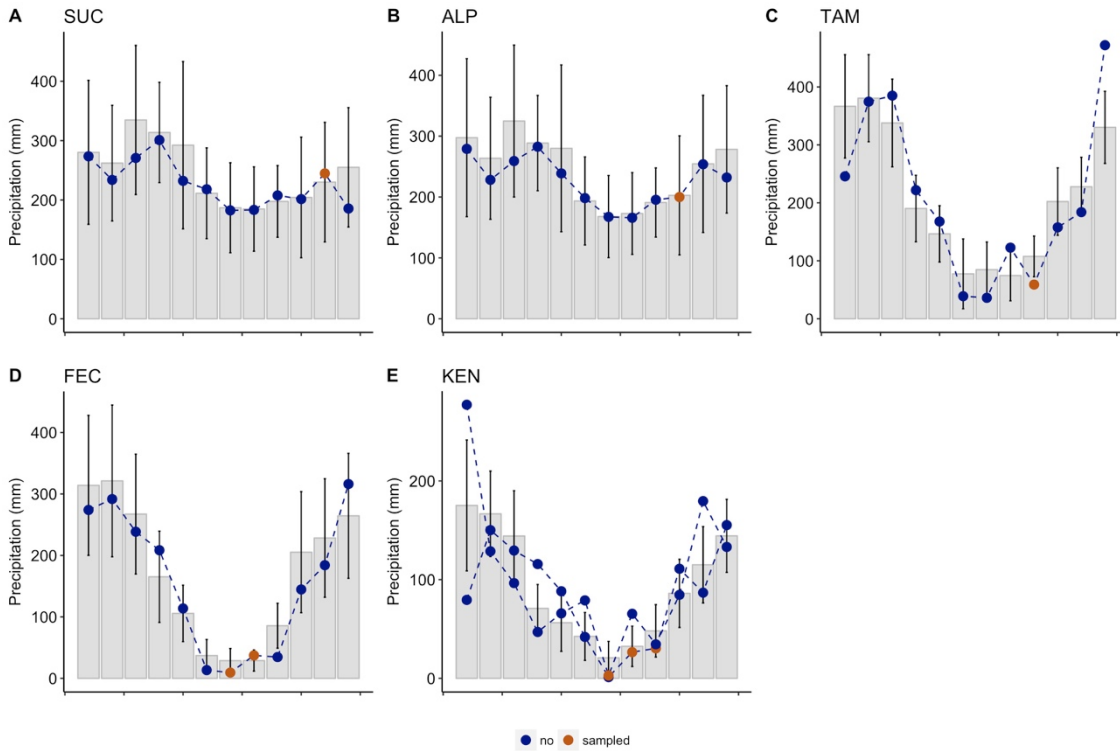


Figure 4. 2 Climatological data when ψ_{\min} was sampled at each site in the Western Amazon. Grey and black bars show the mean and standard deviation of monthly precipitation from 1991 to 2018 (CRU data ts.4.0338). The blue dashed lines represent the year of sampling, while the brown points show the months at which ψ_{\min} was measured. Note that in this chapter I am using only the species sampled in the Western Amazon, representing then a subset from the database shown in the chapters two and three.

Compiled data

To describe Amazonian tree species performance, tree species biogeographic distribution and tree species drought induced mortality, I compiled published data from Coelho de Souza et al. (2016), Esquivel-Muelbert, Baker et al. (2017) and Esquivel-Muelbert et al (2017). Species life-history strategy traits were described by three traits (Coelho de Souza et al., 2016): (1) Species potential size: defined as the 95th percentile of tree diameter distribution from 577 inventory forest plots across the Amazon Basin (2) Species mean growth rate (diameter, cm) and (3) Species mean stem mortality, both calculated using 257 inventory plots across the entire Basin for which data from multiple censuses was available.

To describe Amazonian species-level biogeographical distributions, I used Water Deficit Affiliation (WDA) data (Esquivel-Muelbert et al., 2017a), which describes a

species preference for wet or dry habitat. WDA is calculated as the mean dry season severity across the plots where the species occurs weighted by its relative abundance in each of 513 forest plots broadly distributed in the Western Neotropics. More negative WDA values represent dry affiliated species, while wet affiliated species are represented by less negative WDA values.

Species drought induced mortality data were obtained from Esquivel-Muelbert, Galbraith, et al. (2017). The dataset compiles tree drought induced mortality responses, calculated as the difference (Δm) between mortality rate under drought conditions and baseline mortality rate for each tree species with DBH at least 10 cm and with minimum of 2 individuals. The dataset contains Δm values from two drought experiments (Tapajos - TAP and Caxiuana - CAX) and one natural drought (1982-83 El Nino Barro Colorado Island - BCI). Baseline mortality (mortality under normal conditions) was calculated based on control plot mortality rates for the experimental droughts and post-drought interval mortality rates for the natural drought.

4.2.4 Data analysis

Standardized major axis regressions (SMA) were performed to evaluate the relationship between species mean hydraulic traits and all other evaluated traits. To assess whether there is a relationship between hydraulic traits and life-history traits, I subset the data into *water-limited* forests and *non-water* limited forest. Non-water limited forests include three plots (ALP-1, ALP2, SUC) with mean annual precipitation higher than 2800 mm and no dry season (*i.e.* no months where average monthly precipitation <100 mm), while *water-limited* forests encompass forests with mean annual precipitation ranging from 1127 to 2542 mm and 3 to 6 dry season length (number of months with precipitation <100mm). To investigate whether there is a relationship between hydraulic traits and life-history traits within and across forest types, I used species mean hydraulic traits for water and non-water limited forests. To test whether hydraulic traits are related to drought-induced mortality, I related species mean hydraulic traits to species Δm at each drought site (TAP, CAX, BCI).

4.3 Results

Relationship among hydraulic traits

Among my dataset of 79 species collected in the Western Amazon, for which Ψ_{\min} and HSM were measured, HSM50 is mostly explained by variation of Ψ_{\min} . In contrast, variation in HSM88 is mainly explained by variation in Ψ_{88} . The positive relationship between embolism resistance and Ψ_{\min} is similar for both Ψ_{50} and Ψ_{88} (Fig. 4.3) with species with more resistant xylem reaching more negative Ψ_{\min} .

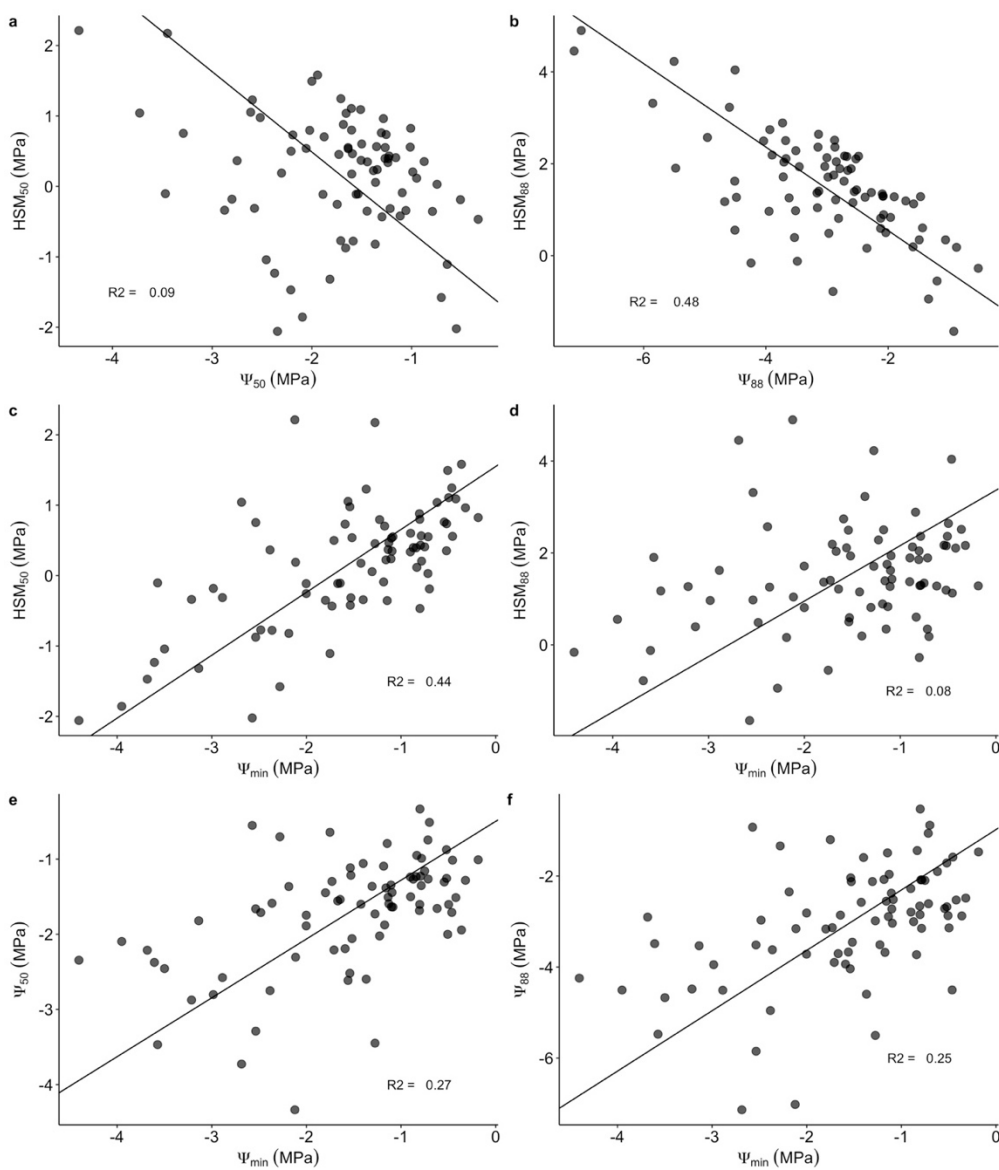


Figure 4.3. Relationship between hydraulic safety margins and Ψ_{\min} and embolism resistance across 79 Western Amazonian tree species. A and B HSM50 versus Ψ_{50}

and Ψ_{\min} , respectively; C and D HSM88 versus Ψ_{88} and Ψ_{\min} , respectively. D and E: embolism resistance versus Ψ_{\min} , Solid lines represent significant ($p \leq 0.05$) standardized major axis (SMA) regression. R² of each regression is displayed on the figure.

Relationship between key hydraulic traits and species biogeographical distribution

I find a moderately strong positive relationship between embolism resistance (ψ_{50} and ψ_{88}), minimum leaf water potential and species water deficit affiliation (WDA) (ψ_{50} : SMA $r^2=0.22$, $p<0.0001$ and ψ_{88} SMA $r^2=0.18$, $p<0.001$, SMA $r^2=0.34$, $p<0.0001$ Fig. 4.4). In our dataset, WDA ranged from -552 to 0. Overall the xylem of wet affiliated species (less negative WDA), which have mesophilic distribution, are more vulnerable to embolism formation, compared to species affiliated to dry conditions (more negative WDA) and that reach more negative minimum leaf water potential. There is no relationship between water deficit affiliation and hydraulic safety margins (HSM) (Fig. 4.4)

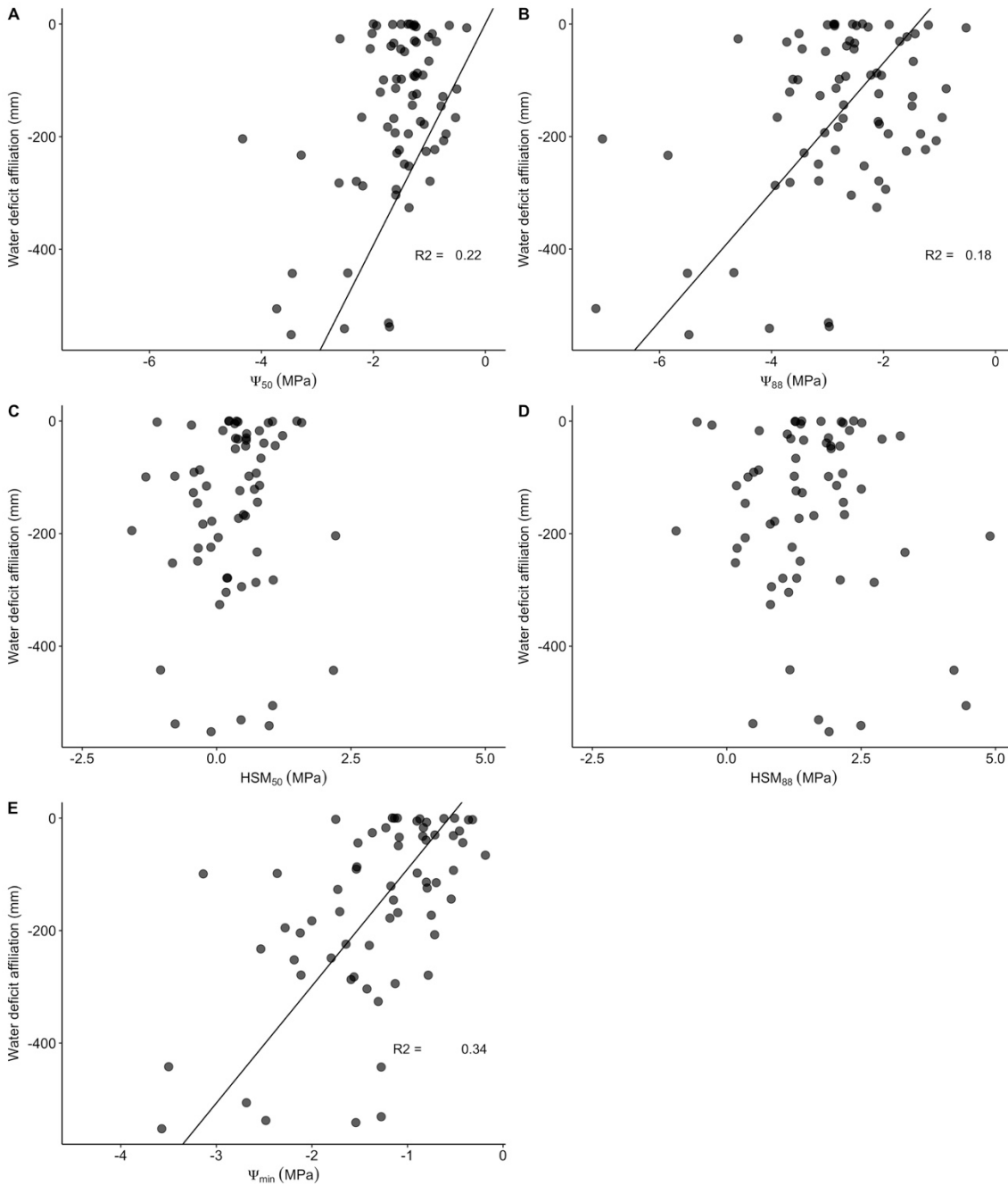


Figure 4.4 Relationship between water deficit affiliation and hydraulic traits: Species mean hydraulic embolism resistance (A, B), species mean hydraulic safety margins (C, D) and minimum leaf water potential (E). Less negative WDA denote wet affiliated species and more negative WDA denote dry affiliated species. WDA data were obtained from (Esquivel-Muelbert et al., 2017a). Significant standard major axis regressions are shown by regression lines.

Relationship between key hydraulic traits and life-history strategy traits

I find that ψ_{88} and HSM_{88} , not ψ_{50} and HSM_{50} , are related to some life-history strategy traits (Fig. 4.5). Mean growth rate decreases significantly with increases of

HSM₈₈ (SMA r²=0.08, p=0.03), with species which have high mean growth rate across the basin, having narrower HSM₈₈ than species with low growth rate. Mean stem mortality rate is positively related to ψ_{88} (SMA r²=0.16, p=0.04), when restricting ψ_{88} sampled to water limited forests. In these forests, species with less resistant xylem (less negative ψ_{88}) are associated with higher mean stem mortality rate across the basin. No relationship is found between potential diameter size and any of the evaluated traits and no relationship is found between ψ_{min} and any of the evaluated life-history traits.

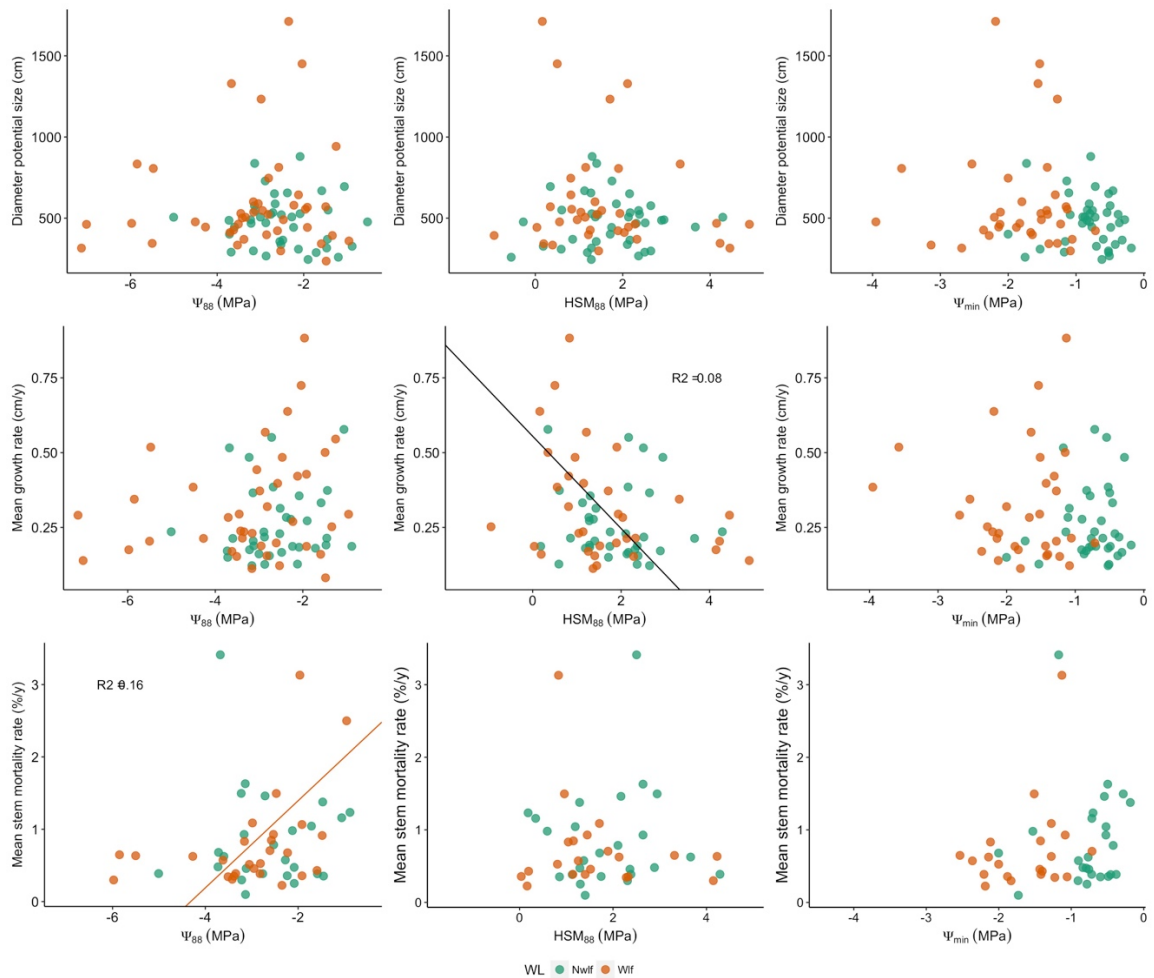


Figure 4.5 Relationship between species mean key hydraulic traits and life-history strategy traits. Species present in water limited forests (seasonal and transitional forests) and non-water limited forests (aseasonal forests) are represented with orange and green points, respectively. Tree performance data at species level were obtained from (Coelho de Souza et al., 2016). Significant standard major axis regressions are shown by regression lines.

Relationship between hydraulic traits and drought induced-mortality

No relationship is found between mortality induced by drought and embolism resistance and minimum leaf water potential. Meanwhile, hydraulic safety margins (HSM_{50} and HSM_{88}) and drought induced mortality are strongly negatively correlated across sites (drought experiments: CAX and TAP and natural drought: BCI) and significant at TAP site individually, indicating that species with narrow hydraulic safety have high mortality under drought (HSM_{50} : SMA $r^2=0.25$, $p=0.03$ and HSM_{88} : SMA $r^2=0.24$, $p=0.03$, Fig. 4.6). Considering only TAP drought experiment, 56% of the variation in species drought induced mortality is explained by HSM_{88} ($p=0.05$), while the relationship with HSM_{50} is marginally insignificant (SMA $r^2=0.53$, $p=0.07$).

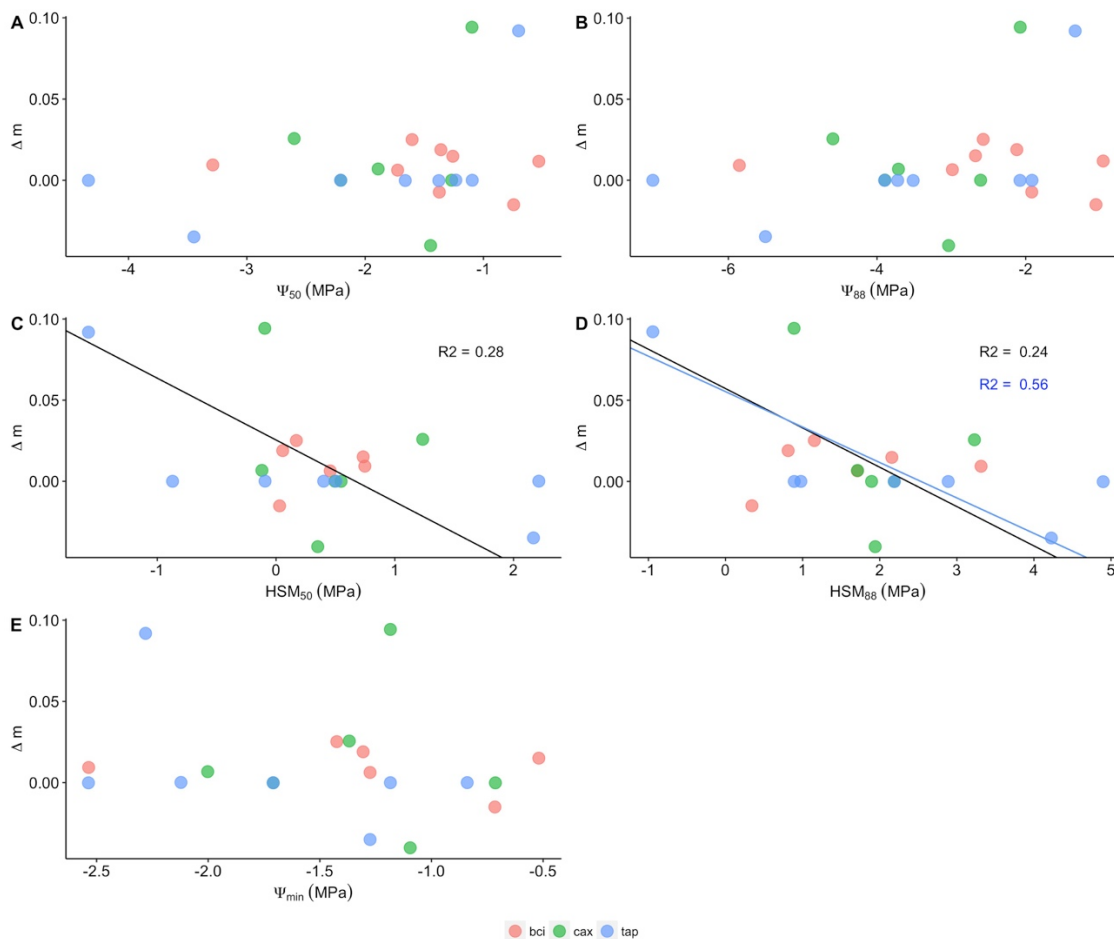


Figure 4.6 Relationship between species mean hydraulic traits and drought induced-mortality. Drought experiments in Caxiutana and Tapajos are represented as green and blue, respectively. Natural drought in BCI (Panama) is represented as red. Data of drought induced mortality at species level were obtained from (Esquivel-Muelbert et al., 2017b). Black line show SMA regression across studies and blue line represents SMA regression within Tapajos drought experiment. Significant standard major axis regressions are shown by regression lines.

To confirm that the observed relationships between embolism resistance vs water deficit affiliation, hydraulic traits vs life-history strategy traits and hydraulic safety margins vs drought-induced mortality were not obtained by chance, I performed SMA regressions with branch wood density and total non-structural carbohydrates (NSC) at branch and leaf levels as alternative predictor variables. These traits were measured for the same individuals on which hydraulic traits were assessed. Despite wood density being correlated with mean growth rate and strongly correlated with stem mortality rate, I found no relationship between wood density and WDA or (Δm). Similarly, NSCs had no predictive power in explaining biogeographical distribution and drought-induced mortality (Fig. 4.7; Table A3. 3). However, different to wood density and embolism resistance, which are traits relatively with less variation within individuals, NSC measurements are more dynamic traits, varying across time (time of the day and seasonally). The results presented in this study must therefore be interpreted carefully, as NSC only represent values for one single point in time (predawn of wet season) per organ per individual.

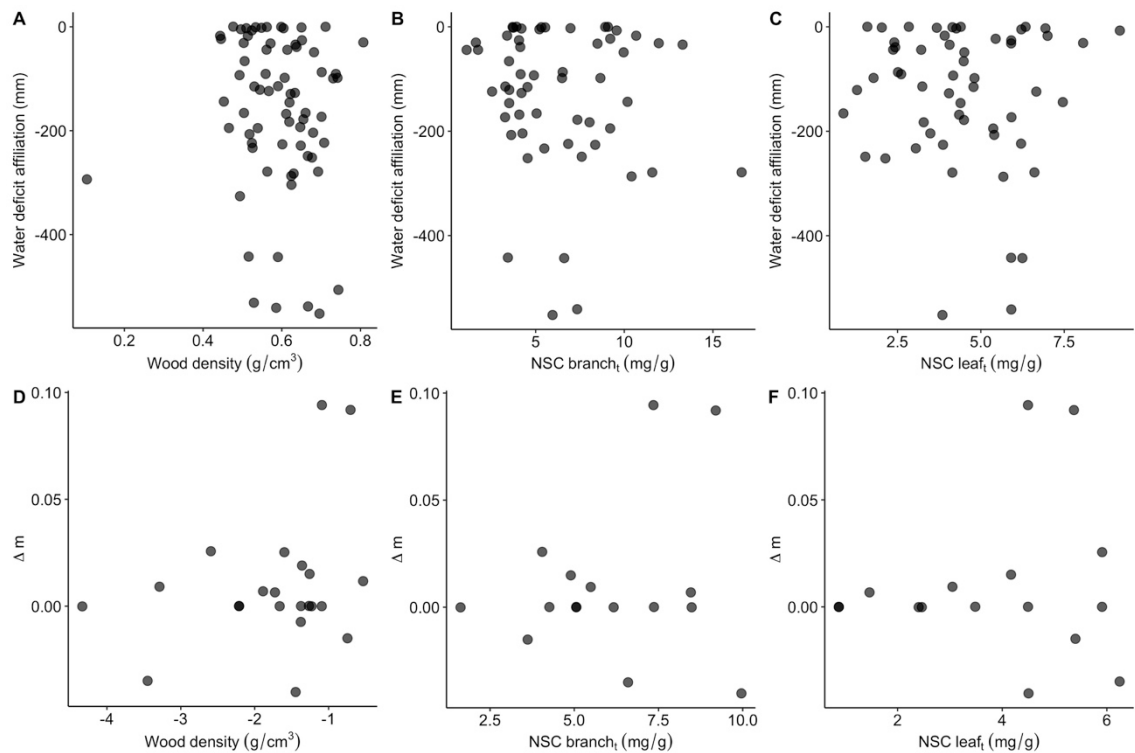


Figure 4.7 Relationship between species mean wood density, Non-structural carbohydrates (NSC) at branch and leaf level with water deficit affiliation (WDA)

and drought induced-mortality (Δm). Δm was investigated in the drought experiments of Caxiuana and Tapajos and in the natural drought occurred in BCI (Panama). Data of drought induced mortality at species level were obtained from (Esquivel-Muelbert et al., 2017b). The absence of regression lines show that no significant relationships were found using standard major axis regressions.

4.4 Discussion

This is the first study to evaluate the extent to which hydraulic traits of Amazonian tree species are related to their biogeographical distribution, life-history strategies and drought-induced mortality. I find that among Amazonian tree species, embolism resistance (Ψ_{50} and Ψ_{88}) reflect species biogeographical distribution. In terms of life-history traits, Ψ_{88} is moderately related (in water-limited forests) to Amazonian species background mortality while HSM_{88} is weakly related to pan-Amazonian species mean growth rate. These relationships do not hold true for Ψ_{50} and HSM_{50} . No relationship is found between evaluated hydraulic traits and pan-Amazonian species mean potential size, inferred from diameter at breast height data. Mortality under drought is explained by both HSM_{50} and HSM_{88} and not by embolism resistance.

Embolism resistance reflect species biogeographical distribution of Amazonian trees

This study demonstrates, for the first time, that embolism resistance is associated with species bioclimatic distribution within Amazonia and that the water deficit affiliation, as calculated by Esquivel-Mulbert et al. (2017) is indeed related to plant physiological characteristics. These findings corroborate the hypothesis that species biogeographical distributions along a precipitation gradient are constrained by physiological features. Indeed, xylem resistance to embolism has been shown to be a fundamental trait underlying species distribution and plant evolution (Maherali et al., 2004; Markesteijn et al., 2011; Trueba et al., 2017; Larter et al., 2017), as it is a key feature to withstand the progressive increase in the xylem tension due to water stress (Tyree & Zimmermann, 2002). For example, a worldwide meta-analysis using multiple methodologies and plant life forms and stages, has demonstrated that the increase of embolism resistance has allowed species to occur in dry habitats (Maherali et al., 2004). In consonance with these findings, I show that embolism resistance explains

approximately 20% of the Amazonian tree species WDA variation, and that wet affiliated species, generally restricted to areas of low or no seasonality, are more vulnerable to embolism. This result is also in line with other tropical study to evaluate the relationship between species occurrence patterns and embolism resistance, which also found positive relationship between embolism resistance and the proportion of 13 species occurrence across sites in New Caledonia (Trueba et al., 2017).

Species with narrower safety margins have higher species mean growth rates and species with more vulnerable xylem in water limited forests have higher background stem mortality rates.

I find that species with narrower HSM_{88} have higher pan-Amazonian species mean growth rate than species with broader HSM_{88} , in agreement with the findings of Eller et al. (2018) for a cloud forest in Brazil. As HSM reflects the coordination of stomata and hydraulic strategies, this result can be understood as high growth rate species opening more their stomata to maximize carbon uptake and grow faster, but at a higher risk of hydraulic failure. Indeed, species with narrow HSM_{88} have vulnerable xylem to embolism formation (SMA: $r^2=0.48$, $p<0.001$, fig A3. 1 and table A3. 1). In line with this explanation, fast-growth species tend to have a shorter life-span than slow-growing species (Reich, 2014). However, I do not find any relationship between HSM_{88} and background mortality rate.

The results from this second analysis (species life-history traits) give some indication about how hydraulic traits relate to demographic traits, but they need to be carefully interpreted. Using Pan-Amazonian values instead of more refined data could potentially be the reason why I find weak or null relationships between some traits. For example, contrary to expectations, species potential size is not related to either embolism resistance or hydraulic safety margins. Additionally, my results suggest no relationship between embolism resistance and growth rate. These results run contrary to expectations. Recent local-scale study in the Atlantic rainforest has proposed the existence of a growth-vulnerability trade-off whereby faster-growing species have more vulnerable xylem (Eller et al., 2018). Although my data do not support such a trade-off across the broader set of Western-Amazonian tree taxa, the absence of a relationship should be interpreted carefully. In contrast to Eller et al. (2018), I did not use individual measurements of

growth. Instead, I used pan-Amazonian species mean growth rates which aggregate across a large range of different site conditions. Further studies using a more refined data (e.g. species mean per site or individual values) are needed to test the generality of these findings among Amazon tree species.

I find a moderate relationship ($r^2 = 0.16$) between background species mean mortality rate and species mean Ψ_{88} across water limited forests. Ψ_{88} has been suggested to be more related to a lethal threshold in Angiosperms (Urli et al., 2013b; Delzon and Cochard, 2014; Choat et al., 2018) and thus it follows expectations that species with lower mortality rates in drought prone systems have more negative Ψ_{88} values. Additionally, in terms of life-history strategies, this finding is consistent with the wood and hydraulic traits spectrum (Chave et al., 2009), where long life-span species (lower background mortality rate), invest more in wood traits and robust xylem (higher embolism resistance) than short life span species.

Low hydraulic safety margins are related to high drought-induced mortality

Finally, I not only investigate the potential relationship between hydraulic traits and background mortality, but also whether these traits are related to drought-induced mortality. Differently from what is found for background mortality, hydraulic safety margins (HSM_{50} and HSM_{88}) and not embolism resistance (Ψ_{88}), determine species mortality responses to drought. However, caution must be applied to these results as hydraulic safety margins were often not determined in the same sites as the drought sites. These results are based only on a set of 22 species, for which it was possible to calculate mortality caused by drought and hydraulic traits were available. The generality of these results requires further testing, perhaps exploring other drought-responses, such as species or tree growth-anomalies following recent extreme drought events in Amazon.

4.5 Implications and Conclusion

In conclusion, this study shows for the first time that Amazonian species dry/wet affiliation is related to hydraulic architecture. As wet affiliated species, which represent a vast portion of Amazonian tree biodiversity (Esquivel-Muelbert et al., 2017a), have vulnerable xylem to embolism, potential future biodiversity decreases can be expected,

with shifts in floristic composition and changes in species distribution. These predictions are in line with observations from previous studies (Esquivel-muelbert et al., n.d.; Fauset et al., 2012; Aguirre-Gutiérrez et al., 2019). Additionally, this study indicates the function of hydraulic safety margin in underpinning species mean growth rate and mortality under drought and consequently, how HSMs affect forest productivity and biomass dynamics, in line with chapter 2 of this thesis. Species with broad HSMs and low growth rate have more buffering capacity to deal with changes in drought regime, which are expected to decrease HSM (Fontes et al., 2018), than fast-growth species with narrow safety margins, which are expected to have high drought-induced mortality. Finally, this work also emphasizes the explanatory power of hydraulic traits in predicting species distribution and mortality under drought which other traits, such as branch wood density and leaf and branch non-structural carbohydrates appear not to have.

Chapter 5: Synthesis and Conclusions

In this final chapter, I synthesise the main objectives and findings from the three data chapters present in this thesis, discuss the implications of my findings and their contribution to the field and suggest future follow-on research.

5.1 Research synthesis and implications

This study investigated hydraulic properties of Amazonian tree across a broad precipitation gradient, spanning a wide set of species and strategies. This involved the collection of the largest tropical database on plant hydraulic traits (embolism resistance and hydraulic safety margins) thus far assembled. This new traits dataset was then related to forest structure data available across multiple inventory plots distributed across the entire Amazonian domain (RAINFOR (Malhi et al., 2002; Lopez-Gonzalez et al., 2011)) to better understand the predictive power of hydraulic traits. The first two data chapters (chapters 2 and 3) focussed on understanding variation of hydraulic traits across forests and within tree taxa. The results from these chapters demonstrated that hydraulic vulnerability is highly variable across sites and that there is a phylogenetic signal to these traits, with most of the variation found across families. In chapter 4, I combined hydraulic traits with demographic and species distribution traits and also tested whether hydraulic traits could explain tree responses under drought. These analyses indicate a key role of hydraulic traits in predicting Amazonian species biogeographical distributions, life history strategies and mortality under drought.

I found that embolism resistance and hydraulic safety margins varied across Amazonian forest types and that site water availability, species composition, soil texture and biogeographic region play important roles in explaining this variation. Integrating the spatial analyses from chapters 2 and and taxon-level analyses from Chapter 3, I constructed the first pan-Amazonian map of embolism resistance.

This study also demonstrates the importance of hydraulic safety margin in explaining community-level biomass sink, species growth rate and drought induced mortality and the importance of xylem embolism resistance in explaining species biogeographical distributions. Other traits evaluated, including wood density and non-

structural carbohydrate concentrations, do not appear to have this predictive capacity. Together, these results provide us with novel insights as to which forests and taxa in Amazonia are likely to be most affected by future amplification of water stress induced by altered rainfall regimes and elevated temperatures. More specifically, I find that tree communities in the Western Amazon, which have the largest species richness in the basin (Phillips and Miller, 2002; Esquivel-Muelbert et al., 2017a), are especially vulnerable to drought, having lower embolism resistance and narrower hydraulic safety margins than other regions. Forests in the southern fringe of the Amazon, where climate has been changing most rapidly and where deforestation has been especially marked, were found to have the most negative hydraulic safety margins and appear to be the forests facing most imminent drought risk. Overall, our results suggest that on-going and future changes in climate in these regions may lead to an increase in tree mortality, biodiversity reduction, changes in species distribution, shifts in forest composition and reduction of the Amazon biomass sink.

My work makes several key contributions to the existing literature in the field. The major contributions are outlined below.

5.1.1 Drought sensitivity and vulnerability is highly variable across Amazonian forests (Chapter 2)

This thesis advances the research field by presenting a novel, fully standardized, pan-Amazonian dataset of hydraulic traits. The dataset encompasses 129 tree species, which account for ~ 24% of the total Amazon aboveground biomass (Fauset et al., 2015), sampled across broad a climatological range, including some of the Amazon's driest and wettest forest regions. The species sampled belong to 36 families, which are among the most dominant families in Amazon in terms of abundance (Ter Steege et al., 2006; Ter Steege et al., 2013) and productivity (Fauset et al., 2015).

Prior to the work undertaken in this thesis, knowledge of the hydraulic characteristics of Amazonian trees could be best described as incipient. Indeed, published records of xylem vulnerability to embolism and hydraulic safety margin existed for only four well-studied sites in the central and eastern Amazon (Caxiuanã, Manaus, Tapajós and Paracou – French Guiana) (Rowland et al., 2015; Powell et al., 2017; Oliveira et al., 2018; Santiago et al., 2018; Brum et al., 2018; Fontes et al., 2018; Barros et al., 2019),

with no data at all for the Western and southern Amazon. My thesis specifically targeted these unstudied regions of the Amazon, making possible the first holistic evaluation of vulnerability to drought across the Basin. Currently, there are only 46 Amazonian adult tree species for which information on hydraulic safety margin and xylem vulnerability to cavitation have been published. My thesis now increases this number to 170, thus effectively trebling the number of species for which we have measurements of critical hydraulic traits. Furthermore, I use a completely standardized approach to sampling and measuring hydraulic traits, allowing a level of comparability across sites and species that is not possible through meta-analyses that pool data from across multiple sampling methods (e.g. Choat et al., 2012).

My results cast a new light on the sensitivity of Amazonian forests to drought. Most of our knowledge to date of drought impacts on Amazon forests had been informed by two drought experiments in eastern Amazonia: Caxiuanã and Tapajós. Following the imposition of drought, both of these forests were characterised by 2-3 years whereby there was a limited effect on tree mortality, followed by marked increases thereafter, especially in the largest trees (e.g. (Nepstad et al., 2007; da Costa et al., 2010; Rowland et al., 2015). Following 7 years of drought in Caxiuanã, the forest had lost approximately 20% of its aboveground biomass (da Costa et al. 2010), rising to over 40% after 12 years. However, my results suggest that the two drought experiment sites may be atypical with respect to their hydraulic properties. For example, community-level ψ_{88} in Tapajós is the lowest recorded across any of our study sites, while in Caxiuanã it is much lower than would be expected given its background rainfall status and is on par with values obtained for the driest regions of the Amazon (see Fig 2.5). My results suggest that large regions of the Amazon are likely to be more sensitive to drought than these two forests, and thus the drought experiments to be expected to underestimate responses in other Amazonian regions.

My results also highlight for the first time the importance of soils in the determination of community-level hydraulic safety margins. Although I found no relationship at all between hydraulic safety margins and background water availability, I find that communities on sandy soils generally have lower hydraulic safety margins than those on clay soils. This adds nuance to previous findings suggesting a global convergence of hydraulic safety margins, as I show that this appears to be true with

respect to background rainfall availability but is not necessarily true with respect to soil texture.

5.1.2 Embolism resistance is phylogenetically constrained within Amazonian tree taxa (Chapter 3)

A fundamental question for understanding the impacts of water stress on plant communities is the extent to which key traits are labile or plastic versus the extent to which they are pre-conditioned genetically. Before this thesis, no study had examined the phylogenetic basis of the drought sensitivity of tropical forest taxa. I used the most up-date molecular-based phylogenetic tree of Amazon tree genera (Coelho de Souza et al., 2019) to demonstrate a strong phylogenetic signature in embolism resistance across Amazonian taxa. Furthermore, this signature was most evident at family level as some families such as the Fabaceae were found to exhibit marked resistance to embolism. This result has important implications for understanding the community-level responses of Amazonian forests to water stress. First, the existence of a strong phylogenetic signal allowed us interpolate community-weighted embolism resistance given species abundance data to gain a better understanding of which communities are most sensitive to water stress. Second, the strong phylogenetic signal implies an important evolutionary control on embolism resistance which may mean that Amazonian taxa have a limited capacity to quickly adjust their hydraulic architecture in response to enhanced water stress. The extension of this limited adaptive capacity to water stress is that continued amplification of water stress in the Amazon would likely lead to compositional changes via floristic sorting, as less-adapted species become less competitive. The relationship I find between embolism resistance and species biogeographical distributions (Chapter 4) further supports this inference.

5.1.3 Hydraulic traits predict species biogeographical distribution, growth rates, background mortality rate and mortality induced by drought (Chapter 4) and community-level carbon sink strength (Chapter 2)

My work reveals that hydraulic traits are important controls on plant function in Amazonia, both at the species level and at the stand-level. While some studies have previously reported relationships between species-level hydraulic properties and growth

rates (e.g. Eller et al. 2018) or hinted at relationships with drought-induced mortality (e.g. Rowland et al. 2015, Powell et al. 2018), these have largely been limited to single sites and a small number of species. Similarly, previous studies have explored the relationship between embolism resistance and species distribution locally (Oliveira et al. 2018), but never at a large-scale. Using the power of the largest tropical forest inventory dataset, I was able to explore the relationships between hydraulic traits and species-level biogeographical distributions, mean growth rates and mean mortality rates across Amazonia. My expanded hydraulic traits database allowed me to test the predictive power of hydraulic traits for explaining drought-induced mortality in two drought experiments and, for the first time, to evaluate the extent to which stand-level carbon sink strength is coordinated with community-level hydraulic attributes.

My findings reveal significant relationships between xylem embolism resistance and species-level background mortality rates and also with water deficit affiliation (biogeographical distribution). Hydraulic safety margin, on the other hand, were found to be important predictors of species-level mean growth, drought-induced mortality and community-level biomass sink strength, thus highlighting the key role that this trait plays not only on plant function but in response to stress and changing environmental conditions. I find that communities characterised by taxa with low hydraulic safety margins (e.g. in Mato Grosso or Acre) are gaining less biomass than those with high safety margins (e.g. in the Tapajos region). This result indicates that high safety margin forests are more able to utilise increasing atmospheric CO₂ concentrations to increase biomass storage than low safety margin forests. This may be due to two mechanisms: 1) low minimal water potentials may induce stomatal closure and thus productivity in low HSM sites or 2) low HSM may result in increased tree mortality losses and thus reduced biomass storage.

The high predictive power of hydraulic traits that I document in this thesis highlights the importance of their inclusion in ecosystem models that predict the effects of climate change on the composition and function of tropical forests. A new generation of ‘trait-based’ models now simulate ecosystem functioning based on commonly-measured traits such as leaf mass per area and wood density (e.g. Fyllas et al., 2014). The inclusion of hydraulic traits in this context is a very recent development (e.g.

Christoffersen et al., 2016), but one which my findings suggest is pivotal for robust simulation of the impacts of climate change on ecosystem function.

5.2 Future research directions

5.2.1 Expanded site sampling of hydraulic traits

In this thesis I measured hydraulic traits (embolism resistance and hydraulic safety margins) for 129 Amazonian species across a wide environmental gradient to test whether there are differences in hydraulic vulnerability across Amazon forests (Chapter 2) and used these measurements to impute community-level hydraulic traits for 582 forests across the Amazon (Chapter 3). Although my results allow for a first large-scale perspective of hydraulic trait variation across Amazonia, they are still only based on 11 sites and further sampling is necessary to confirm some of the patterns we observe. In terms of additional sampling across Amazonian forests, I identify three immediate priorities: 1) measuring more sites along the southern fringe of the Amazon, 2) measuring sites in the Guiana Shield and 3) measuring more extensively along a sand-clay soil gradient.

In Chapter 2, I found that the most vulnerable site, in terms of community-weighted hydraulic safety margins, was found in the southern fringe of the central Amazon, in Mato Grosso state. This region of the Amazon has faced the greatest recent climatic changes (Fu et al., 2013; Nobre et al., 2016) of all Amazonian regions, both in terms of strengthening of the dry season and increases in maximum air temperatures. The very low hydraulic safety margins observed in this site point to substantial hydraulic stress and may indicate that this region of the Amazon is most imminently at risk. However, this finding is based on only one forest in which I have hydraulic traits. Future studies expanding sampling in this region are important for testing the generality of this pattern.

The pan-Amazonian map of xylem resistance to embolism constructed in Chapter 3 suggests that forests in the Guiana Shield have a relatively high resistance to embolism. This result emerges from the phylogenetic imputation applied to the species abundance data available for this region. However, I made no actual measurements in this region. To confirm the validity of the map, it is essential that hydraulic traits are sampled in this region of the Amazon, which is characterised by high biomass and productivity but low

turnover (Johnson et al., 2016). More generally, broader sampling is needed to fully validate the map. For example, the map suggests that Ecuadorian forests in general have xylem properties that render them sensitive to water stress, while Venezuelan forests have more robust xylem. However, we did not specifically measure hydraulic traits in Ecuador or Venezuela.

Finally, more work is needed to fully confirm the role of soil texture in modulating hydraulic safety margins. In Chapter 2, I find that plant communities on sandy soils have lower hydraulic safety margins than those on clay soils. However, our sites were unevenly distributed along the sand-clay axis. Most (6/11) sites actually had low clay content (<25% clay). To increase confidence in this result, more sampling in higher-clay sites is important. Given the important role of background rainfall as a predictor of xylem resistance to embolism, studies which span a soil texture gradient but share the same climate would be especially useful.

Finally, other tropical forests beyond Amazonia remain poorly characterised with respect to their hydraulic traits. Hydraulic trait data is missing for large swathes of tropical forests. For example, no hydraulic trait information is available for the Congo Basin, the world's second-largest expanse of tropical forest. Similarly, the hydraulic attributes of Southeast Asian rainforests are effectively unknown. To compare continental patterns of drought sensitivity and vulnerability, it is important to expand sampling to also include these Paleotropical forests.

5.2.2 Calculating phylogenetic signal using an inevitably incomplete phylogeny

The analyses presented in the third chapter were all conducted at genus-level and using an incomplete phylogeny. Thus, the extent of phylogenetic signal in the present study may be an outcome of the taxonomic scale and the incomplete phylogeny used. However, because trait variation is often greater among than within genera (i.e. species belonging to the same genera tend to be more similar to each other than different genera belonging to the same family), I expect that refining the taxonomic level would increase even more the strength of similarity among lineages.

I cannot easily predict how including more lineages would affect the extent of signal found here because the impact of adding more lineages will strongly depend on which lineages are missing. For example, although this study includes a wide range of

climate and soil types, the majority of samples forest sites are moist forests on relatively nutrient poor soils. Including lineages restricted to seasonally dry tropical forests (STDFs), where water is limited and soils are generally richer, could possibly reduce the extent of signal found here. Lineages occurring in STDFs are generally widespread across the phylogeny and due to water limitation may have evolved particularly hydraulic properties to survive in this environment. In contrast, I expect that including temperate lineages may increase even more the extent of the signal found here. Temperate lineages are clustered within angiosperms (Judd et al., 1994) and may also have evolved specifically hydraulic properties to survive in freezing environments. Therefore, because the magnitude of the signal could possibly change with complete phylogenetic and trait information, investigating the link between hydraulic properties and evolutionary relationships among lineages merits further studies.

5.2.3 Intraspecific variation in hydraulic traits

In this study, I measured hydraulic traits for 8 species that occurred in at least 3 sites differing by at least 50 mm in maximum climatological water deficit. This sample size of common species did not allow me to adequately address intraspecific variation across different precipitation regimes. Furthermore, the low number of replicates per species (~3 individuals per species) also made it difficult to study intraspecific variation. The phylogenetic signal found for embolism resistance (Chapter 3) suggests low lability of this trait. In agreement with this finding, most of the embolism resistance variation found across a broad climatic gradient in Catalonian forests was due to interspecific, rather than intra-specific variation (Rosas et al., 2019). However, Oliveira *et al.* (2018) found some evidence of plasticity in embolism resistance along topographical gradients, despite species maintaining their relative rank degrees of embolism resistance. Further studies are needed, ideally tracking individual species across broad edapho-climatic gradients, to quantify the extent of lability in hydraulic traits for Amazonian species.

5.2.4 The anatomical underpinnings of embolism resistance

In Chapter 3, I found that lineages that have been shown to consistently have pit vesturing are more emboli-resistant than those where this feature is consistently absent. This analysis provided the first indication that vested pits may increase embolism

resistance in Amazonian taxa. However, I did not specifically determine whether the individuals sampled possessed vestured pits or not. Future studies should adopt a more refined approach and evaluate the presence or absence of vestured pits in the same species or even on the same individuals for which embolism resistance is measured.

5.2.5 Relating hydraulic traits to function

In Chapter 4, I assessed the potential relationship between hydraulic traits and life-history strategy traits, as well as drought induced mortality. I found that hydraulic safety margin and not embolism resistance is related to species mean growth rate. The absence of relationships between embolism resistance and growth rate (Eller et al., 2018) and potential size are unexpected (Rowland et al., 2015; Bennett et al., 2015) and may possibly be explained by the fact I used pan-Amazonian species, which aggregate one value per species across the whole basin. Further investigation using a more refined approach (e.g. species mean per site or individual values) is needed to fully corroborate these findings. Similarly, the generality of the relationship found between hydraulic safety margins and species drought induced mortality needs further testing. This relationship is particularly remarkable within the context that species hydraulic safety margins were not determined at the same sites as the drought sites. This implies that there is a species-level signature to hydraulic safety margins, but this needs to be tested much more broadly. Repeated measurements of *in situ* leaf water potential, which allow hydraulic safety margins to be tracked over time for trees experiencing drought are critical for fully validating this relationship.

I also find in Chapter 4 that wood density and non-structural carbohydrates have no power in predicting species-level biogeographical distributions, life history traits or mortality under drought. This suggests a differential role for hydraulic traits in terms of their ability to predict function. To fully evaluate this, I intend to extend the analyses undertaken in Chapter 4 to include other trait data for my target species including commonly measured leaf economic traits such as leaf mass per area (LMA) and leaf nutrient concentrations. Lack of predictive power for these traits would further support the case that hydraulic traits represent ‘supertraits’ that have much more predictive power in explaining whole-tree function than other traits.

Finally, in future work, I plan to relate the evaluated traits to other hydraulic traits such as xylem and leaf specific conductance, leaf area to sapwood area ratio, leaf water potential regulation and stomatal control. I collected these traits during my field campaigns but they remain unanalysed. This further work will allow me to understand the coordination of xylem resistance and stomatal control and also allow me to assess the evidence for the existence of a hydraulic safety-efficiency trade-off across Amazonian species.

5.3 Final remarks

This thesis has enabled significant advances in our understanding of how sensitive Amazonian forests are to water stress. These advances include: 1) the first large-scale mapping of hydraulic properties across Amazonia, 2) the first analysis to link forest-level carbon sink strength with community-level hydraulic traits, 3) the documentation of strong phylogenetic signal in xylem embolism resistance across Amazonian taxa and 4) elucidation of the important role of hydraulic traits in predicting species-level biogeography, life history strategies and response to drought. These advances have allowed the scientific community to understand which Amazon forests and taxa are most sensitive/vulnerable to drought and provide the modelling community with invaluable mechanistic insights for developing more accurate predictions of the future impact of climate change on Amazonian forests.

References

Adams, H.D., Zeppel, M.J.B., Anderegg, W.R.L., Hartmann, H., Landhäusser, S.M., Tissue, D.T., Huxman, T.E., Hudson, P.J., Franz, T.E., Allen, C.D., Anderegg, L.D.L., Barron-Gafford, G.A., Beerling, D.J., Breshears, D.D., Brodrigg, T.J., Bugmann, H., Cobb, R.C., Collins, A.D., Dickman, L.T., Duan, H., Ewers, B.E., Galiano, L., Galvez, D.A., Garcia-Forner, N., Gaylord, M.L., Germino, M.J., Gessler, A., Hacke, U.G., Hakamada, R., Hector, A., Jenkins, M.W., Kane, J.M., Kolb, T.E., Law, D.J., Lewis, J.D., Limousin, J.M., Love, D.M., Macalady, A.K., Martínez-Vilalta, J., Mencuccini, M., Mitchell, P.J., Muss, J.D., O'Brien, M.J., O'Grady, A.P., Pangle, R.E., Pinkard, E.A., Piper, F.I., Plaut, J.A., Pockman, W.T., Quirk, J., Reinhardt, K., Ripullone, F., Ryan, M.G., Sala, A., Sevanto, S., Sperry, J.S., Vargas, R., Vennetier, M., Way, D.A., Xu, C., Yopez, E.A. and McDowell, N.G. 2017. A multi-species synthesis of physiological mechanisms in drought-induced tree mortality. *Nature Ecology and Evolution*. **1**(9), pp.1285–1291.

Aguirre-Gutiérrez, J., Oliveras, I., Rifai, S., Fauset, S., Adu-Bredu, S., Affum-Baffoe, K., Baker, T.R., Feldpausch, T.R., Gvozdevaite, A., Hubau, W., Kraft, N.J.B., Lewis, S.L., Moore, S., Niinemets, Ü., Peprah, T., Phillips, O.L., Ziemnińska, K., Enquist, B., Malhi, Y. and Sciences, E. 2019. Drier tropical forests are susceptible to functional changes in response to a long-term drought. *Ecology Letters*. **22**(5), pp.855-865.

Anderegg, W.R.L., Berry, J.A. and Field, C.B. 2012. Linking definitions, mechanisms, and modeling of drought-induced tree death. *Trends in Plant Science*. **17**(12), pp.693–700.

Anderegg, W.R.L., Klein, T., Bartlett, M., Sack, L., Pellegrini, A.F.A., Choat, B. and Jansen, S. 2016. Meta-analysis reveals that hydraulic traits explain cross-species patterns of drought-induced tree mortality across the globe. *Proceedings of the National Academy of Sciences*. **113**(18), pp.5024–5029.

Aragão, L.E.O.C., Malhi, Y., Roman-Cuesta, R.M., Saatchi, S., Anderson, L.O. and Shimabukuro, Y.E. 2007. Spatial patterns and fire response of recent Amazonian droughts. *Geophysical Research Letters*. **34**(7), p.L07701.

Araujo-Murakami, A., Doughty, C.E., Metcalfe, D.B., Silva-Espejo, J.E., Arroyo, L., Heredia, J.P., Flores, M., Sibling, R., Mendizabal, L.M., Pardo-Toledo, E., Vega, M., Moreno, L., Rojas-Landivar, V.D., Halladay, K., Girardin, C.A.J., Killeen, T.J. and Malhi, Y. 2014. The productivity, allocation and cycling of carbon in forests at the dry margin of the Amazon forest in Bolivia. *Plant Ecology and Diversity*. **7**(1–2), pp.55–69.

Barros, F. de V., Bittencourt, P.R.L., Brum, M., Restrepo-Coupe, N., Pereira, L., Teodoro, G.S., Saleska, S.R., Borma, L.S., Christoffersen, B.O., Penha, D., Alves, L.F., Lima, A.J.N., Carneiro, V.M.C., Gentine, P., Lee, J.E., Aragão, L.E.O.C., Ivanov, V., Leal, L.S.M., Araujo, A.C. and Oliveira, R.S. 2019. Hydraulic traits explain differential responses of Amazonian forests to the 2015 El Niño-induced drought. *New Phytologist*. **223**(3), pp.1253–1266.

Batterman, S.A., Hedin, L.O., Van Breugel, M., Ransijn, J., Craven, D.J. and Hall, J.S. 2013. Key role of symbiotic dinitrogen fixation in tropical forest secondary succession. *Nature*. **502**(7470), pp.224–227.

Bennett, A.C., Mcdowell, N.G., Allen, C.D. and Anderson-Teixeira, K.J. 2015. Larger trees suffer most during drought in forests worldwide. *Nature Plants*. **1**(10), pp.1–5.
Bittencourt, P., Pereira, L. and Oliveira, R. 2018. Pneumatic Method to Measure Plant Xylem Embolism. *Bio-Protocol*. **8**(20), pp.1–14.

Blomberg, S.P., Garland, T. and Ives, A.R. 2003. Testing for phylogenetic signal in comparative data: Behavioral traits are more labile. *Evolution*. **57**(4), pp.717–745.

Boyle, B., Hopkins, N., Lu, Z., Raygoza Garay, J.A., Mozzherin, D., Rees, T., Matasci, N., Narro, M.L., Piel, W.H., Mckay, S.J., Lowry, S., Freeland, C., Peet, R.K. and Enquist, B.J. 2013. The taxonomic name resolution service: An online tool for automated standardization of plant names. *BMC Bioinformatics*. **14**(1), p.16.

Brienen, R.J.W., Phillips, O.L., Feldpausch, T.R., Gloor, E., Baker, T.R., Lloyd, J., Lopez-Gonzalez, G., Monteagudo-Mendoza, A., Malhi, Y., Lewis, S.L., Vásquez-Martinez, R., Alexiades, M., Álvarez Dávila, E., Alvarez-Loayza, P., Andrade, A., Aragaõ, L.E.O.C., Araujo-Murakami, A., Arets, E.J.M.M., Arroyo, L., Aymard C., G.A., Bánki, O.S., Baraloto, C., Barroso, J., Bonal, D., Boot, R.G.A., Camargo, J.L.C., Castilho, C. V., Chama, V., Chao, K.J., Chave, J., Comiskey, J.A., Cornejo Valverde, F., Da Costa, L., De Oliveira, E.A., Di Fiore, A., Erwin, T.L., Fauset, S., Forsthofer, M., Galbraith, D.R., Grahame, E.S., Groot, N., Hérault, B., Higuchi, N., Honorio Coronado, E.N., Keeling, H., Killeen, T.J., Laurance, W.F., Laurance, S., Licona, J., Magnussen, W.E., Marimon, B.S., Marimon-Junior, B.H., Mendoza, C., Neill, D.A., Nogueira, E.M., Núñez, P., Pallqui Camacho, N.C., Parada, A., Pardo-Molina, G., Peacock, J., Penã-Claros, M., Pickavance, G.C., Pitman, N.C.A., Poorter, L., Prieto, A., Quesada, C.A., Ramírez, F., Ramírez-Angulo, H., Restrepo, Z., Roopsind, A., Rudas, A., Salomaõ, R.P., Schwarz, M., Silva, N., Silva-Espejo, J.E., Silveira, M., Stropp, J., Talbot, J., Ter Steege, H., Teran-Aguilar, J., Terborgh, J., Thomas-Caesar, R., Toledo, M., Torello-Raventos, M., Umetsu, R.K., Van Der Heijden, G.M.F., Van Der Hout, P., Guimarães Vieira, I.C., Vieira, S.A., Vilanova, E., Vos, V.A. and Zagt, R.J. 2015. Long-term decline of the Amazon carbon sink. *Nature*. **519**(7543), pp.344–348.

Brodribb, T.J. 2017. Progressing from ‘functional’ to mechanistic traits. *New Phytologist*. **215**(1), pp.9–11.

Brodribb, T.J., Bowman, D.J.M.S., Nichols, S., Delzon, S. and Burslem, R. 2010. Xylem function and growth rate interact to determine recovery rates after exposure to extreme water deficit. *New Phytologist*. **188**(2), pp.533–542.

Brum, M., Vadeboncoeur, M.A., Ivanov, V., Asbjornsen, H., Saleska, S., Alves, L.F., Penha, D., Dias, J.D., Aragaõ, L.E.O.C., Barros, F., Bittencourt, P., Pereira, L. and Oliveira, R.S. 2018. Hydrological niche segregation defines forest structure and drought tolerance strategies in a seasonal Amazon forest. *Journal of Ecology*. **107**(1), pp.318-333.

Chao, K.J., Phillips, O.L., Gloor, E.G., Monteagudo, A., Torres-Lezama, A. and Martinez, R.V. 2008. Growth and wood density predict tree mortality in Amazon forests. *Journal of Ecology* 96:281-292.

Chave, J., Coomes, D., Jansen, S., Lewis, S.L., Swenson, N.G. and Zanne, A.E. 2009. Towards a worldwide wood economics spectrum. *Ecology Letters*. **12**(4), pp.351–366.

Chave, J., Réjou-Méchain, M., Búrquez, A., Chidumayo, E., Colgan, M.S., Delitti, W.B.C., Duque, A., Eid, T., Fearnside, P.M., Goodman, R.C., Henry, M., Martínez-Yrizar, A., Mugasha, W.A., Muller-Landau, H.C., Mencuccini, M., Nelson, B.W., Ngomanda, A., Nogueira, E.M., Ortiz-Malavassi, E., Pélissier, R., Ploton, P., Ryan, C.M., Saldarriaga, J.G. and Vieilledent, G. 2014. Improved allometric models to estimate the aboveground biomass of tropical trees. *Global Change Biology*. **20**(10), pp.3177-3190.

Choat, B., Drayton, W.M., Brodersen, C., Matthews, M.A., Shackel, K.A., Wada, H. and McElrone, A.J., 2010. Measurement of vulnerability to water stress-induced cavitation in

grapevine: a comparison of four techniques applied to a long-vesseled species. *Plant, Cell & Environment*, **33**(9), pp.1502-1512.

Choat, B., Brodribb, T.J., Brodersen, C.R., Duursma, R.A., López, R. and Medlyn, B.E. 2018. Triggers of tree mortality under drought. *Nature*. **558**(7711), pp.531–539.

Choat, B., Cobb, A.R. and Jansen, S. 2008. Structure and function of bordered pits: New discoveries and impacts on whole-plant hydraulic function. *New Phytologist*. **177**(3), pp.608–626.

Choat, B., Jansen, S., Brodribb, T.J., Cochard, H., Delzon, S., Bhaskar, R., Bucci, S.J., Feild, T.S., Gleason, S.M., Hacke, U.G., Jacobsen, A.L., Lens, F., Maherali, H., Martínez-Vilalta, J., Mayr, S., Mencuccini, M., Mitchell, P.J., Nardini, A., Pittermann, J., Pratt, R.B., Sperry, J.S., Westoby, M., Wright, I.J. and Zanne, A.E. 2012. Global convergence in the vulnerability of forests to drought. *Nature*. **491**(7426), pp.752–755.

Choat, B., Jansen, S., Zwieniecki, M.A., Smets, E. and Holbrook, N.M. 2004. Changes in pit membrane porosity due to deflection and stretching: The role of vested pits. *Journal of Experimental Botany*. **55**(402), pp.1569–1575.

Christenhusz, M.J. and Byng, J.W., 2016. The number of known plants species in the world and its annual increase. *Phytotaxa*, **261**(3), pp.201-217.

Christoffersen, B.O., Gloor, M., Fauset, S., Fyllas, N.M., Galbraith, D.R., Baker, T.R., Kruijt, B., Rowland, L., Fisher, R.A., Binks, O.J., Sevanto, S., Xu, C., Jansen, S., Choat, B., Mencuccini, M., McDowell, N.G. and Meir, P. 2016. Linking hydraulic traits to tropical forest function in a size-structured and trait-driven model (TFS v.1-Hydro). *Geoscientific Model Development*. **9**(11), pp.4227–4255.

Cierner, C., Boers, N., Hirota, M., Kurths, J., Müller-Hansen, F., Oliveira, R.S. and Winkelmann, R. 2019. Higher resilience to climatic disturbances in tropical vegetation exposed to more variable rainfall. *Nature Geoscience*. **12**(3), pp.174-179.

Clinebell, R.R., Phillips, O.L., Gentry, A.H., Stark, N. and Zuuring, H. 1995. Prediction of neotropical tree and liana species richness from soil and climatic data. *Biodiversity and Conservation*. **4**(1), pp.56–90.

Cochard, H. and Delzon, S. 2013a. Hydraulic failure and repair are not routine in trees. *Annals of Forest Science*. **70**(7), pp.659–661.

Cochard, H., Badel, E., Herbette, S., Delzon, S., Choat, B. and Jansen, S., 2013b. Methods for measuring plant vulnerability to cavitation: a critical review. *Journal of Experimental Botany*, **64**(15), pp.4779-4791.

Coelho de Souza, F., Dexter, K.G., Phillips, O.L., Brienen, R.J.W., Chave, J., Galbraith, D.R., Gonzalez, G.L., Mendoza, A.M., Toby Pennington, R., Poorter, L., Alexiades, M., Álvarez-Dávila, E., Andrade, A., Aragão, L.E.O.C., Araujo-Murakami, A., Arets, E.J.M.M., Aymard C., G.A., Baraloto, C., Barroso, J.G., Bonal, D., Boot, R.G.A., Camargo, J.L.C., Comiskey, J.A., Valverde, F.C., De Camargo, P.B., Di Fiore, A., Elias,

F., Erwin, T.L., Feldpausch, T.R., Ferreira, L., Fyllas, N.M., Gloor, E., Herault, B., Herrera, R., Higuchi, N., Coronado, E.N.H., Killeen, T.J., Laurance, W.F., Laurance, S., Lloyd, J., Lovejoy, T.E., Malhi, Y., Maracahipes, L., Marimon, B.S., Marimon-Junior, B.H., Mendoza, C., Morandi, P., Neill, D.A., Vargas, P.N., Oliveira, E.A., Lenza, E., Palacios, W.A., Peñuela-Mora, M.C., Pipoly, J.J., Pitman, N.C.A., Prieto, A., Quesada, C.A., Ramirez-Angulo, H., Rudas, A., Ruokolainen, K., Salomão, R.P., Silveira, M., Stropp, J., Steege, H. Ter, Thomas-Caesar, R., Van Der Hout, P., Van Der Heijden, G.M.F., Van Der Meer, P.J., Vasquez, R. V., Vieira, S.A., Vilanova, E., Vos, V.A., Wang, O., Young, K.R., Zagt, R.J. and Baker, T.R. 2016. Evolutionary heritage influences amazon tree ecology. *Proceedings of the Royal Society B: Biological Sciences*. **283**(1844), p.20161587.

Coelho de Souza, F.C., Dexter, K.G., Phillips, O.L., Pennington, R.T., Neves, D., Sullivan, M.J., Alvarez-Davila, E., Alves, Á., Amaral, I., Andrade, A. and Aragao, L.E., 2019. Evolutionary diversity is associated with wood productivity in Amazonian forests. *Nature ecology & evolution*, **3**(12), pp.1754-1761.

Crisp, M.D. and Cook, L.G., 2012. Phylogenetic niche conservatism: what are the underlying evolutionary and ecological causes?. *New Phytologist*, **196**(3), pp.681-694.

da Costa, A.C.L., Galbraith, D., Almeida, S., Fisher, R., Phillips, O., Metcalfe, D., Levy, P., Portela, B., Costa, M. and Meir, P. 2010. Effect of seven years of experimental drought on the aboveground biomass storage of an eastern Amazonian rainforest. *New Phytologist*. **187**(3), pp.579–591.

Cox, P.M., Betts, R.A., Jones, C.D., Spall, S.A. and Totterdell, I.J. 2000. Acceleration of global warming due to carbon-cycle feedbacks in a coupled climate model. *Nature*. **408**(6809), pp.184–187.

Cox, P.M., Harris, P.P., Huntingford, C., Betts, R.A., Collins, M., Jones, C.D., Jupp, T.E., Marengo, J.A. and Nobre, C.A. 2008. Increasing risk of Amazonian drought due to decreasing aerosol pollution. *Nature*. **453**(7192), pp.212–215.

Crisp, M.D., Arroyo, M.T.K., Cook, L.G., Gandolfo, M.A., Jordan, G.J., McGlone, M.S., Weston, P.H., Westoby, M., Wilf, P. and Linder, H.P. 2009. Phylogenetic biome conservatism on a global scale. *Nature*. **458**(7239), pp.754–756.

Currie, D.J., Mittelbach, G.G., Cornell, H. V., Field, R., Guégan, J.F., Hawkins, B.A., Kaufman, D.M., Kerr, J.T., Oberdorff, T., O'Brien, E. and Turner, J.R.G. 2004. Predictions and tests of climate-based hypotheses of broad-scale variation in taxonomic richness. *Ecology Letters*. **7**(12), pp.1121–1134.

Delzon, S. and Cochard, H. 2014. Recent advances in tree hydraulics highlight the ecological significance of the hydraulic safety margin. *New Phytologist*. **203**(2), pp.355–358.

Dexter, K. and Chave, J. 2016. Evolutionary patterns of range size, abundance and species richness in Amazonian angiosperm trees. *PeerJ*. **4**, p.e2402.

Diaz, S., Grigulis, K., Robson, T.M., Lavorel, S., Bello, Francesco De, Que, F., Lavorel, S., de Bello, F., Quetier, F., Grigulis, K. and Robson, T.M. 2007. Incorporating plant functional diversity effects in ecosystem service assessments. *Proceedings of the National Academy of Sciences*. **104**(52), pp.20684–20689.

Dixon, H.H. 1914. *Transpiration and the Ascent of Sap in Plants*. London: Macmillan.
Domec, J.C. and Gartner, B.L. 2001. Cavitation and water storage capacity in bole xylem segments of mature and young Douglas-fir trees. *Trees - Structure and Function*. **15**(4), pp.204–214.

Duffy, P.B., Brando, P., Asner, G.P. and Field, C.B. 2015. Projections of future meteorological drought and wet periods in the Amazon. *Proceedings of the National Academy of Sciences*. **112**(43), pp.13172-13177.

Eller, C.B., Barros, F.V., Bittencourt, P.R.L., Rowland, L., Mencuccini, M. and Oliveira, R.S. 2018. Xylem hydraulic safety and construction costs determine tropical tree growth. *Plant Cell and Environment*. **41**(3), pp.548–562.

Engelbrecht, B.M.J., Comita, L.S., Condit, R., Kursar, T.A., Tyree, M.T., Turner, B.L. and Hubbell, S.P. 2007. Drought sensitivity shapes species distribution patterns in tropical forests. *Nature*. **447**(7140), pp.80–82.

Esquivel-Muelbert, A., Baker, T.R., Dexter, K.G., Lewis, S.L., Brienen, R.J.W., Feldpausch, T.R., Lloyd, J., Monteagudo-Mendoza, A., Arroyo, L., Álvarez-Dávila, E., Higuchi, N., Marimon, B.S., Marimon-Junior, B.H., Silveira, M., Vilanova, E., Gloor, E., Malhi, Y., Chave, J., Barlow, J., Bonal, D., Davila Cardozo, N., Erwin, T., Fauset, S., Hérault, B., Laurance, S., Poorter, L., Qie, L., Stahl, C., Sullivan, M.J.P., ter Steege, H., Vos, V.A., Zuidema, P.A., Almeida, E., Almeida de Oliveira, E., Andrade, A., Vieira, S.A., Aragão, L., Araujo-Murakami, A., Arets, E., Aymard C, G.A., Camargo, P.B., Barroso, J.G., Bongers, F., Boot, R., Camargo, J.L., Castro, W., Chama Moscoso, V., Comiskey, J., Cornejo Valverde, F., Lola da Costa, A.C., del Aguila Pasquel, J., Di Fiore, T., Fernanda Duque, L., Elias, F., Engel, J., Flores Llampazo, G., Galbraith, D., Herrera Fernández, R., Honorio Coronado, E., Hubau, W., Jimenez-Rojas, E., Lima, A.J.N., Umetsu, R.K., Laurance, W., Lopez-Gonzalez, G., Lovejoy, T., Aurelio Melo Cruz, O., Morandi, P.S., Neill, D., Núñez Vargas, P., Pallqui, N.C., Parada Gutierrez, A., Pardo, G., Peacock, J., Peña-Claros, M., Peñuela-Mora, M.C., Petronelli, P., Pickavance, G.C., Pitman, N., Prieto, A., Quesada, C., Ramírez-Angulo, H., Réjou-Méchain, M., Restrepo Correa, Z., Roopsind, A., Rudas, A., Salomão, R., Silva, N., Silva Espejo, J., Singh, J., Stropp, J., Terborgh, J., Thomas, R., Toledo, M., Torres-Lezama, A., Valenzuela Gamarra, L., van de Meer, P.J., van der Heijden, G., van der Hout, P., Vasquez Martinez, R., Vela, C., Vieira, I.C.G. and Phillips, O.L. 2018. Compositional response of Amazon forests to climate change. *Global Change Biology*. **25**(1), pp.39-56.

Esquivel-Muelbert, A., Baker, T.R., Dexter, K.G., Lewis, S.L., ter Steege, H., Lopez-Gonzalez, G., Monteagudo Mendoza, A., Brienen, R., Feldpausch, T.R., Pitman, N., Alonso, A., van der Heijden, G., Peña-Claros, M., Ahuite, M., Alexiades, M., Álvarez Dávila, E., Murakami, A.A., Arroyo, L., Aulestia, M., Balslev, H., Barroso, J., Boot, R.,

Cano, A., Chama Moscoso, V., Comiskey, J.A., Cornejo, F., Dallmeier, F., Daly, D.C., Dávila, N., Duivenvoorden, J.F., Duque Montoya, A.J., Erwin, T., Di Fiore, A., Fredericksen, T., Fuentes, A., García-Villacorta, R., Gonzales, T., Guevara Andino, J.E., Honorio Coronado, E.N., Huamantupa-Chuquimaco, I., Killeen, T.J., Malhi, Y., Mendoza, C., Mogollón, H., Jørgensen, P.M., Montero, J.C., Mostacedo, B., Nauray, W., Neill, D., Vargas, P.N., Palacios, S., Palacios Cuenca, W., Pallqui Camacho, N.C., Peacock, J., Phillips, J.F., Pickavance, G., Quesada, C.A., Ramírez-Angulo, H., Restrepo, Z., Reynel Rodríguez, C., Paredes, M.R., Sierra, R., Silveira, M., Stevenson, P., Stropp, J., Terborgh, J., Tirado, M., Toledo, M., Torres-Lezama, A., Umaña, M.N., Urrego, L.E., Vasquez Martínez, R., Gamarra, L.V., Vela, C.I.A., Vilanova Torre, E., Vos, V., von Hildebrand, P., Vriesendorp, C., Wang, O., Young, K.R., Zartman, C.E. and Phillips, O.L. 2017a. Seasonal drought limits tree species across the Neotropics. *Ecography*. **40**(5), pp.618–629.

Esquivel-Muelbert, A., Galbraith, D., Dexter, K.G., Baker, T.R., Lewis, S.L., Meir, P., Rowland, L., Da Costa, A.C.L., Nepstad, D. and Phillips, O.L. 2017b. Biogeographic distributions of neotropical trees reflect their directly measured drought tolerances. *Scientific Reports*. **7**(1), pp.1–11.

Fauset, S., Baker, T.R., Lewis, S.L., Feldpausch, T.R., Affum-Baffoe, K., Foli, E.G., Hamer, K.C. and Swaine, M.D. 2012. Drought-induced shifts in the floristic and functional composition of tropical forests in Ghana. *Ecology Letters*. **15**(10), pp.1120–1129.

Fauset, S., Johnson, M.O., Gloor, M., Baker, T.R., Monteagudo M., A., Brien, R.J.W., Feldpausch, T.R., Lopez-Gonzalez, G., Malhi, Y., Ter Steege, H., Pitman, N.C.A., Baraloto, C., Engel, J., Pétronelli, P., Andrade, A., Camargo, J.L.C., Laurance, S.G.W., Laurance, W.F., Chave, J., Allie, E., Vargas, P.N., Terborgh, J.W., Ruokolainen, K., Silveira, M., Aymard C., G.A., Arroyo, L., Bonal, D., Ramírez-Angulo, H., Araujo-Murakami, A., Neill, D., Hérault, B., Dourdain, A., Torres-Lezama, A., Marimon, B.S., Salomão, R.P., Comiskey, J.A., Réjou-Méchain, M., Toledo, M., Licona, J.C., Alarcón, A., Prieto, A., Rudas, A., Van Der Meer, P.J., Killeen, T.J., Marimon Junior, B.H., Poorter, L., Boot, R.G.A., Stergios, B., Torre, E.V., Costa, F.R.C., Levis, C., Schiatti, J., Souza, P., Groot, N., Arets, E., Moscoso, V.C., Castro, W., Coronado, E.N.H., Peña-Claros, M., Stahl, C., Barroso, J., Talbot, J., Vieira, I.C.G., Van Der Heijden, G., Thomas, R., Vos, V.A., Almeida, E.C., Davila, E.Á., Aragão, L.E.O.C., Erwin, T.L., Morandi, P.S., De Oliveira, E.A., Valadão, M.B.X., Zagt, R.J., Van Der Hout, P., Loayza, P.A., Pipoly, J.J., Wang, O., Alexiades, M., Cerón, C.E., Huamantupa-Chuquimaco, I., Di Fiore, A., Peacock, J., Camacho, N.C.P., Umetsu, R.K., De Camargo, P.B., Burnham, R.J., Herrera, R., Quesada, C.A., Stropp, J., Vieira, S.A., Steininger, M., Rodríguez, C.R., Restrepo, Z., Muelbert, A.E., Lewis, S.L., Pickavance, G.C. and Phillips, O.L. 2015. Hyperdominance in Amazonian forest carbon cycling. *Nature Communications*. **6**(1), pp.1–9.

Feldpausch, T.R., Lloyd, J., Lewis, S.L., Brien, R.J.W., Gloor, M., Monteagudo Mendoza, A., Lopez-Gonzalez, G., Banin, L., Abu Salim, K., Affum-Baffoe, K., Alexiades, M., Almeida, S., Amaral, I., Andrade, A., Aragão, L.E.O.C., Araujo Murakami, A., Arets, E.J.M., Arroyo, L., Aymard C., G.A., Baker, T.R., Bánki, O.S.,

Berry, N.J., Cardozo, N., Chave, J., Comiskey, J.A., Alvarez, E., De Oliveira, A., Di Fiore, A., Djangbletey, G., Domingues, T.F., Erwin, T.L., Fearnside, P.M., França, M.B., Freitas, M.A., Higuchi, N., Honorio C., E., Iida, Y., Jiménez, E., Kassim, A.R., Killeen, T.J., Laurance, W.F., Lovett, J.C., Malhi, Y., Marimon, B.S., Marimon-Junior, B.H., Lenza, E., Marshall, A.R., Mendoza, C., Metcalfe, D.J., Mitchard, E.T.A., Neill, D.A., Nelson, B.W., Nilus, R., Nogueira, E.M., Parada, A., S.-H. Peh, K., Pena Cruz, A., Peñuela, M.C., Pitman, N.C.A., Prieto, A., Quesada, C.A., Ramírez, F., Ramírez-Angulo, H., Reitsma, J.M., Rudas, A., Saiz, G., Salomão, R.P., Schwarz, M., Silva, N., Silva-Espejo, J.E., Silveira, M., Sonké, B., Stropp, J., Taedoumg, H.E., Tan, S., Ter Steege, H., Terborgh, J., Torello-Raventos, M., Van Der Heijden, G.M.F., Vásquez, R., Vilanova, E., Vos, V.A., White, L., Willcock, S., Woell, H. and Phillips, O.L. 2012. Tree height integrated into pantropical forest biomass estimates. *Biogeosciences*. **9**(8), pp.3381–3403.

Fisher, R.A., Williams, M., de Lourdes Ruivo, M., de Costa, A.L. and Meir, P. 2008. Evaluating climatic and soil water controls on evapotranspiration at two Amazonian rainforest sites. *Agricultural and Forest Meteorology*. **148**(6–7), pp.850–861.

Fontes, C.G., Dawson, T.E., Jardine, K., McDowell, N., Gimenez, B.O., Anderegg, L., Negrón-Juárez, R., Higuchi, N., Fine, P.V.A., Araújo, A.C. and Chambers, J.Q. 2018. Dry and hot: the hydraulic consequences of a climate change-type drought for Amazonian trees. *Philosophical transactions of the Royal Society of London. Series B, Biological sciences*. **373**(1760), p.20180209.

Fu, R., Yin, L., Li, W., Arias, P.A., Dickinson, R.E., Huang, L., Chakraborty, S., Fernandes, K., Liebmann, B., Fisher, R. and Myneni, R.B. 2013. Increased dry-season length over southern Amazonia in recent decades and its implication for future climate projection. *Proceedings of the National Academy of Sciences*. **110**(45), pp.18110–18115.

Fyllas, N.M., Gloor, E., Mercado, L.M., Sitch, S., Quesada, C.A., Domingues, T.F., Galbraith, D.R., Torre-Lezama, A., Vilanova, E., Ramírez-Angulo, H., Higuchi, N., Neill, D.A., Silveira, M., Ferreira, L., Aymard C., G.A., Malhi, Y., Phillips, O.L. and Lloyd, J. 2014. Analysing Amazonian forest productivity using a new individual and trait-based model (TFS v.1). *Geoscientific Model Development*. **7**(4), pp.1251–1269.

Gei, M., Rozendaal, D.M.A., Poorter, L., Bongers, F., Sprent, J.I., Garner, M.D., Aide, T.M., Andrade, J.L., Balvanera, P., Becknell, J.M., Brancalion, P.H.S., Cabral, G.A.L., César, R.G., Chazdon, R.L., Cole, R.J., Colletta, G.D., De Jong, B., Denslow, J.S., Dent, D.H., Dewalt, S.J., Dupuy, J.M., Durán, S.M., Do Espírito Santo, M.M., Fernandes, G.W., Nunes, Y.R.F., Finegan, B., Moser, V.G., Hall, J.S., Hernández-Stefanoni, J.L., Junqueira, A.B., Kennard, D., Lebrija-Trejos, E., Letcher, S.G., Lohbeck, M., Marín-Spiotta, E., Martínez-Ramos, M., Meave, J.A., Menge, D.N.L., Mora, F., Muñoz, R., Muscarella, R., Ochoa-Gaona, S., Orihuela-Belmonte, E., Ostertag, R., Peña-Claros, M., Pérez-García, E.A., Piotto, D., Reich, P.B., Reyes-García, C., Rodríguez-Velázquez, J., Romero-Pérez, I.E., Sanaphre-Villanueva, L., Sanchez-Azofeifa, A., Schwartz, N.B., De Almeida, A.S., Almeida-Cortez, J.S., Silver, W., De Souza Moreno, V., Sullivan, B.W., Swenson, N.G., Uriarte, M., Van Breugel, M., Van Der Wal, H., Veloso, M.D.D.M., Vester, H.F.M., Vieira, I.C.G., Zimmerman, J.K. and Powers, J.S. 2018. Legume abundance along successional and rainfall gradients in Neotropical forests. *Nature Ecology and Evolution*. **2**(7), pp.1104–1111.

- Gentry, A.H 1988. Changes in Plant Community Diversity and Floristic Composition on Environmental and Geographical Gradients. *Annals of the Missouri Botanical Garden*. **75**(1), pp.1–34.
- Hacke, U.G., Sperry, J.S., Pockman, W.T., Davis, S.D. and McCulloh, K.A. 2001. Trends in wood density and structure are linked to prevention of xylem implosion by negative pressure. *Oecologia*. **126**(4), pp.457–461.
- Harris, I., Jones, P.D., Osborn, T.J. and Lister, D.H. 2014. Updated high-resolution grids of monthly climatic observations - the CRU TS3.10 Dataset. *International Journal of Climatology*. **34**(3), pp.623-642.
- Hodnett, M.G., Silva, L.P., Rocha, H.R. and Senna, R.C. 1995. Seasonal soil water storage changes beneath central Amazonian rainforest and pasture. . **170**, pp.233–254.
- Hodnett, M.G. and Tomasella, J. 2002. Marked differences between van Genuchten soil water-retention parameters for temperate and tropical soils: A new water-retention pedo-transfer functions developed for tropical soils. *Geoderma*. **108**(3–4), pp.155–180.
- Holbrook, N.M., Burns, M.J. and Field, C.B., 1995. Negative xylem pressures in plants: a test of the balancing pressure technique. *Science*, **270**(5239), pp.1193-1194.
- Jansen, S., Baas, P., Gasson, P., Lens, F. and Smets, E. 2004. Variation in xylem structure from tropics to tundra: Evidence from vestured pits. *Proceedings of the National Academy of Sciences*. **101**(23), pp.8833–8837.
- Jansen, S., Baas, P., Gasson, P. and Smets, E. 2003. Vestured Pits : Do They Promote Safer Water Transport ? *International Journal of Plant Sciences*. **164**(3), pp.405–413.
- Jansen, S., Baas, P. and Smets, E. 2001. Vestured Pits : Their Occurrence and Systematic Importance in Eudicots. *Taxon*. **50**(1), pp.135–167.
- Jansen, S., Choat, B. and Pletsers, A. 2009. Morphological variation of intervessel pit membranes and implications to xylem function in angiosperms. *American Journal of Botany*. **96**(2), pp.409–419.
- Jansen, S., Smets, E. and Baas, P. 1998. Vestures in woody plants: A review. *IAWA Journal*. **19**(4), pp.347–382.
- Janzen, D.H. 1967. Why Mountain Passes are Higher in the Tropics. *The American Naturalist*. **101**(919), pp.233–249.
- Jiménez-Muñoz, J.C., Mattar, C., Barichivich, J., Santamaría-Artigas, A., Takahashi, K., Malhi, Y., Sobrino, J.A. and Schrier, G. Van Der 2016. Record-breaking warming and extreme drought in the Amazon rainforest during the course of El Niño 2015-2016. *Scientific Reports*. **6**(May), pp.1–7.

Jiménez-Muñoz, J.C., Sobrino, J.A., Mattar, C. and Malhi, Y. 2013. Spatial and temporal patterns of the recent warming of the Amazon forest. *Journal of Geophysical Research Atmospheres*. **118**(11), pp.5204–5215.

Johnson, M.O., Galbraith, D., Gloor, M., De Deurwaerder, H., Guimberteau, M., Rammig, A., Thonicke, K., Verbeeck, H., von Randow, C., Monteagudo, A., Phillips, O.L., Brienen, R.J.W., Feldpausch, T.R., Lopez Gonzalez, G., Fauset, S., Quesada, C.A., Christoffersen, B., Ciais, P., Sampaio, G., Kruijt, B., Meir, P., Moorcroft, P., Zhang, K., Alvarez-Davila, E., Alves de Oliveira, A., Amaral, I., Andrade, A., Aragao, L.E.O.C., Araujo-Murakami, A., Arets, E.J.M.M., Arroyo, L., Aymard, G.A., Baraloto, C., Barroso, J., Bonal, D., Boot, R., Camargo, J., Chave, J., Cogollo, A., Cornejo Valverde, F., Lola da Costa, A.C., Di Fiore, A., Ferreira, L., Higuchi, N., Honorio, E.N., Killeen, T.J., Laurance, S.G., Laurance, W.F., Licona, J., Lovejoy, T., Malhi, Y., Marimon, B., Marimon, B.H., Matos, D.C.L., Mendoza, C., Neill, D.A., Pardo, G., Peña-Claros, M., Pitman, N.C.A., Poorter, L., Prieto, A., Ramirez-Angulo, H., Roopsind, A., Rudas, A., Salomao, R.P., Silveira, M., Stropp, J., ter Steege, H., Terborgh, J., Thomas, R., Toledo, M., Torres-Lezama, A., van der Heijden, G.M.F., Vasquez, R., Guimarães Vieira, I.C., Vilanova, E., Vos, V.A. and Baker, T.R. 2016. Variation in stem mortality rates determines patterns of above-ground biomass in Amazonian forests: implications for dynamic global vegetation models. *Global Change Biology*. **22**(12), pp.3996–4013.

Judd, W.S., SANDERS, R.W. and DONOGHUE, M.J., 1994. Angiosperm family pairs: preliminary phylogenetic analyses. *Harvard papers in botany*, pp.1-51.

Larter, M., Pfautsch, S., Domec, J.C., Trueba, S., Nagalingum, N. and Delzon, S. 2017. Aridity drove the evolution of extreme embolism resistance and the radiation of conifer genus *Callitris*. *New Phytologist*. **215**(1), pp.97–112.

Lavergne, S., Mouquet, N., Thuiller, W. and Ronce, O. 2010. Biodiversity and Climate Change: Integrating Evolutionary and Ecological Responses of Species and Communities. *Annual Review of Ecology, Evolution, and Systematics*. **41**(1), pp.321–350.

Lewis, S.L., Brando, P.M., Phillips, O.L., Van Der Heijden, G.M.F. and Nepstad, D. 2011. The 2010 Amazon drought. *Science*. **331**(6017), pp.554-554.

Lopez-Gonzalez, G., Lewis, S.L., Burkitt, M., Baker, T.R. and Phillips, O.L. 2009. ForestPlots.net Database. [Accessed 1 September 2018]. Available from: www.forestplots.net.

Lopez-Gonzalez, G., Lewis, S.L., Burkitt, M. and Phillips, O.L. 2011. ForestPlots.net: A web application and research tool to manage and analyse tropical forest plot data. *Journal of Vegetation Science*. **22**(4), pp.610-613.

Losos, J.B., 2008. Phylogenetic niche conservatism, phylogenetic signal and the relationship between phylogenetic relatedness and ecological similarity among species. *Ecology letters*, **11**(10), pp.995-1003.

Ruivo, M.D.L.P., Barreiros, J.A.P., Bonaldo, A.B., da Silva, R.M., Sá, L.D.A. and Lopes, E.L.N. 2007. LBA-ESECAFLOR artificially induced drought in Caxiuanã reserve, eastern Amazonia: Soil properties and litter spider fauna. *Earth Interactions*. **11**(8), pp.1–13.

Maherali, H., Pockman, W.T. and Jackson, R.B. 2004. Adaptive variation in the vulnerability of woody plants to xylem cavitation. *Ecology*. **85**(8), pp.2184–2199.

Malhi, Y., Aragao, L.E.O.C., Galbraith, D., Huntingford, C., Fisher, R., Zelazowski, P., Sitch, S., McSweeney, C. and Meir, P. 2009. Exploring the likelihood and mechanism of a climate-change-induced dieback of the Amazon rainforest. *Proceedings of the National Academy of Sciences*. **106**(49), pp.20610–20615.

Malhi, Y., Doughty, C.E., Goldsmith, G.R., Metcalfe, D.B., Girardin, C.A.J., Marthews, T.R., del Aguila-Pasquel, J., Aragão, L.E.O.C., Araujo-Murakami, A., Brando, P., da Costa, A.C.L., Silva-Espejo, J.E., Farfán Amézquita, F., Galbraith, D.R., Quesada, C.A., Rocha, W., Salinas-Revilla, N., Silvério, D., Meir, P. and Phillips, O.L. 2015. The linkages between photosynthesis, productivity, growth and biomass in lowland Amazonian forests. *Global Change Biology*. **21**(6), pp.2283–2295.

Malhi, Y., Phillips, O.L., Lloyd, J., Baker, T., Wright, J., Almeida, S., Arroyo, L., Frederiksen, T., Grace, J., Higuchi, N., Killeen, T., Laurance, W.F., Leão, C., Lewis, S., Meir, P., Monteagudo, A., Neill, D., Núñez Vargas, P., Panfil, S.N., Patiño, S., Pitman, N., Quesada, C.A., Ruelas-Ll., A., Salomão, R., Saleska, S., Silva, N., Silveira, M., Sombroek, W.G., Valencia, R., Vásquez Martínez, R., Vieira, I.C.G. and Vinceti, B. 2002. An international network to monitor the structure, composition and dynamics of Amazonian forests (RAINFOR). *Journal of Vegetation Science*. **13**(3), pp.439–450.

Malhi, Y., Roberts, J.T., Betts, R.A., Killeen, T.J., Li, W. and Nobre, C.A. 2008. The Fate of the Amazon. *Science*. **319**(5860), pp.169–172.

Marengo, J.A., Nobre, C.A., Tomasella, J., Oyama, M.D., de Oliveira, G.S., de Oliveira, R., Camargo, H., Alves, L.M. and Brown, I.F. 2008. The drought of Amazonia in 2005. *Journal of Climate*. **21**(3), pp.495–516.

Marengo, J.A., Souza, C.M., Thonicke, K., Burton, C., Halladay, K., Betts, R.A., Alves, L.M. and Soares, W.R. 2018. Changes in Climate and Land Use Over the Amazon Region: Current and Future Variability and Trends. *Frontiers in Earth Science*. **6**, p.228.

Markesteyn, L., Poorter, L., Paz, H., Sack, L. and Bongers, F. 2011. Ecological differentiation in xylem cavitation resistance is associated with stem and leaf structural traits. *Plant, Cell and Environment*. **34**(1), pp.137–148.

Martinez-Vilalta, J., Anderegg, W.R.L., Sapes, G. and Sala, A. 2019. Greater focus on water pools may improve our ability to understand and anticipate drought-induced mortality in plants. *New Phytologist*. **223**(1), pp.22–32.

Martínez-Vilalta, J. and Garcia-Forner, N. 2017. Water potential regulation, stomatal behaviour and hydraulic transport under drought: deconstructing the iso/anisohydric concept. *Plant Cell and Environment*. **40**(6), pp.962–976.

Martinez-Vilalta, J., Sala, A., Asensio, D., Galliano, L., Hoch, G., Palacio, S., Piper, F. and Lloret, F. 2016. Dynamics of non-structural carbohydrates in terrestrial plants: a global synthesis. *Ecological monographs* 86: 495-516.

McDowell, N., Allen, C.D., Anderson-Teixeira, K., Brando, P., Brien, R., Chambers, J., Christoffersen, B., Davies, S., Doughty, C., Duque, A., Espirito-Santo, F., Fisher, R., Fontes, C.G., Galbraith, D., Goodsman, D., Grossiord, C., Hartmann, H., Holm, J., Johnson, D.J., Kassim, A.R., Keller, M., Koven, C., Kueppers, L., Kumagai, T., Malhi, Y., McMahon, S.M., Mencuccini, M., Meir, P., Moorcroft, P., Muller-Landau, H.C., Phillips, O.L., Powell, T., Sierra, C.A., Sperry, J., Warren, J., Xu, C. and Xu, X. 2018. Drivers and mechanisms of tree mortality in moist tropical forests. *New Phytologist*. **219**(3), pp.851–869.

McDowell, N.G. 2018. Deriving pattern from complexity in the processes underlying tropical forest drought impacts. *New Phytologist*. **219**(3), pp.841–844.

McDowell, N., Pockman, W.T., Allen, C.D., Breshears, D.D., Cobb, N., Kolb, T., Plaut, J., Sperry, J., West, A., Williams, D.G. and Yezzer, E.A., 2008. Mechanisms of plant survival and mortality during drought: why do some plants survive while others succumb to drought?. *New phytologist*, **178**(4), pp.719-739.

McDowell, N.G. and Allen, C.D. 2015. Darcy's law predicts widespread forest mortality under climate warming. *Nature Climate Change*. **5**(7), pp.669–672.

Medeiros, J.S., Lens, F., Maherali, H. and Jansen, S. 2018. Vascular pits and scalariform perforation plate morphology modify the relationships between angiosperm vessel diameter, climate and maximum plant height. *New Phytologist*. **221**(4), pp.1802-1813.

Meir, P., Wood, T.E., Galbraith, D.R., Brando, P.M., Da Costa, A.C.L., Rowland, L. and Ferreira, L. V. 2015. Threshold Responses to Soil Moisture Deficit by Trees and Soil in Tropical Rain Forests: Insights from Field Experiments. *BioScience*. **65**(9), pp.882–892.

Mencuccini, M. 2003. The ecological significance of long-distance water transport: Short-term regulation, long-term acclimation and the hydraulic costs of stature across plant life forms. *Plant, Cell and Environment*. **26**(1), pp.163–182.

Mencuccini, M., Minunno, F., Salmon, Y., Martínez-Vilalta, J. and Hölttä, T. 2015. Coordination of physiological traits involved in drought-induced mortality of woody plants. *New Phytologist*. **208**(2), pp.396–409.

Nepstad, D.C. 2002. The effects of partial throughfall exclusion on canopy processes, aboveground production, and biogeochemistry of an Amazon forest. *Journal of Geophysical Research*. **107**(D20), pp LBA-53.

Nepstad, D.C., Tohver, I.M., Ray, D., Moutinho, P. and Cardinot, G. 2007. Mortality of large trees and lianas following experimental drought in an Amazon forest. *Ecology*. **88**(9), pp.2259–69.

Nobre, C.A., Sampaio, G., Borma, L.S., Castilla-Rubio, J.C., Silva, J.S. and Cardoso, M. 2016. Land-use and climate change risks in the Amazon and the need of a novel sustainable development paradigm. *Proceedings of the National Academy of Sciences*. **113**(39), pp.10759-10768.

O'Brien, M., Leuzinger, S., Phillipson, C.D., Tay, J. and Hector, A. 2014. Drought survival of tropical tree seedlings enhanced by non-structural carbohydrate levels. *Nature Climate Change*.

de Oliveira Junior, R.C., Keller, M., Patrick Michael Crill, Beldini, T.P. and Camargo, P.B. de 2010. Comportamento anual da água no solo sob loresta natural e plantio de grãos em latossolo amarelo na região de Belterra-PA. *Embrapa Amazônia Oriental-Artigo em periódico indexado (ALICE)*. **11**(05).

Oliveira, R.S., Costa, F.R.C., van Baalen, E., de Jonge, A., Bittencourt, P.R., Almanza, Y., Barros, F. de V., Cordoba, E.C., Fagundes, M. V., Garcia, S., Guimaraes, Z.T.T.M., Hertel, M., Schiatti, J., Rodrigues-Souza, J. and Poorter, L. 2018. Embolism resistance drives the distribution of Amazonian rainforest tree species along hydro-topographic gradients. *New Phytologist*. **221**(3), pp.1457-1465.

Pammenter NW and Vander Willigen C 1998. A mathematical and statistical analysis of the curves illustrating vulnerability of xylem to cavitation. *Tree Physiology*. **18**(8-9), pp.589–593.

Peacock, J., Baker, T.R., Lewis, S.L., Lopez-Gonzalez, G. and Phillips, O.L. 2007. The RAINFOR database: monitoring forest biomass and dynamics. *Journal of Vegetation Science*. **18**(4), pp.535–542.

Pereira, L., Bittencourt, P.R.L., Oliveira, R.S., Junior, M.B.M., Barros, F. V, Ribeiro, R. V and Mazzafera, P. 2016. Plant pneumatics: stem air flow is related to embolism – new perspectives on methods in plant hydraulics. *New Phytologist*, **211**(1), pp.357-370.

Phillips, O. and Miller, J.S. 2002. Global patterns of plant diversity: Alwyn H. Gentry's forest transect data set. *Missouri Botanical Press*.

Phillips, O. L, Aragão, L.E.O.C., Lewis, S.L., Fisher, J.B., Lloyd, J., López-González, G., Malhi, Y., Monteagudo, A., Peacock, J., Quesada, C. a, Van Der Heijden, G., Almeida, S., Amaral, I., Arroyo, L., Aymard, G., Baker, T.R., Bánki, O., Blanc, L., Bonal, D., Brando, P., Chave, J., De Oliveira, A.C.A., Cardozo, N.D., Czimczik, C.I., Feldpausch, T.R., Freitas, M.A., Gloor, E., Higuchi, N., Jiménez, E., Lloyd, G., Meir, P., Mendoza, C., Morel, A., Neill, D. a, Nepstad, D., Patiño, S., Peñuela, M.C., Prieto, A., Ramírez, F., Schwarz, M., Silva, J., Silveira, M., Thomas, A.S., Steege, H. Ter, Stropp, J., Vásquez, R., Zelazowski, P., Alvarez Dávila, E., Andelman, S., Andrade, A., Chao, K.-J., Erwin, T., Di Fiore, A., Honorio C, E., Keeling, H., Killeen, T.J., Laurance, W.F.,

Peña Cruz, A., Pitman, N.C. a, Núñez Vargas, P., Ramírez-Angulo, H., Rudas, A., Salamão, R., Silva, N., Terborgh, J. and Torres-Lezama, A. 2009. Drought sensitivity of the Amazon rainforest. *Science*. **323**(5919), pp.1344–7.

Pla, L., Casanoves, F. and Di Rienzo, J. 2012. Functional Diversity Indices *In: Quantifying Functional Biodiversity*. Springer, London, UK.

Pockman, W.T., Sperry, J.S. and O'Leary, J.W., 1995. Sustained and significant negative water pressure in xylem. *Nature*, **378**(6558), pp.715-716.

Powell, T.L., Wheeler, J.K., de Oliveira, A.A.R., da Costa, A.C.L., Saleska, S.R., Meir, P. and Moorcroft, P.R. 2017. Differences in xylem and leaf hydraulic traits explain differences in drought tolerance among mature Amazon rainforest trees. *Global Change Biology*. **23**(10), pp.4280–4293.

Quesada, C.A., Lloyd, J., Schwarz, M., Patiño, S., Baker, T.R., Czimczik, C., Fyllas, N.M., Martinelli, L., Nardoto, G.B., Schmerler, J., Santos, A.J.B., Hodnett, M.G., Herrera, R., Luizão, F.J., Arneith, A., Lloyd, G., Dezzeo, N., Hilke, I., Kuhlmann, I., Raessler, M., Brand, W.A., Geilmann, H., Filho, J.O.M., Carvalho, F.P., Filho, R.N.A., Chaves, J.E., Cruz, O.F., Pimentel, T.P. and Paiva, R. 2010. Variations in chemical and physical properties of Amazon forest soils in relation to their genesis. *Biogeosciences*. **7**(5), pp.1515–1541.

Quesada, C.A., Phillips, O.L., Schwarz, M., Czimczik, C.I., Baker, T.R., Patiño, S., Fyllas, N.M., Hodnett, M.G., Herrera, R., Almeida, S., Alvarez Dávila, E., Arneith, A., Arroyo, L., Chao, K.J., Dezzeo, N., Erwin, T., Di Fiore, A., Higuchi, N., Honorio Coronado, E., Jimenez, E.M., Killeen, T., Lezama, A.T., Lloyd, G., López-González, G., Luizão, F.J., Malhi, Y., Monteagudo, A., Neill, D.A., Núñez Vargas, P., Paiva, R., Peacock, J., Peñuela, M.C., Peña Cruz, A., Pitman, N., Priante Filho, N., Prieto, A., Ramírez, H., Rudas, A., Salomão, R., Santos, A.J.B., Schmerler, J., Silva, N., Silveira, M., Vásquez, R., Vieira, I., Terborgh, J. and Lloyd, J. 2012. Basin-wide variations in Amazon forest structure and function are mediated by both soils and climate. *Biogeosciences*. **9**(6), pp.2203–2246.

Quintero, I. and Wiens, J.J. 2013. Rates of projected climate change dramatically exceed past rates of climatic niche evolution among vertebrate species. *Ecology Letters*. **16**(8), pp.1095–1103.

Rammig, A., Jupp, T., Thonicke, K., Tietjen, B., Heinke, J., Ostberg, S., Lucht, W., Cramer, W. and Cox, P. 2010. Estimating the risk of Amazonian forest dieback. *New Phytologist*. **187**(3), pp.694–706.

Reich, P.B. 2014. The world-wide ‘fast-slow’ plant economics spectrum: A traits manifesto. *Journal of Ecology*. **102**(2), pp.275–301.

Revell, L.J., Harmon, L.J. and Collar, D.C., 2008. Phylogenetic signal, evolutionary process, and rate. *Systematic biology*, **57**(4), pp.591-601.

- Rosas, T., Martínez-Vilalta, J., Mencuccini, M., Cochard, H., Barba, J. and Saura-Mas, S. 2019. Adjustments and coordination of hydraulic, leaf and stem traits along a water availability gradient. *New Phytologist*. **223**(2), pp.632-646.
- Rowland, L., Da Costa, A.C.L., Galbraith, D.R., Oliveira, R.S., Binks, O.J., Oliveira, A.A.R., Pullen, A.M., Doughty, C.E., Metcalfe, D.B., Vasconcelos, S.S., Ferreira, L. V., Malhi, Y., Grace, J., Mencuccini, M. and Meir, P. 2015. Death from drought in tropical forests is triggered by hydraulics not carbon starvation. *Nature*. **528**(7580), pp.119–122.
- Santiago, L.S., De Guzman, M.E., Baraloto, C., Vogenberg, J.E., Brodie, M., Hérault, B., Fortunel, C. and Bonal, D. 2018. Coordination and trade-offs among hydraulic safety, efficiency and drought avoidance traits in Amazonian rainforest canopy tree species. *New Phytologist*. **218**(3), pp.1015–1024.
- Sevanto, S., McDowell, N.G., Dickman, L.T., Pangle, R. and Pockman, W.T. 2014. How do trees die? A test of the hydraulic failure and carbon starvation hypotheses. *Plant, Cell and Environment*. **37**(1), pp.153–161.
- Skelton, R.P., Anderegg, L.D.L. and Lamarque, L.J. 2019. Examining variation in hydraulic and resource acquisition traits along climatic gradients tests our understanding of plant form and function. *New Phytologist*. **223**(2), pp.505-507.
- Sperry, J. 2013. Cutting-edge research or cutting-edge artefact? An overdue control experiment complicates the xylem refilling story. *Plant, Cell and Environment*. **36**(11), pp.1916–1918.
- Sperry, J.S. and Saliendra, N.Z., 1994. Intra-and inter-plant variation in xylem cavitation in *Betula occidentalis*. *Plant, Cell & Environment*, **17**(11), pp.1233-1241.
- Sperry, J.S., Donnelly, J.R. and Tyree, M.T. 1988. A method for measuring hydraulic conductivity and embolism in xylem. *Plant, Cell & Environment*. **11**(1), pp.35–40.
- Sperry, J.S., Hacke, U.G. and Pittermann, J. 2006. Size and function in conifer tracheids and angiosperm vessels. *American Journal of Botany*. **93**(10), pp.1490–1500.
- Sperry, J.S., Venturas, M.D., Anderegg, W.R.L., Mencuccini, M., Mackay, D.S., Wang, Y. and Love, D.M. 2017. Predicting stomatal responses to the environment from the optimization of photosynthetic gain and hydraulic cost. *Plant Cell and Environment*. **40**(6), pp.816–830.
- Ter Steege, H., Pitman, N.C.A., Phillips, O.L., Chave, J., Sabatier, D., Duque, A., Molino, J.F., Prévost, M.F., Spichiger, R., Castellanos, H., Von Hildebrand, P. and Vásquez, R. 2006. Continental-scale patterns of canopy tree composition and function across Amazonia. *Nature*. **443**(7110), pp.444–447.
- Ter Steege, H., Pitman, N.C.A., Sabatier, D., Baraloto, C., Salomão, R.P., Guevara, J.E., Phillips, O.L., Castilho, C. V., Magnusson, W.E., Molino, J.F., Monteagudo, A., Vargas, P.N., Montero, J.C., Feldpausch, T.R., Coronado, E.N.H., Killeen, T.J., Mostacedo, B.,

Vasquez, R., Assis, R.L., Terborgh, J., Wittmann, F., Andrade, A., Laurance, W.F., Laurance, S.G.W., Marimon, B.S., Marimon, B.H., Vieira, I.C.G., Amaral, I.L., Brienen, R., Castellanos, H., López, D.C., Duivenvoorden, J.F., Mogollón, H.F., Matos, F.D.D.A., Dávila, N., García-Villacorta, R., Diaz, P.R.S., Costa, F., Emilio, T., Levis, C., Schiatti, J., Souza, P., Alonso, A., Dallmeier, F., Montoya, A.J.D., Piedade, M.T.F., Araujo-Murakami, A., Arroyo, L., Gribel, R., Fine, P.V.A., Peres, C.A., Toledo, M., Aymard C., G.A., Baker, T.R., Cerón, C., Engel, J., Henkel, T.W., Maas, P., Petronelli, P., Stropp, J., Zartman, C.E., Daly, D., Neill, D., Silveira, M., Paredes, M.R., Chave, J., Lima Filho, D.D.A., Jørgensen, P.M., Fuentes, A., Schöngart, J., Valverde, F.C., Di Fiore, A., Jimenez, E.M., Mora, M.C.P., Phillips, J.F., Rivas, G., Van Andel, T.R., Von Hildebrand, P., Hoffman, B., Zent, E.L., Malhi, Y., Prieto, A., Rudas, A., Ruschell, A.R., Silva, N., Vos, V., Zent, S., Oliveira, A.A., Schutz, A.C., Gonzales, T., Nascimento, M.T., Ramirez-Angulo, H., Sierra, R., Tirado, M., Medina, M.N.U., Van Der Heijden, G., Vela, C.I.A., Torre, E.V., Vriesendorp, C., Wang, O., Young, K.R., Baider, C., Balslev, H., Ferreira, C., Mesones, I., Torres-Lezama, A., Giraldo, L.E.U., Zagt, R., Alexiades, M.N., Hernandez, L., Huamantupa-Chuquimaco, I., Milliken, W., Cuenca, W.P., Pauletto, D., Sandoval, E.V., Gamarra, L.V., Dexter, K.G., Feeley, K., Lopez-Gonzalez, G. and Silman, M.R. 2013. Hyperdominance in the Amazonian tree flora. *Science*. **342**(6156). p.1243092.

Ter Steege, H., Pitman, N., Sabatier, D., Castellanos, H., Van Der Hout, P., Daly, D.C., Silveira, M., Phillips, O., Vasquez, R., Van Andel, T. and Duivenvoorden, J., 2003. A spatial model of tree α -diversity and tree density for the Amazon. *Biodiversity & Conservation*, *12*(11), pp.2255-2277.

Trueba, S., Pouteau, R., Lens, F., Feild, T.S., Isnard, S., Olson, M.E. and Delzon, S. 2017. Vulnerability to xylem embolism as a major correlate of the environmental distribution of rain forest species on a tropical island. *Plant Cell and Environment*. **40**(2), pp.277–289.

Tyree, M. T., & Zimmermann, M.H. 2002. *Xylem Structure and the Ascent of Sap* (Springer, ed.). Berlin: Heidelberg.

Tyree, M.T. and Dixon, M.A. 1986. Water stress induced cavitation and embolism in some woody plants. *Physiologia Plantarum*. **66**(3), pp.397–405.

Tyree, M.T., Salleo, S., Nardini, A., Lo Gullo, M.A. and Mosca, R. 1999. Refilling of embolized vessels in young stems of laurel. Do we need a new paradigm? *Plant Physiology*. **120**(1), pp.11–21.

Tyree, M.T. and Sperry, J.S., 1989. Vulnerability of xylem to cavitation and embolism. *Annual review of plant biology*, *40*(1), pp.19-36.

Tyree, M.T. and Sperry, J.S. 1988. Do woody plants operate near the point of catastrophic xylem dysfunction caused by dynamic water stress? : answers from a model. *Plant physiology*. **88**(3), pp.574–80.

Urli, M., Porté, A.J., Cochard, H., Guengant, Y., Burlett, R. and Delzon, S. 2013. Xylem embolism threshold for catastrophic hydraulic failure in angiosperm trees. *Tree Physiology*. **33**(7), pp.672–683.

Yoon, J.H. and Zeng, N. 2010. An Atlantic influence on Amazon rainfall. *Climate Dynamics*. **34**(2), pp.249–264.

Zanne, A.E., Lopez-Gonzalez, G., Coomes, D. a., Ilic, J., Jansen, S., Lewis, S.L.S.L., Miller, R.B.B., Swenson, N.G.G., Wiemann, M.C.C. and Chave, J. 2009. *Data from: Towards a worldwide wood economics spectrum*. *Ecology letters*, **12**(4), pp.351-366.

Zhang, Y., Lamarque, L.J., Torres-Ruiz, J.M., Schuldt, B., Karimi, Z., Li, S., Qin, D.W., Bittencourt, P., Burlett, R., Cao, K.F., Delzon, S., Oliveira, R., Pereira, L. and Jansen, S. 2018. Testing the plant pneumatic method to estimate xylem embolism resistance in stems of temperate trees. *Tree Physiology*. **38**(7), pp.1016–1025.

Zhao, M. and Running, S.W. 2010. Drought-Induced Reduction in Global. *Science*. **329**(5994), pp.940–943.

Appendices

Appendix 1:

Supplementary Information for Chapter 2

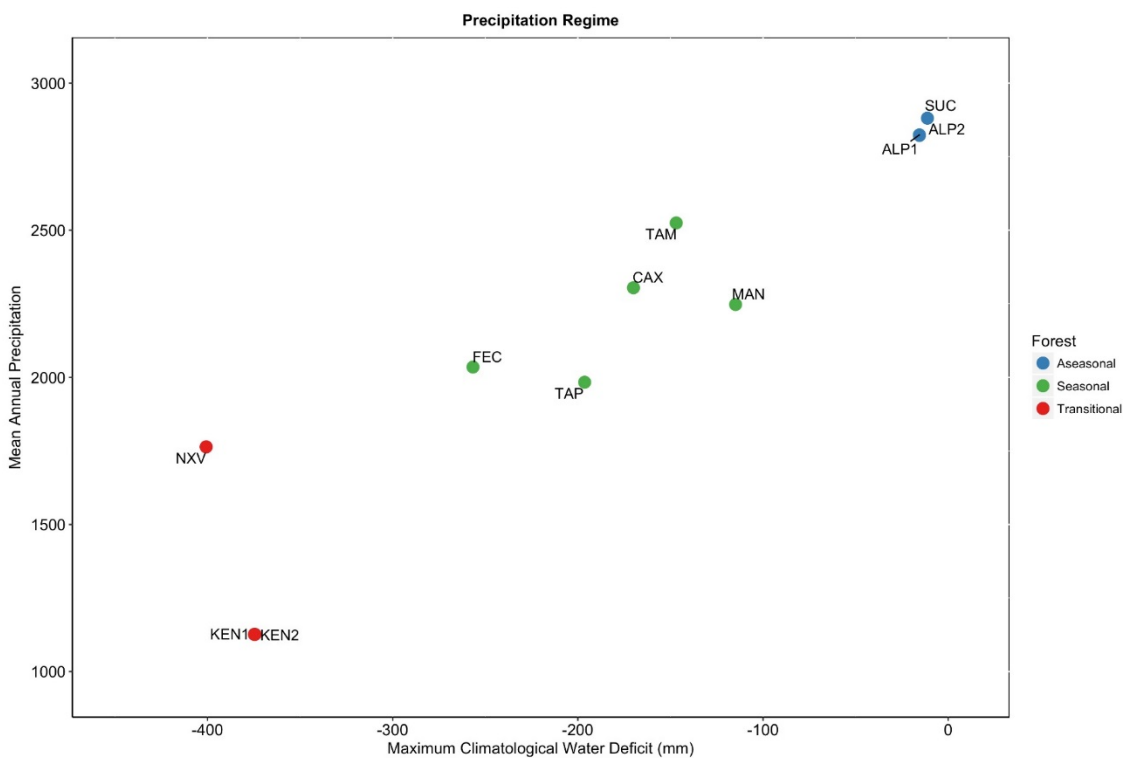


Figure A1. 1 Sites precipitation regime. Precipitation regime across the 11 sampled forest sites: Precipitation data were obtained from CRU (Climatic Research Unit) at 0.5o spatial resolution from 1960-2015 (quote Harris). Maximum cumulative water deficit (MCWD) was calculated following Aragão et al (2007). MCWD is defined as the maximum climatologically-induced water deficit. Sites which MCWD~0 do not experience seasonality, while in sites with very negative MCWD values are strongly seasonally water-stressed⁴⁸. Based on that I gathered the sites into forest types: Aseasonal (blue): SUC, ALP1 and ALP2; Seasonal (green): TAM, CAM, MAN, TAP and FEC and Transitional forests (red): NVX, KEN1 and KEN2.

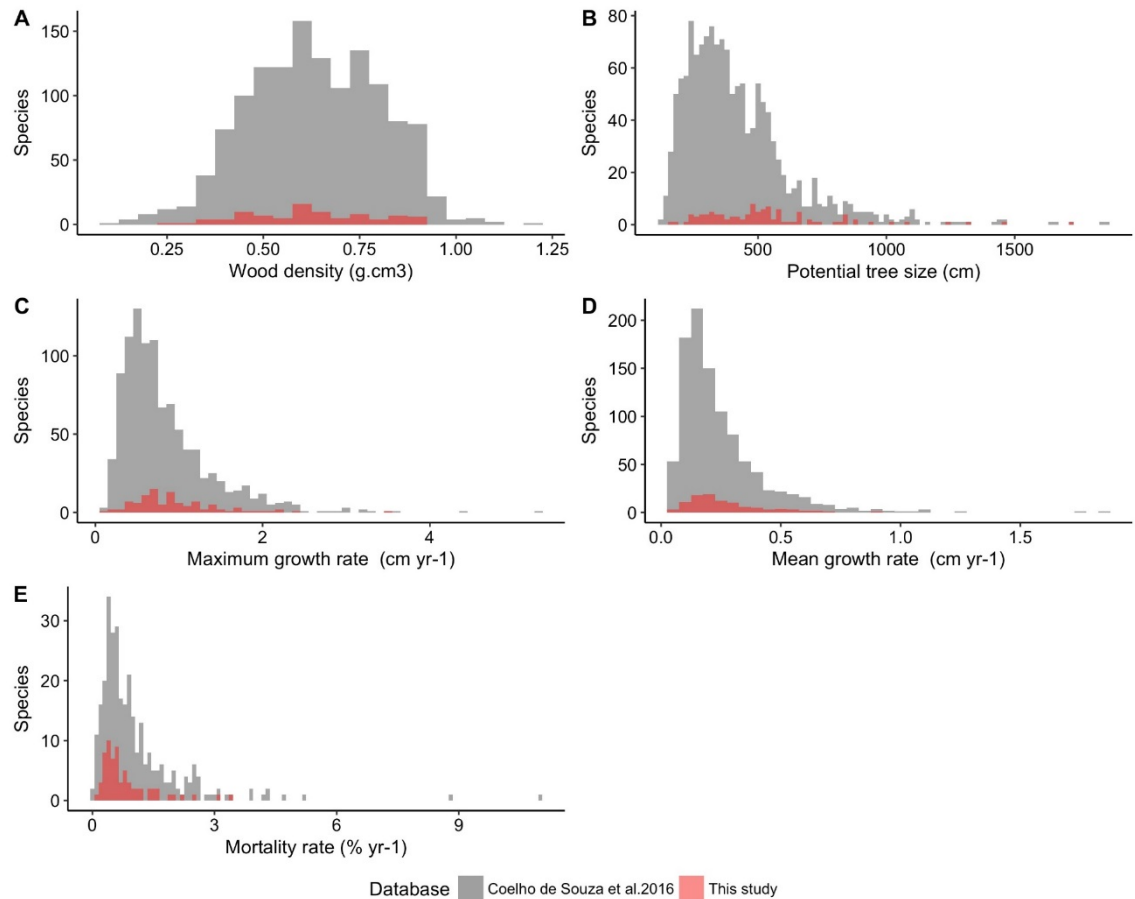


Figure A1. 2 Sampled species functional trait range. Histograms of life-history related traits range of the sampled species (red) in relation to pan-Amazonian life-history range (grey). A) Species mean wood density (g.cm^3) (Zanne et al., 2009; Chave et al., 2014); B) Species Potential size, calculated as the 95th percentile of diameter distribution (cm); C) Species Maximum growth, calculated as the 95th percentile of growth rates distribution (cm yr^{-1}); D) Species Mean growth rate (cm yr^{-1}); E) Species mortality rate ($\% \text{ yr}^{-1}$). All trait data shown in this figure were extracted from Coelho de Souza et al. (2016).

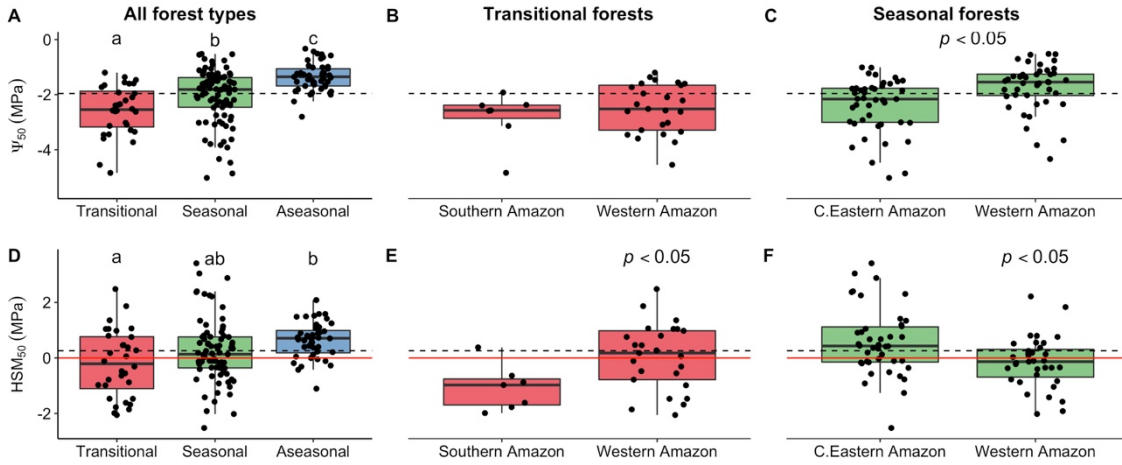


Figure A1.3 Hydraulic traits variation within and across Amazon forest types. A) and D) Hydraulic traits variation across all three forest types, B and E) Hydraulic traits variation within transitional forests (red). C and F) Hydraulic traits variation within seasonal forests (green). A, B and C) xylem water potential on which 50% (ψ_{50}) of the conductance is lost. D, E and F) hydraulic safety margins related to ψ_{50} (HSM_{50}). Dashed lines show the mean value of each trait across all tree taxa. Red line, the hydraulic safety margins equal to zero. Significant differences at $p < 0.05$ are shown by letters above each boxplot (panels A and D: Anova and Tukey HSD Pos Hoc) or displayed on the figure (panels B, C, E, F: Wilcoxon rank sum tests). ψ_{88} values for were cubic-root transformed to meet the assumption of normal distribution of the errors (A). Each point represents one species per site. Transitional, seasonal and aseasonal forets encompass 3, 5 and 3 forest sites, respectively.

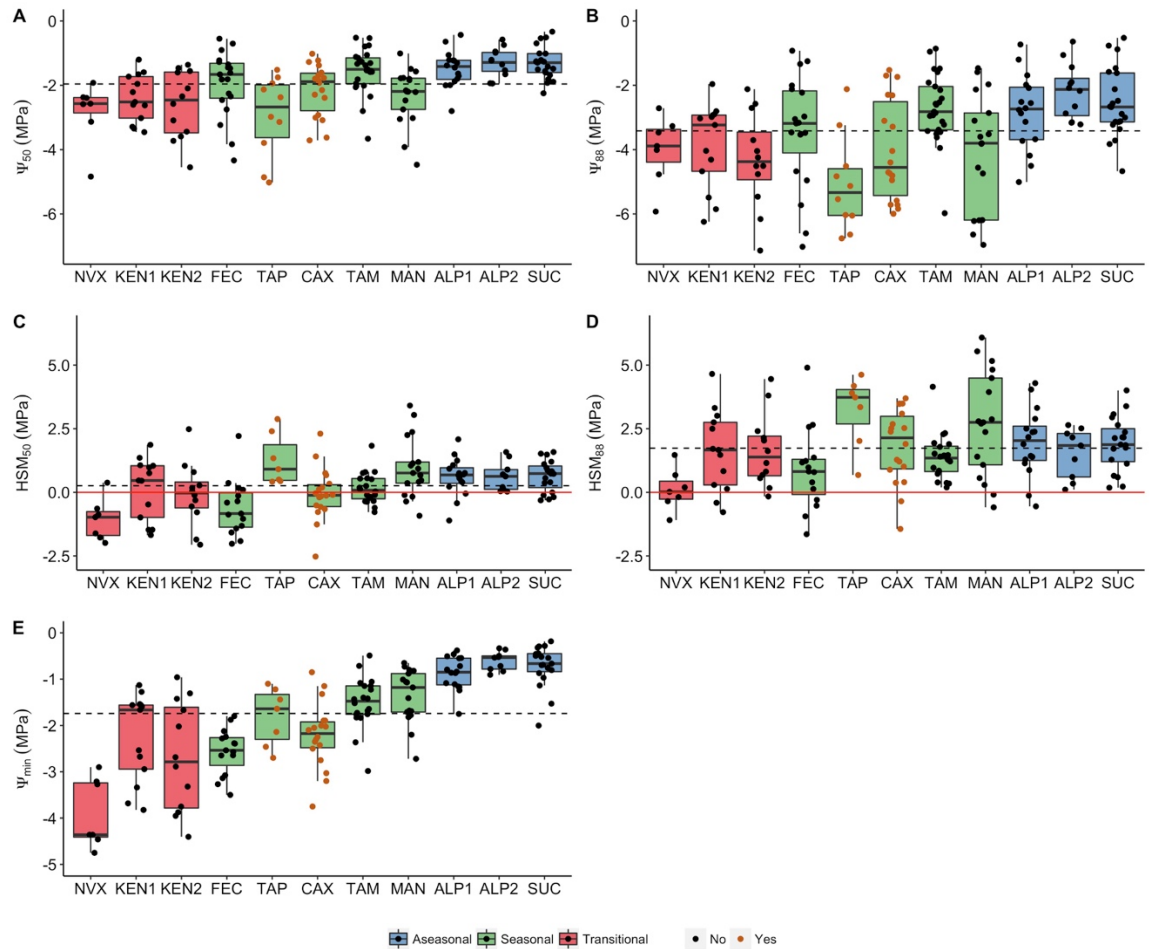


Figure A1.4 Hydraulic traits variation across Amazon forest sites. a) xylem water potential on which 50% (ψ_{50}); b) xylem water potential on which 88% (ψ_{88}) of the conductance is lost, respectively; c) hydraulic safety margins related to ψ_{50} (HSM50) and d) hydraulic safety margins related to ψ_{88} (HSM88). Dashed lines show the mean value of each trait across all tree taxa. Red line, the hydraulic safety margins equal to zero. Sites are sorted by increase in water availability. Red, green and blue colors represent sites from transitional, seasonal and aseasonal forests. Each point represents species per site. Brown points show species of forest plots in drought experiment locations (TAP and CAX). Note that I only used data from the control plots.

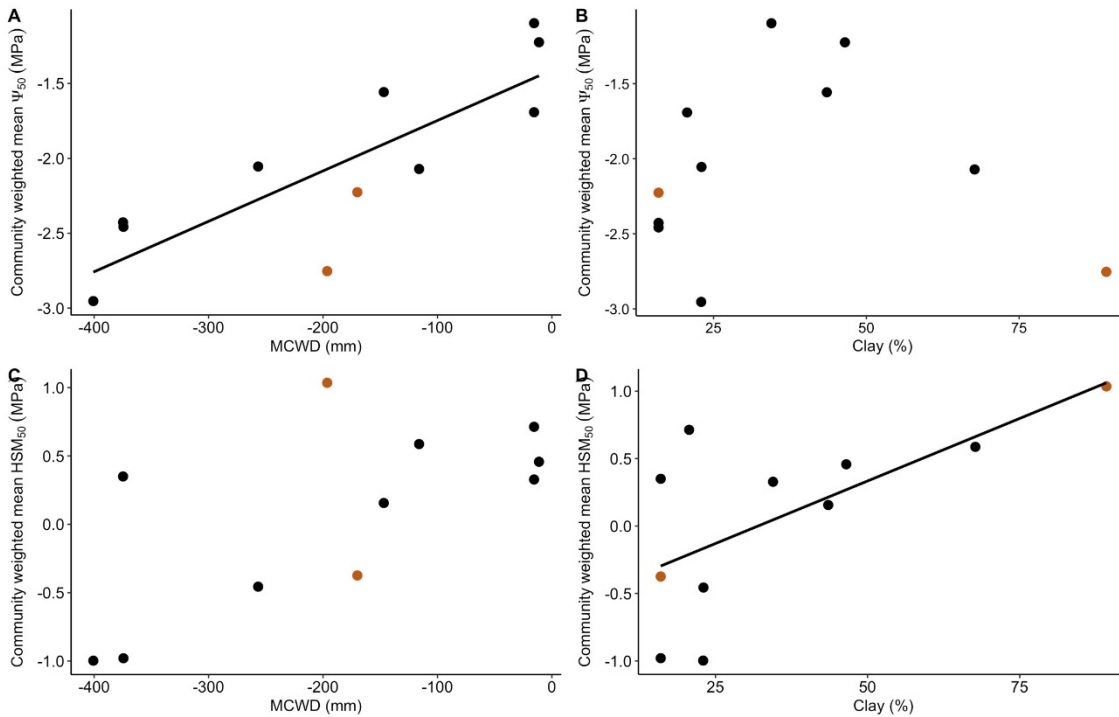


Figure A1.5 Relationship between tree community hydraulic traits and environmental variables. a) and c) Community weighted mean ψ_{50} (xylem water potential on which 50% of the conductance is lost) and Community weighted mean HSM₅₀, respectively, in relation to Maximum Cumulative Water Deficit (MCWD), $n=11$; b) and d) Community weighted mean ψ_{50} and Community weighted mean HSM₅₀, respectively, in relation to Soil Clay Percentage, $n=11$. Significant linear relations are shown by regression line: a) $R^2 = 0.68$, $p < 0.01$, c) $R^2 = 0.43$, $p = 0.03$ and d) $R^2 = 0.45$, $p = 0.04$. Further information available on SI Table 3. Brown points show forest plots in drought experiment locations (TAP and CAX). Note that I only used data from the control plots.

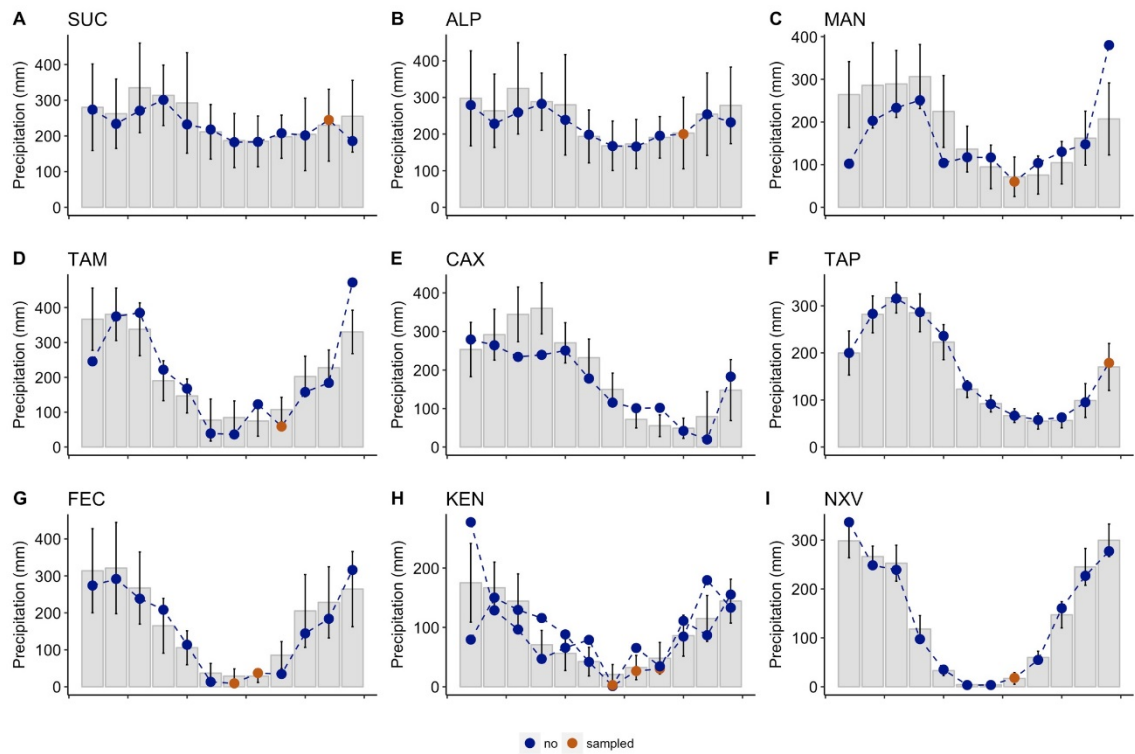


Figure A1.6 Climatological data when ψ_{\min} was sampled at each site. Grey and black bars show the mean and standard deviation of monthly precipitation from 1991 to 2018 (CRU data ts.4.0338). The blue dashed lines represent the year of sampling, while the brown points show the months at which ψ_{\min} was measured. TAP hydraulic traits data were obtained from Brum et al (2018).

Table A1. 1 Sampling design summary: Site environmental characteristics.

Forest type	Biogeographic Region	Site	MCWD (mm)	MAP (mm)	DSL (months)	Soil type	Clay (%)	Ptotal (mg.kg-1)	Sampled Soil Depth (cm)	Soil data source
Aseasonal	Western Amazon	ALP1	-15.55	2824	0	Sandy clay loam	20.67	110.3	0-30	Quesada 2010 (AI)
		ALP2	-15.52	2824	0	Clay loam	34.46	110.24	0-30	Quesada 2010 (AI)
		SUC	-11.22	2880	0	Clay	46.49	284.62	0-30	Quesada 2010 (SUC-02)
Seasonal	Western Amazon	FEC	-256.65	2035	4-5	Clay loam	23.02	478.17	0-30	Quesada Lloyd unpublisl
		TAM	-146.87	2542	3-4	Clay	43.53	256.29	0-30	Quesada 2010 (TA 05)
	C.Eastern Amazon	CAX	-169.97	2301	4	Sandy loam	16	37.4	0-20	Ruivo et 2007 ; M al 2015
		MAN	-116.02	2247	2-3	Clay	67.71	101.78	0-30	Quesada 2010 (ML 12)
		TAP	-196.34	1983	5	Clay	89.25	192.34	0-30	Quesada 2010 (TA)
Transitional	Western Amazon	KEN2	-374.38	1127	6-7	Sandy loam	16	224.7	0-30	Araujo-Murakarr 2014; M et al 2014

		KEN1	-374.72	1127	6-7	Sandy loam	16	447.1	0-30	Araujo-Murakami 2014; Melián et al 2015
	Southern Amazon	NVX	-400.7	1764	5	NA	22.98	NA	0-30	Quesada Lloyd unpublished

*Data accessed from Forest.plots database. Maximum climatological water deficit (MCWD); Mean annual precipitation (MAP); Dry season length (DSL) = number of months with <100mm precipitation.

Table A1. 2 Sampling design summary: Site biotic characteristics.

Forest type	Biogeographic Region	Site	Relative sampled basal area for ψ_{50} , ψ_{88} (%)	N sampled species (ψ_{50} , ψ_{88})	Relative sampled basal area for HSMs(%)	N sampled species (HSMs)	Plot				HSM5		HSM8			
							Area (ha)	p50 mean	p50 sd	p88 mean	p88 sd	0 mean	HSM5 0 sd	8 mean	F 8	
Aseasonal	Western Amazon	ALP 1	27.16	16	27.16	16	27.91	0.48	-1.49	0.57	-2.83	1.18	0.61	0.75	1.96	1
		ALP 2	27.32	12	22.41	9	26.16	0.44	-1.34	0.44	-2.19	0.85	0.62	0.59	1.54	0
		SUC	21.91	21	17.26	19	15.04	2	-1.31	0.58	-2.54	1.08	0.64	0.61	1.9	1
Seasonal	Western Amazon	FEC	58.85	19	43.61	15	34.11	1	-1.95	1.02	-3.43	1.72	-0.6	1.08	0.91	1
		TAM	56.65	25	42.46	20	29.07	1	-1.56	0.78	-2.71	1.08	0.17	0.61	1.39	0

	C.Easter n Amazon	CA X	16.37	18	16.37	18	10.6 6	1	-2.15	2	0.8	7	1.5	-0.06	1.03	1.81	1
		MA N	13.69	17	13.45	16	10.7	3.6	-2.34	9	0.8	3	1.8	0.97	1.19	2.72	2
		TAP	37.03	10	26.28	7	NA	4	-2.95	6	1.2	9	1.4	1.27	1	3.21	1
Transition al	Western Amazon	KE N2	54.66	12	54.66	12	43.4 2	1	-2.62	5	1.0	7	1.4	-0.07	1.23	1.64	1
		KE N1	75.16	13	75.16	13	60.8 4	1	-2.4	4	0.7	4	1.3	0.15	1.21	1.63	1
	Southern Amazon	NV X	51.38	7	51.38	7	56.7 5	1	-2.83	6	0.9	6	1.0	-1.07	0.81	0.1	0

CD5= cumulative dominance of the 5 most dominant species, in terms of basal area

Table A1. 3 Linear models relating Community weighted mean hydraulic traits and environmental variable.

Variable	Models	Residual standard error	Multiple R- squared	Ajusted R- squared	fstatisti c	p- value	Intercep t	Intercept SE	Slop e	Slope SE	AIC
P50	CWM_P50~CWD	0.36	0.68	0.65	19.38	0.00	-1.41	0.18	0.00	0.00	12.3 2
	CWM_P50~CWD+Ptotal	0.34	0.70	0.61	8.04	0.02	-1.61	0.21	0.00	0.00	11.3 8
	CWM_P50~CWD+Clay	0.32	0.78	0.72	13.86	0.00	-1.04	0.26	0.00	0.00	10.5 0
	CWM_P50~CWD+Ptotal+Clay	0.29	0.81	0.72	8.54	0.01	-1.24	0.27	0.00	0.00	8.68 21.0
	CWM_P50~Ptotal	0.57	0.02	-0.10	0.19	0.67	-1.83	0.34	0.00	0.00	7

	CWM_P50~Clay	0.63	0.00	-0.11	0.00	0.97	-2.04	0.36	0.00	0.01	24.9
	CWM_P50~Ptotal+Clay	0.61	0.05	-0.23	0.17	0.84	-1.67	0.52	0.00	0.00	22.8
	CWM_P50~MAP	0.40	0.60	0.56	13.60	0.01	-3.65	0.45	0.00	0.00	14.8
	CWM_P50~MAP+Ptotal	0.35	0.69	0.60	7.68	0.02	-3.88	0.57	0.00	0.00	11.6
	CWM_P50~MAP+Clay	0.40	0.65	0.56	7.33	0.02	-3.57	0.46	0.00	0.00	15.5
	CWM_P50~MAP+Ptotal+Clay	0.33	0.76	0.65	6.46	0.03	-3.70	0.55	0.00	0.00	10.8
	CWM_P50~DSL	0.36	0.68	0.65	19.43	0.00	-1.36	0.19	-	0.05	12.3
	CWM_P50~DSL+Ptotal	0.29	0.79	0.72	12.84	0.00	-1.51	0.18	0.21	0.04	7.90
	CWM_P50~DSL+Clay	0.37	0.70	0.63	9.48	0.01	-1.22	0.28	-	0.05	13.5
	CWM_P50~DSL+Ptotal+Clay	0.29	0.82	0.73	9.09	0.01	-1.32	0.25	0.21	0.04	9
											8.18
P88	CWM_P88~CWD	0.60	0.54	0.49	10.48	0.01	-2.69	0.30	0.00	0.00	23.6
	CWM_P88~CWD+Ptotal	0.55	0.67	0.58	7.13	0.02	-2.99	0.34	0.01	0.00	4
	CWM_P88~CWD+Clay	0.58	0.61	0.51	6.24	0.02	-2.23	0.48	0.00	0.00	20.9
	CWM_P88~CWD+Ptotal+Clay	0.54	0.73	0.60	5.49	0.04	-2.57	0.49	0.01	0.00	23.7
											9
											20.8
											5

	CWM_P88~Ptotal	0.90	0.00	-0.12	0.03	0.86	-3.32	0.54	0.00	0.00	30.0
	CWM_P88~Clay	0.88	0.00	-0.11	0.00	0.98	-3.46	0.49	0.00	0.01	32.1
	CWM_P88~Ptotal+Clay	0.96	0.01	-0.27	0.03	0.97	-3.21	0.82	0.00	0.00	31.9
	CWM_P88~MAP	0.59	0.55	0.50	10.87	0.01	-5.59	0.67	0.00	0.00	23.4
	CWM_P88~MAP+Ptotal	0.60	0.62	0.51	5.64	0.03	-6.38	0.98	0.00	0.00	22.4
	CWM_P88~MAP+Clay	0.60	0.59	0.48	5.67	0.03	-5.48	0.69	0.00	0.00	24.4
	CWM_P88~MAP+Ptotal+Clay	0.61	0.65	0.48	3.75	0.08	-6.19	1.04	0.00	0.00	23.5
	CWM_P88~DSL	0.50	0.67	0.64	18.64	0.00	-2.53	0.26	-	0.06	19.7
	CWM_P88~DSL+Ptotal	0.47	0.76	0.70	11.37	0.01	-2.83	0.30	0.28	0.07	9
	CWM_P88~DSL+Clay	0.52	0.69	0.62	9.01	0.01	-2.34	0.39	-	0.07	17.5
	CWM_P88~DSL+Ptotal+Clay	0.49	0.77	0.66	6.87	0.02	-2.67	0.44	0.28	0.07	21.1
	CWM_HSM_p50~CWD	0.54	0.43	0.36	6.68	0.03	0.64	0.27	-	0.00	19.1
	CWM_HSM_p50~CWD+Ptotal	0.58	0.30	0.10	1.52	0.28	0.52	0.36	0.32	0.07	6
	CWM_HSM_p50~CWD+Clay	0.46	0.64	0.55	7.15	0.02	0.00	0.37	0.00	0.00	21.5
HSM50											9
											21.8
											8
											18.4
											2

	CWM_HSM_p50~CWD+Ptotal+Clay	0.47	0.60	0.40	3.01	0.12	-0.15	0.43	0.00	0.00	18.31	
	CWM_HSM_p50~Ptotal	0.64	0.04	-0.08	0.32	0.59	0.36	0.38	0.00	0.00	23.10	
	CWM_HSM_p50~Clay	0.54	0.43	0.37	6.78	0.03	-0.59	0.30	0.02	0.01	21.53	
	CWM_HSM_p50~Ptotal+Clay	0.51	0.45	0.30	2.88	0.12	-0.36	0.44	0.00	0.00	19.49	
	CWM_HSM_p50~MAP	0.63	0.22	0.14	2.57	0.14	-1.03	0.71	0.00	0.00	24.94	
	CWM_HSM_p50~MAP+Ptotal	0.62	0.19	-0.04	0.83	0.48	-0.73	1.03	0.00	0.00	23.38	
	CWM_HSM_p50~MAP+Clay	0.52	0.53	0.41	4.51	0.05	-1.28	0.60	0.00	0.00	21.39	
	CWM_HSM_p50~MAP+Ptotal+Clay	0.51	0.54	0.31	2.36	0.17	-1.16	0.86	0.00	0.00	19.71	
	CWM_HSM_p50~DSL	0.63	0.24	0.15	2.82	0.13	0.53	0.33	-	0.13	0.08	24.71
	CWM_HSM_p50~DSL+Ptotal	0.62	0.20	-0.02	0.90	0.45	0.53	0.39	-	0.11	0.09	23.20
	CWM_HSM_p50~DSL+Clay	0.49	0.58	0.48	5.59	0.03	-0.16	0.37	-	0.11	0.06	20.08
	CWM_HSM_p50~DSL+Ptotal+Clay	0.47	0.60	0.40	3.01	0.12	-0.19	0.42	-	0.10	0.07	18.32
HSM88	CWM_HSM_p88~CWD	0.64	0.20	0.11	2.28	0.17	1.87	0.32	0.00	0.00	25.31	
	CWM_HSM_p88~CWD+Ptotal	0.60	0.07	-0.19	0.27	0.77	1.84	0.37	0.00	0.00	22.68	

CWM_HSM_p88~CWD+Clay	0.58	0.43	0.29	3.02	0.11	1.20	0.47	0.00	0.00	23.61
CWM_HSM_p88~CWD+Ptotal+Clay	0.51	0.43	0.14	1.51	0.31	1.18	0.46	0.00	0.00	19.81
CWM_HSM_p88~Ptotal	0.57	0.06	-0.05	0.55	0.48	1.82	0.34	0.00	0.00	20.77
CWM_HSM_p88~Clay	0.58	0.36	0.29	5.06	0.05	0.86	0.32	0.02	0.01	22.88
CWM_HSM_p88~Ptotal+Clay	0.47	0.43	0.27	2.62	0.14	1.20	0.41	0.00	0.00	17.84
CWM_HSM_p88~MAP	0.70	0.05	-0.05	0.49	0.50	0.94	0.79	0.00	0.00	27.20
CWM_HSM_p88~MAP+Ptotal	0.61	0.06	-0.20	0.24	0.79	1.78	1.00	0.00	0.00	22.77
CWM_HSM_p88~MAP+Clay	0.61	0.37	0.21	2.31	0.16	0.69	0.70	0.00	0.00	24.77
CWM_HSM_p88~MAP+Ptotal+Clay	0.51	0.43	0.15	1.53	0.30	1.38	0.86	0.00	0.00	19.74
CWM_HSM_p88~DSL	0.71	0.03	-0.07	0.31	0.59	1.64	0.37	-	-	27.42
CWM_HSM_p88~DSL+Ptotal	0.60	0.07	-0.20	0.25	0.78	1.80	0.39	0.01	0.09	22.74
CWM_HSM_p88~DSL+Clay	0.61	0.37	0.21	2.33	0.16	0.96	0.46	-	-	24.74
CWM_HSM_p88~DSL+Ptotal+Clay	0.51	0.43	0.15	1.54	0.30	1.17	0.45	0.02	0.07	19.73

Table A1. 4 Results of Kendall tau correlations among environmental variables.

Variables		tau	z	p-value
Clay	Ptotal	-0.05	-0.18	0.86
Clay	MCWD	0.34	1.42	0.16
Ptotal	MCWD	-0.24	-0.98	0.32

Table A1. 5 Linear models describing the relationship between hydraulic traits and relative dominance per species per site.

Site	Model	Intercept	Slope	pvalue	r2	r2ajust
ALP1	p50 ~ Domin_relat	-1.36	-0.07	0.56	0.08	0.02
	p88 ~ Domin_relat	-2.73	-0.06	1.21	0.01	-0.06
	HSM_p50 ~ Domin_relat	0.54	0.04	0.77	0.01	-0.06
	HSM_p88 ~ Domin_relat	1.91	0.03	1.38	0.00	-0.07
ALP2	p50 ~ Domin_relat	-1.47	0.07	0.41	0.20	0.12
	p88 ~ Domin_relat	-2.31	0.05	0.88	0.02	-0.07
	HSM_p50 ~ Domin_relat	0.87	-0.10	0.55	0.24	0.13
	HSM_p88 ~ Domin_relat	1.83	-0.12	0.98	0.12	0.00
CAX	p50 ~ Domin_relat	-2.07	-0.09	0.84	0.01	-0.05
	p88 ~ Domin_relat	-3.81	-0.23	1.61	0.02	-0.04
	HSM_p50 ~ Domin_relat	0.27	-0.36	1.01	0.10	0.05
	HSM_p88 ~ Domin_relat	2.01	-0.22	1.51	0.02	-0.04
FEC	p50 ~ Domin_relat	-1.78	-0.06	1.04	0.02	-0.04
	p88 ~ Domin_relat	-3.28	-0.05	1.76	0.00	-0.05
	HSM_p50 ~ Domin_relat	-0.81	0.07	1.11	0.03	-0.05
	HSM_p88 ~ Domin_relat	0.77	0.05	1.67	0.01	-0.07
KEN1	p50 ~ Domin_relat	-2.38	0.00	0.77	0.00	-0.09
	p88 ~ Domin_relat	-3.90	0.00	1.40	0.00	-0.09
	HSM_p50 ~ Domin_relat	-0.04	0.03	1.25	0.03	-0.06
	HSM_p88 ~ Domin_relat	1.49	0.02	1.66	0.01	-0.08
KEN2	p50 ~ Domin_relat	-2.72	0.02	1.10	0.02	-0.08
	p88 ~ Domin_relat	-4.35	0.01	1.54	0.00	-0.10
	HSM_p50 ~ Domin_relat	0.53	-0.13	1.01	0.39	0.33
	HSM_p88 ~ Domin_relat	2.16	-0.11	1.31	0.22	0.15
MAN	p50 ~ Domin_relat	-2.64	0.38	0.86	0.11	0.05
	p88 ~ Domin_relat	-5.00	1.14	1.66	0.23	0.18
	HSM_p50 ~ Domin_relat	1.42	-0.56	1.15	0.13	0.07

	HSM_p88 ~ Domin_relat	3.77	-1.31	1.86	0.24	0.19
NXV	p50 ~ Domin_relat	-1.78	-0.14	0.96	0.16	0.00
	p88 ~ Domin_relat	-3.21	-0.11	1.12	0.08	-0.11
	HSM_p50 ~ Domin_relat	-1.70	0.09	0.85	0.08	-0.10
	HSM_p88 ~ Domin_relat	-0.27	0.05	0.87	0.03	-0.16
	p50 ~ Domin_relat	-1.41	0.10	0.50	0.04	-0.01
SUC	p88 ~ Domin_relat	-2.62	0.07	1.10	0.00	-0.05
	HSM_p50 ~ Domin_relat	1.00	-0.39	0.57	0.19	0.14
	HSM_p88 ~ Domin_relat	2.47	-0.63	1.00	0.16	0.11
	p50 ~ Domin_relat	-1.55	0.00	0.72	0.00	-0.04
	p88 ~ Domin_relat	-2.71	0.00	1.10	0.00	-0.04
TAM	HSM_p50 ~ Domin_relat	0.18	-0.01	0.63	0.00	-0.06
	HSM_p88 ~ Domin_relat	1.36	0.01	0.93	0.00	-0.05
	p50 ~ Domin_relat	-3.19	0.06	1.31	0.03	-0.09
	p88 ~ Domin_relat	-5.64	0.15	1.47	0.13	0.02
	HSM_p50 ~ Domin_relat	1.53	-0.07	1.06	0.07	-0.12
TAP	HSM_p88 ~ Domin_relat	3.70	-0.13	1.41	0.14	-0.04

Table A1. 6 Summary of clusters and forest plots used to investigate changes in net biomass.

Cluster	Plot code	Date initial census	Date final census	Census length
ALP	ALP-12	2001.03	2016.9045	15.8745
	ALP-11	2001.03	2016.9045	15.8745
	ALP-02	2001.03	2016.906	15.876
CAX	CAX-01	2002.8765	2009.953	7.0765
	CAX-02	1995.501	2009.953	14.452
	CAX-06	2004.607	2009.953	5.346
	TEC-01	2002.871	2012.806	9.935
	TEC-02	2003.189	2012.814	9.625
	TEC-03	2003.219	2012.82	9.601
	TEC-04	2003.31	2012.817	9.507
	TEC-05	2003.4755	2012.811	9.3355
	TEC-06	2003.329	2012.809	9.48

FEC	FEC-01	2000.858	2018.396	17.538
	RFH-01	2004.331	2018.4025	14.0715
MAN	BNT-01	2001.542	2012.454	10.912
	BNT-02	2001.542	2012.454	10.912
	BNT-04	2001.542	2012.454	10.912
	JAC-01	2002.501	2011.452	8.951
	JAC-02	2002.501	2011.452	8.951
SUC	SUC-01	2001.06	2016.631	15.571
	SUC-02	2001.071	2016.637	15.566
	SUC-04	2001.159	2016.658	15.499
	SUC-05	2001.121	2016.661	15.54
TAM	TAM-01	2000.5955	2017.723	17.1275
	TAM-02	2000.5765	2017.74	17.1635
	TAM-05	2000.5615	2017.748	17.1865
	TAM-06	2000.549	2017.718	17.169
	TAM-07	2003.722	2017.7615	14.0395
	TAM-08	2001.529	2017.753	16.224
	TAM-09	2010.6865	2017.734	7.0475
TAP	TAP-50	1983.501	1995.501	12
	TAP-51	1983.501	1995.501	12
	TAP-52	1983.501	1995.501	12
	TAP-53	1983.501	1995.501	12
	TAP-54	1983.501	1995.501	12
	TAP-55	1983.501	1995.501	12
	TAP-56	1983.501	1995.501	12
	TAP-57	1983.501	1995.501	12
	TAP-58	1983.501	1995.501	12
	TAP-59	1983.501	1995.501	12
	TAP-60	1983.501	1995.501	12
	TAP-61	1983.501	1995.501	12
	TAP-80	1999.958	2005.458	5.5
NXV	VCR-02	2003.585	2018.4985	14.9135
	VCR-01	2004.5	2018.6205	14.1205

Appendix 2: Supplementary Information for Chapter 3

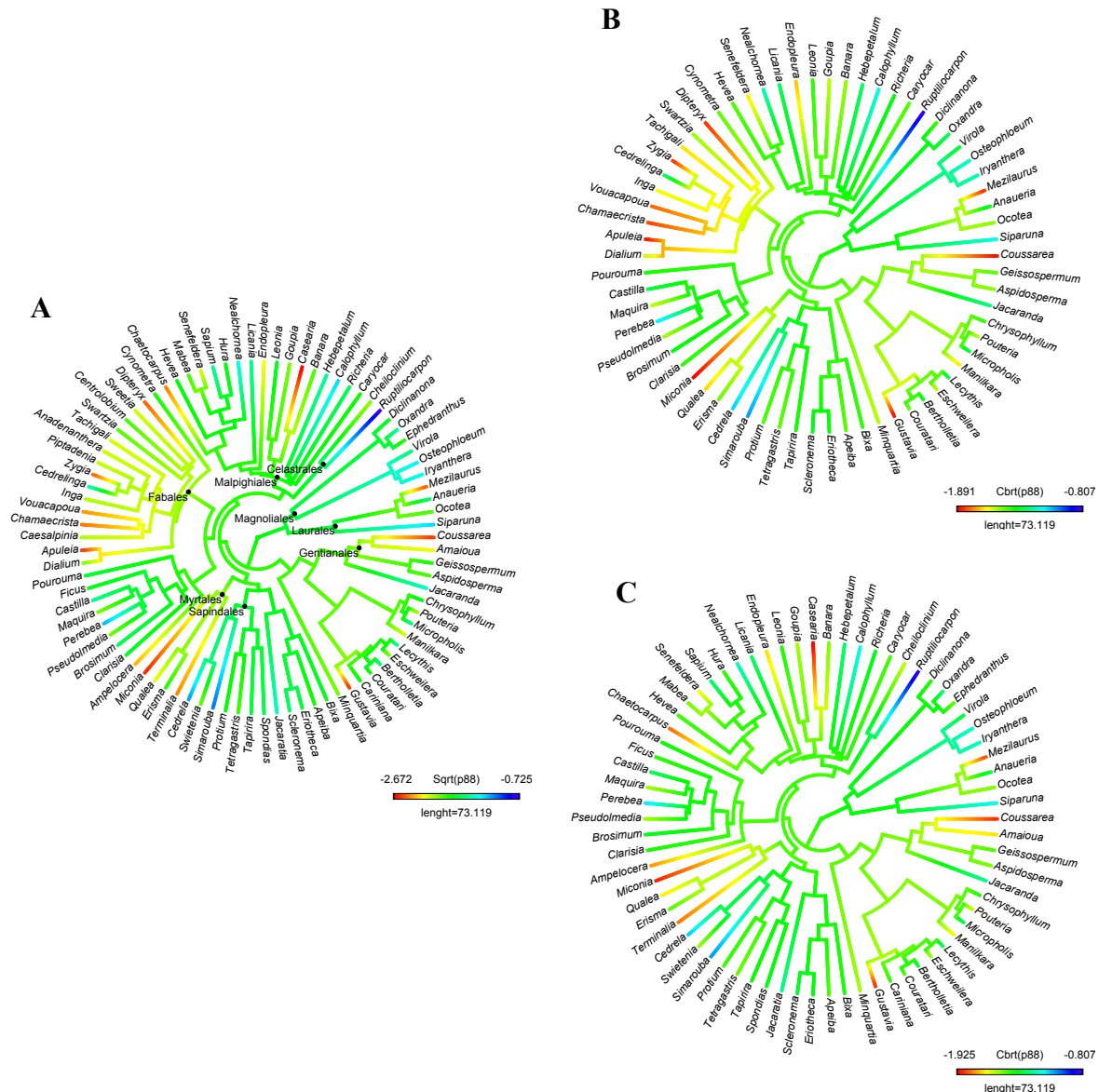


Figure A2. 1 Phylogenetic tree (Coelho et al 2019) of Amazonian tree genera with branches coloured as: absolute mean Ψ_{88} value per genus, $n=87$ genera (A), Phylogenetic signal for Ψ_{88} account for environmental variation: excluding transitional forests, $n=67$ genera (B) and for unbalance sampling: excluding Fabaceae, the most abundant family in the dataset, $n=71$ genera (C).

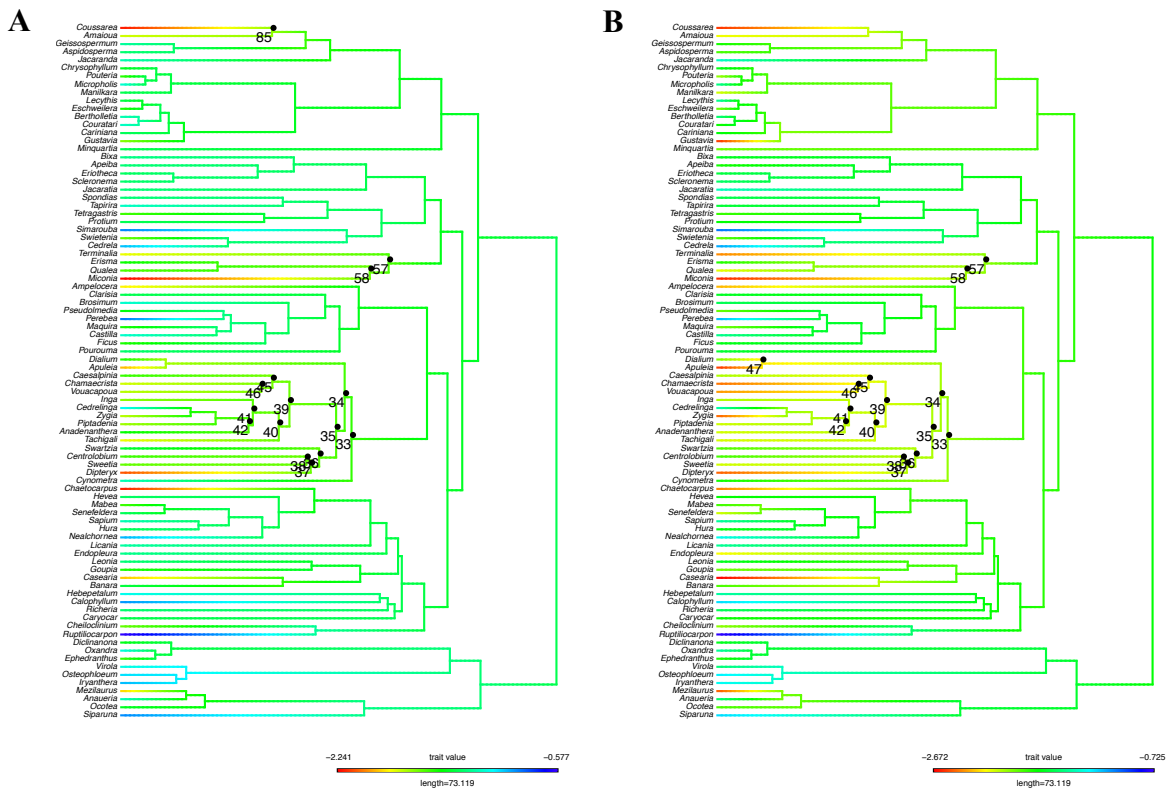


Figure A2. 2 Map of phylogenetic signal at genus-level for Ψ_{50} (A) and Ψ_{88} (B). The circles show individual nodes which have lower values than expected randomly, at 0.05 level of significance, using randomization approach of Dexter et al. (2016).

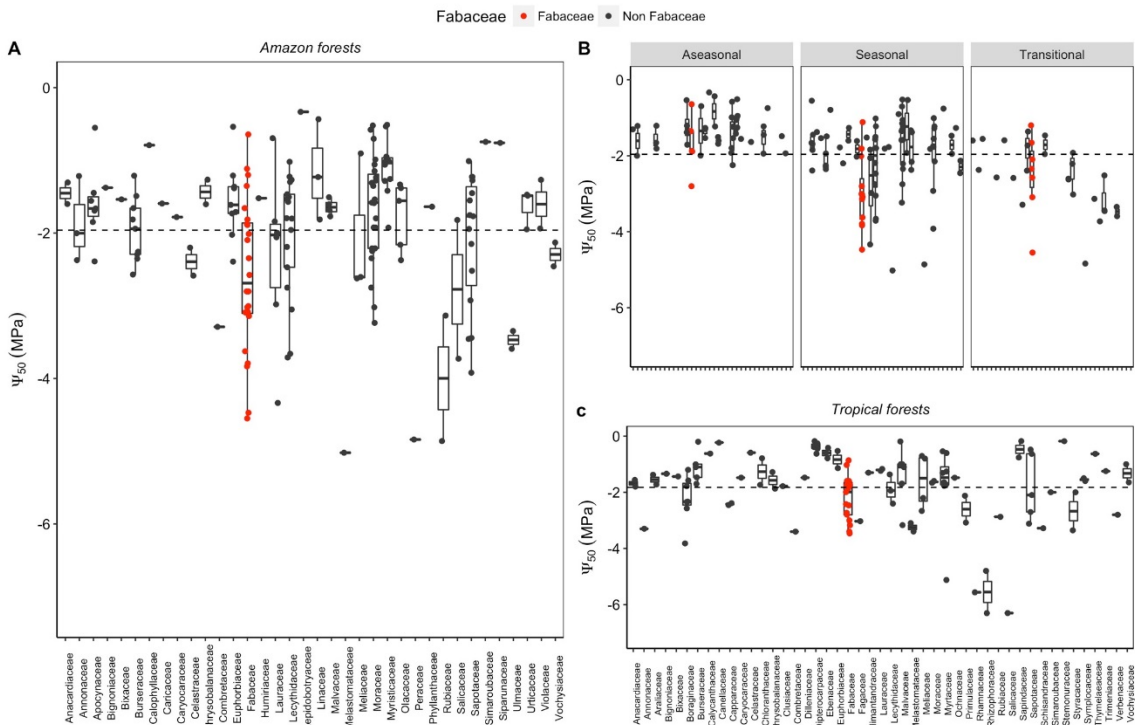


Figure A2. 3 Difference in embolism resistance (Ψ_{50}) among families across (A) and within (B) Amazonian forests and across tropical rainforests (C). Dashed horizontal lines show mean trait value across pan-Amazonian dataset (A, B) and compiled dataset (C).

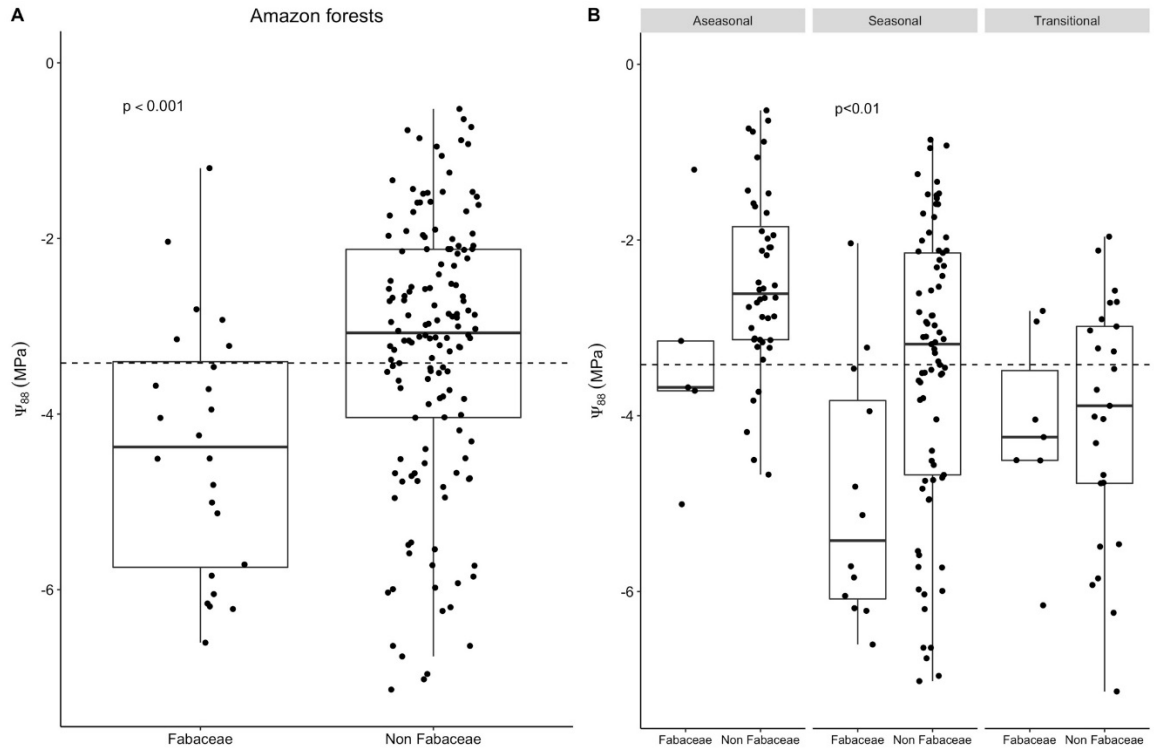


Figure A2. 4 Difference in embolism resistance (Ψ_{88}) between Fabaceae and Non-Fabaceae across (A) and within (B) Amazonian forests. Dashed vertical lines show mean trait value across pan-Amazonian dataset. Statistical differences at $p < 0.05$ using Wilcoxon rank sum tests are displayed on the figure.

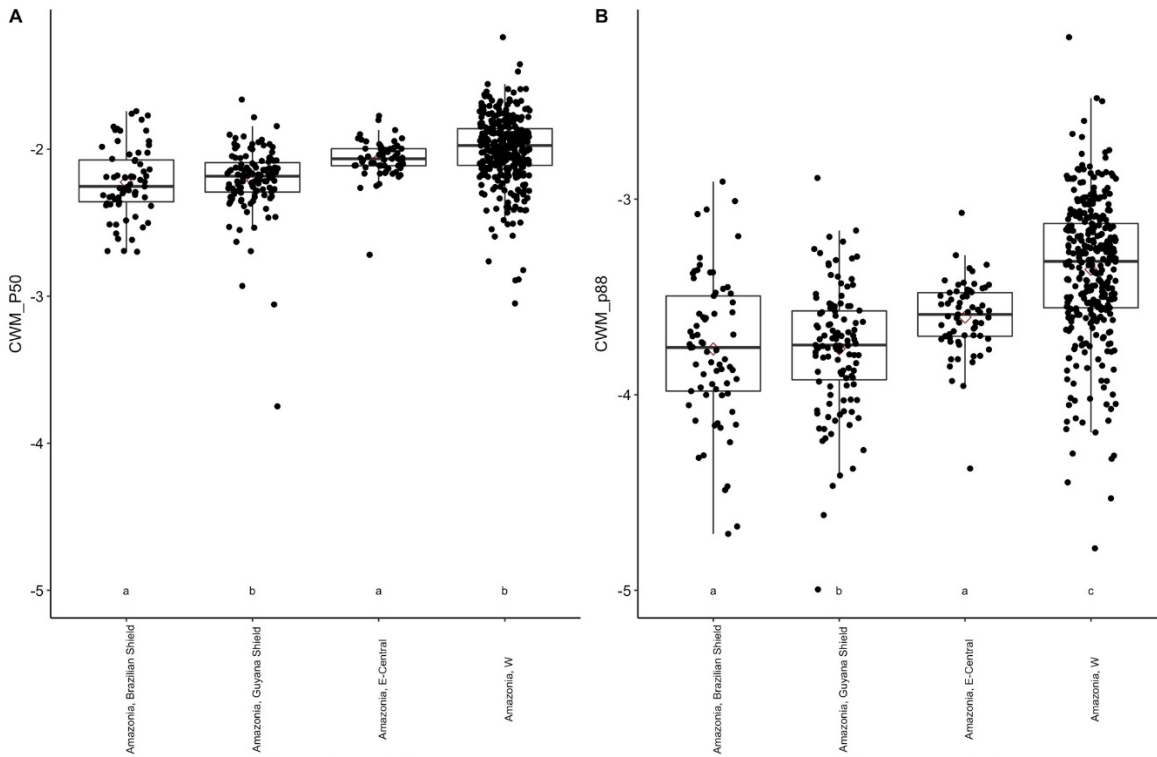


Figure A2.5 Community-weighted mean embolism resistance across Amazonian regions (Feldpausch et al. 2011): Ψ_{50} (A), Ψ_{88} (B). Differences at 0.05 level of significance using Anova and Tukey HSD *Pos Hoc* tests are indicated by letters below each boxplot. Black points represent forest sites (n=587).

Appendix 3:
Supplementary Information for Chapter 4

Table A3. 1 Summary of environments conditions of Western Amazonia.

Biogeographic Region	Forest type	Site	MCWD (mm)	MAP (mm)	DSL (months)	Soil type	Clay (%)	Ptotal (mg.kg-1)	Sampled Soil Depth (cm)	Soil data source
Western Amazon	Non-water limited	ALP1	-15.55	2824	0	Sandy clay loam	20.67	110.3	0-30	Quesada et al 2010 (ALP11)
		ALP2	-15.52	2824	0	Clay loam	34.46	110.24	0-30	Quesada et al 2010 (ALP22)
		SUC	-11.22	2880	0	Clay	46.49	284.62	0-30	Quesada et al 2010 (SUC01; SUC-02)
	Water limited	FEC	-256.65	2035	4-5	Clay loam	23.02	478.17	0-30	Quesada and Lloyd unpublished
		TAM	-146.87	2542	3-4	Clay	43.53	256.29	0-30	Quesada et al 2010 (TAM05)
		KEN2	-374.38	1127	6-7	Sandy loam	16	224.7	0-30	Araujo-Murakami et al 2014; Mallhi et al 2015
		KEN1	-374.72	1127	6-7	Sandy loam	16	447.1	0-30	Araujo-Murakami et al 2014; Mallhi et al 2015

Table A3. 2 Models and respective values of the relationship between hydraulic safety margins and Ψ_{min} and embolism resistance for 79 Western Amazonian tree species. The first third of the table contains the selected models and values for the group all which comprises both non water limited forests and water limited forests. Selected models for non water limited forests and water limited forests only are shown at the second and bottom thirds respectively.

group	Model	n	r2	pval	Slope	Slope lowCI	Slope highCI	Int	Int lowCI	Int highCI	
all	HSM_p50~p50	79	0.086	0.01	-1.14	-1.42	-0.92	-	1.79	-2.28	-1.31
	HSM_p50~Psi_min	79	0.439	0.00	0.89	0.75	1.06	1.55	1.26	1.84	
	HSM_p88~p88	79	0.479	0.00	-0.91	-1.07	-0.77	-	1.27	-1.77	-0.77
	HSM_p88~Psi_min	79	0.079	0.01	1.21	0.97	1.50	3.37	2.85	3.88	
Nwlf	HSM_p50~p50	41	0.575	0.00	-1.27	-1.49	-1.08	-	1.16	-1.47	-0.85
	HSM_p50~Psi_min	41	0.452	0.00	1.31	1.10	1.56	1.62	1.39	1.86	
	HSM_p88~p88	41	0.829	0.00	-1.05	-1.17	-0.94	-	0.89	-1.22	-0.57
	HSM_p88~Psi_min	41	0.116	0.03	1.95	1.57	2.41	3.34	2.87	3.81	
Wlf	HSM_p50~p50	47	0.301	0.00	-1.27	-1.49	-1.08	-	2.68	-3.19	-2.17
	HSM_p50~Psi_min	47	0.343	0.00	1.31	1.10	1.56	2.69	2.13	3.25	
	HSM_p88~p88	47	0.632	0.00	-1.05	-1.17	-0.94	-	2.30	-2.78	-1.82
	HSM_p88~Psi_min	47	0.072	0.07	1.95	1.57	2.41	5.52	4.48	6.55	

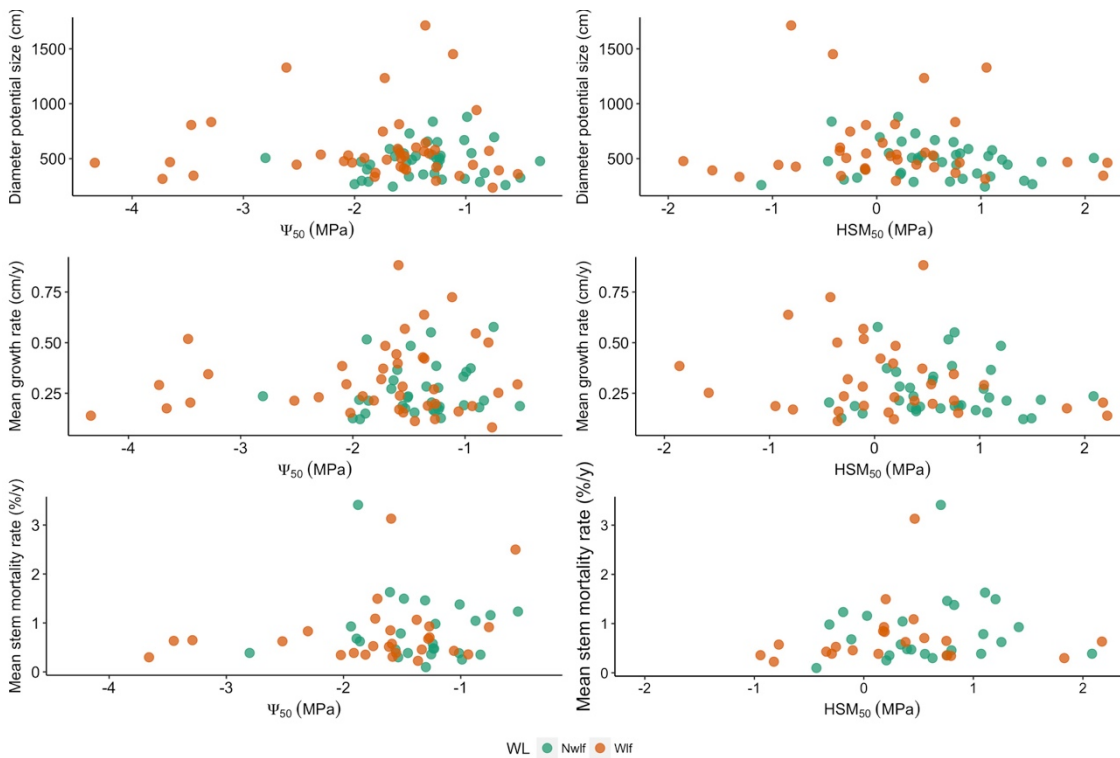


Figure A3. 1 Relationship between species mean Ψ_{50} and HSM_{50} and life-history strategy traits. Species present in water limited forests (seasonal and transitional forests) and non-water limited forests (aseasonal forests) are represented with orange and green points, respectively. Tree performance data at species level were obtained from (Coelho de Souza et al., 2016). Solid lines represent significant ($p \leq 0.05$) standardized major axis (SMA) regression.

Table A3. 3 Summary of standard maor axis (SMA) regressions between hydraulic traits and water deficit affiliation.

		group	Model	n	r2	pval	Slope	Slope lowCI	Slope highCI	Int	Int lowCI	Int highCI
Water Deficit Affiliation	all		WDA~p50	71	0.222	0.00	196.33	159.09	242.29	151.85	76.18	227.51
			WDA~p88	71	0.181	0.00	114.93	92.63	142.59	160.96	81.33	240.59
			WDA~HSM_p50	64	0.006	0.55	209.81	163.31	269.53	-224.92	-280.90	-168.94
			WDA~HSM_p88	64	0.020	0.27	143.17	183.61	111.63	63.88	-12.33	140.09
Life history traits	all	MaxD	MaxD~p50	72	0.002	0.68	366.43	463.91	289.42	-27.26	-190.92	136.40
			MaxD~p88	72	0.000	0.94	211.38	267.69	166.92	-43.02	-210.96	124.92
			MaxD~HSM_p50	65	0.020	0.26	364.76	466.85	285.00	663.37	568.20	758.54
			MaxD~HSM_p88	65	0.015	0.34	256.37	328.33	200.18	956.21	819.49	1092.92
		MeangrD	MeangrD~p50	66	0.005	0.57	0.22	0.17	0.28	0.65	0.55	0.75
			MeangrD~p88	66	0.022	0.24	0.13	0.10	0.16	0.66	0.56	0.76
			MeangrD~HSM_p50	59	0.051	0.08	-0.22	-0.29	-0.17	0.38	0.32	0.43
			MeangrD~HSM_p88	59	0.080	0.03	-0.15	-0.20	-0.12	0.55	0.47	0.64
		Mort	Mort~p50	43	0.014	0.45	1.16	0.85	1.57	2.62	2.00	3.24
			Mort~p88	43	0.044	0.18	0.65	0.48	0.88	2.65	2.03	3.27
			Mort~HSM_p50	37	0.038	0.25	1.22	0.87	1.69	0.38	0.04	0.72
			Mort~HSM_p88	37	0.000	0.99	0.76	0.54	1.06	-0.40	-0.95	0.14
		Nwlf	MaxD	MaxD~p50+Forest	39	0.007	0.61	346.96	276.95	434.74	952.48	822.44

		MaxD~p88+Forest	39	0.006	0.63	192.75	153.79	241.70	962.37	825.35	1099.40	
		MaxD~HSM_p50+Forest	39	0.014	0.47	298.77	379.72	234.74	649.95	563.64	736.25	
		MaxD~HSM_p88+Forest	39	0.001	0.84	198.94	253.15	155.99	823.54	705.51	941.57	
	MeangrD	MeangrD~p50	35	0.021	0.41	0.23	0.18	0.30	0.59	0.49	0.68	
		MeangrD~p88	35	0.013	0.51	0.13	0.10	0.16	0.59	0.50	0.69	
		MeangrD~HSM_p50	35	0.001	0.84	-0.21	-0.27	-0.17	0.40	0.33	0.47	
		MeangrD~HSM_p88	35	0.005	0.68	-0.14	-0.18	-0.11	0.52	0.43	0.60	
	Mort	Mort~p50	25	0.005	0.73	1.11	0.83	1.48	2.37	1.78	2.95	
		Mort~p88	25	0.001	0.86	0.60	0.46	0.79	2.43	1.84	3.03	
		Mort~HSM_p50	25	0.010	0.64	0.99	0.73	1.36	0.25	-0.16	0.66	
		Mort~HSM_p88	25	0.003	0.81	-0.62	-0.84	-0.46	2.02	1.48	2.57	
	Wlf	MaxD~p50+Forest	42	0.000	0.90	346.96	276.95	434.74	1226.60	1025.92	1427.28	
		MaxD~p88+Forest	42	0.011	0.51	192.75	153.79	241.70	1210.51	1019.95	1401.06	
		MaxD	MaxD~HSM_p50+Forest	35	0.005	0.69	298.77	379.72	234.74	642.90	496.90	788.90
			MaxD~HSM_p88+Forest	35	0.031	0.31	198.94	253.15	155.99	922.72	767.34	1078.09
		MeangrD	MeangrD~p50	40	0.019	0.40	0.23	0.18	0.30	0.74	0.61	0.87
			MeangrD~p88	40	0.055	0.14	0.13	0.10	0.16	0.73	0.61	0.85
			MeangrD~HSM_p50	33	0.046	0.23	-0.21	-0.27	-0.17	0.35	0.26	0.43
			MeangrD~HSM_p88	33	0.108	0.06	-0.14	-0.18	-0.11	0.54	0.45	0.64
		Mort	Mort~p50	27	0.062	0.21	1.11	0.83	1.48	2.71	2.03	3.38
			Mort~p88	27	0.165	0.04	0.60	0.46	0.79	2.60	2.00	3.20
			Mort~HSM_p50	21	0.009	0.68	0.99	0.73	1.36	0.47	0.02	0.92
			Mort~HSM_p88	21	0.026	0.49	-0.62	-0.84	-0.46	1.73	1.21	2.25
	all	AMD~p50	22	0.086	0.19	0.03	0.02	0.05	0.07	0.04	0.10	

Drought induced mortality		AMD~p88	22	0.087	0.18	0.02	0.01	0.03	0.07	0.04	0.11	
		AMD~HSM_p50	19	0.249	0.03	-0.04	-0.06	-0.02	0.03	0.01	0.04	
		AMD~HSM_p88	19	0.241	0.03	-0.02	-0.04	-0.02	0.06	0.03	0.08	
	tap		AMD~p50+study	8	0.280	0.18	0.03	0.02	0.05	0.07	0.02	0.11
			AMD~p88+study	8	0.319	0.14	0.02	0.01	0.03	0.07	0.02	0.12
			AMD~HSM_p50+study	7	0.526	0.07	-0.04	-0.07	-0.02	0.02	-0.02	0.07
			AMD~HSM_p88+study	7	0.557	0.05	-0.02	-0.04	-0.01	0.06	0.01	0.10
	cax		AMD~p50+study	6	0.042	0.70	0.03	0.02	0.05	0.07	0.00	0.13
			AMD~p88+study	6	0.117	0.51	0.02	0.01	0.03	0.07	0.01	0.14
			AMD~HSM_p50+study	6	0.058	0.64	-0.04	-0.07	-0.02	0.03	-0.03	0.09
			AMD~HSM_p88+study	6	0.174	0.41	-0.02	-0.04	-0.01	0.06	0.00	0.12
	bci		AMD~p50+study	8	0.043	0.62	0.03	0.02	0.05	0.05	0.01	0.09
			AMD~p88+study	8	0.072	0.52	0.02	0.01	0.03	0.05	0.01	0.09
		AMD~HSM_p50+study	6	0.031	0.74	-0.04	-0.07	-0.02	0.02	0.00	0.05	
		AMD~HSM_p88+study	6	0.064	0.63	-0.02	-0.04	-0.01	0.04	0.00	0.09	

Table A3. 4 Drought induced mortality as a function of wood density at branch level and branch and leaves total non-structural carbohydrates concentrations

	group	Model	n	r2	pval	Slope	Slope lowCI	Slope highCI	Int	Int lowCI	Int highCI
Water Deficit Affiliation			5	0.01	0.4				135.2		
		WDA~Branch_NSC_wet	6	2	3	-42.38	-55.41	-32.42	9	48.25	222.32
			5	0.00	0.6				195.1		
	all	WDA~Leaf_NSC_wet	6	4	6	-73.75	-96.53	-56.36	8	93.33	297.03

	bci	AMD~wd_b+study	8	0.23	0.2	0.41	0.24	0.68	-0.20	-0.33	-0.08
		AMD~Branch_NSC_wet+study	3	0.77	0.3	0.02	0.01	0.03	-0.08	-0.36	0.20
		AMD~Leaf_NSC_wet+study	3	0.60	0.4	-0.02	-0.04	-0.01	0.08	-0.24	0.40
	cax	AMD~wd_b+study	6	0.10	0.5	0.41	0.24	0.68	-0.27	-0.47	-0.07
		AMD~Branch_NSC_wet+study	6	0.01	0.8	0.02	0.01	0.03	-0.09	-0.22	0.03
		AMD~Leaf_NSC_wet+study	6	0.07	0.6	-0.02	-0.04	-0.01	0.07	-0.02	0.17

Table A3. 5 Relationship between drought induce mortality (ΔM) and hydraulic traits for common species of seasonal and aseasnal forest

Drought induced mortality assessed from study	Species	Hydraulic traits measured from					
		Site	Forest type	ΔM	Psi min	HSM p50	HSM p88
TAP Seasonal Forest	Aspidosperma auriculatum	FEC	Seasonal	0	-2.54	-0.87	0.98
		ALP2	Aseasonal	0	-0.53	0.04	0.11
	Brosimum guianense	FEC	Seasonal	0	-3.27	-1.92	-0.30
		SUC	Aseasonal	0	-0.44	1.48	3.38
	TAM	Seasonal	0	-0.49	0.03	0.37	
	Brosimum rubescens	ALP1	Aseasonal	0	-0.84	0.39	2.89

		ALP1	Aseasonal	0	-0.72	2.08	4.29
	Dialium guianense	FEC	Seasonal	0	-2.65	-0.83	0.82
		TAM	Seasonal	0	-1.76	0.25	1.46
	Mezilaurus itauba	FEC	Seasonal	0	-2.12	2.21	4.90
	Perebea mollis	FEC	Seasonal	0.0920	-2.28	-1.58	-0.94
				-			
	Pouteria macrophylla	KEN2	Transitional	0.0349	-0.96	2.48	3.80
				-			
		KEN1	Transitional	0.0349	-1.59	1.87	4.65
		ALP2	Aseasonal	0.0943	-0.53	0.04	0.11
	Brosimum guianense	FEC	Seasonal	0.0943	-3.27	-1.92	-0.30
		SUC	Aseasonal	0.0943	-0.44	1.48	3.38
		TAM	Seasonal	0.0943	-0.49	0.03	0.37
		ALP1	Aseasonal	0	-0.72	2.08	4.29
	Dialium guianense	FEC	Seasonal	0	-2.65	-0.83	0.82
		TAM	Seasonal	0	-1.76	0.25	1.46
CAX Seasonal Forest	Eschweilera coriacea	ALP2	Aseasonal	0.0257	-0.91	0.63	2.31
		TAM	Seasonal	0.0257	-1.83	1.83	4.15
	Licania heteromorpha	TAM	Seasonal	0.0000	-0.71	0.55	1.89
				-			
	Minuartia guianensis	SUC	Aseasonal	0.0403	-0.76	0.80	2.36
				-			
		TAM	Seasonal	0.0403	-1.43	-0.10	1.52
	Swartzia racemosa	SUC	Aseasonal	0.0068	-2.00	-0.11	1.71
BCI Seasonal Forest*	Hura crepitans	KEN1	Transitional	0.0064	-1.28	0.45	1.71

<i>Sapium glandulosum</i>	KEN2	Transitional	0.0189	-1.31	0.06	0.81
			-			
<i>Simarouba amara</i>	ALP2	Aseasonal	0.0150	-0.72	0.03	0.34
<i>Spondias mombin</i>	KEN2	Transitional	0.0251	-1.42	0.18	1.15
<i>Terminalia amazonia</i>	KEN1	Transitional	0.0093	-2.54	0.75	3.32
<i>Virola surinamensis</i>	SUC	Aseasonal	0.0150	-0.52	0.74	2.16

*Powell et al 2018

